BIOCHEMICAL ANALYSIS OF THE DROSOPHILA

RNAI PATHWAY

APPROVED BY SUPERVISORY COMMITTEE

Qinghua Liu, Ph.D.

Kristen W. Lynch, Ph.D.

Steven L. McKnight, Ph.D.

Xiaodong Wang, Ph.D.

DEDICATION

In honor of my parents, Zhongping Jiang 江仲屏,

and Xiurong Dai 戴秀榕

BIOCHEMICAL ANALYSIS OF THE DROSOPHILA RNAI PATHWAY

by

FENG JIANG

DISSERTATION

Presented to the Faculty of the Graduate School of Biomedical Sciences

The University of Texas Southwestern Medical Center at Dallas

In Partial Fulfillment of the Requirements

For the Degree of

DOCTOR OF PHILOSOPHY

The University of Texas Southwestern Medical Center at Dallas

Dallas, Texas

September 2008

ACKNOWLEDGEMENTS

I am very grateful to my mentor, Dr. Qinghua Liu, who gave me this great opportunity to work in the exciting field of RNA interference, despite the fact that I hardly knew anything about science about four years ago. Through the years, his guidance, patience, and encouragement have made my thesis work an enjoyable and exciting experience. I appreciate the freedom and independence that he has given me, to explore my own research interests. He impresses me as the most hard-working person with never-ending passion about science. I have benefited tremendously from his constant inspiration, his high standard on experimental data and critical thinking.

My deep gratitude also goes to my dissertation committee members. Dr. Xiaodong Wang has always welcomed me to discuss with him about my projects and provided innovative ideas about research directions and problem solving. Dr. Kristen Lynch, as my committee chair, has always kept me in the right track so that I was able to make progress every year and eventually finish my study in time. Dr. Steven McKnight, despite his busy schedule, has always made time for my committee meetings and provided critical suggestions. I am also obliged to Dr. McKnight for sponsoring me with the Sara and McKnight Fellowship.

I feel fortunate to have worked with all my labmates, who have made the Liu Lab a stimulating environment with constant discussion and support among each other. My appreciation goes to especially Rosie Addison and Tamara Strauss for their invaluable friendship.

I am also truly thankful to Nancy McKinney, who offered me the opportunity to start my Ph.D. study in the spring semester due to the delay caused by visa issues. Her constant support helped me to catch up with the rest of the class and find the labs for my rotation. She also became my non-science mentor, who taught me the nuance of the English language and western culture. Her comfort strengthened me during difficult times and gave me an appreciation of how meaningful the smallest act of compassion can be.

Finally, I would like to thank my families for their unconditional love and support. My parents, Zhongping Jiang and Xiurong Dai, instilled in me a strong sense of self-motivation and independence, which provide the foundation for all my academic pursuits. My husband, Zhigao Wang, who is also a biomedical researcher, not only stands by me all the time through happiness and sadness, but contributes intellectual input to my research projects.

BIOCHEMICAL ANALYSIS OF THE DROSOPHILA RNAI PATHWAY

FENG JIANG, Ph.D.

The University of Texas Southwestern Medical Center at Dallas, 2008

QINGHUA LIU, Ph.D.

RNA interference is post-transcriptional gene silencing mediated by (21-26 nt) miRNAs and siRNAs. In *Drosophila*, the RNase III enzymes Dicer-1 and Dicer-2 generate miRNAs and siRNAs, respectively. Nascent miRNA and siRNA duplexes are assembled into distinct RNA induced silencing complexes termed miRISC and siRISC, of which AGO1 and AGO2 are the respective catalytic subunits. My dissertation project is focused on identifying new RNAi components and understanding mechanisms of RISC assembly by biochemical reconstitution.

Our group previously identified a novel dsRNA-binding protein named R2D2 which functioned in complex with Dicer-2 to process dsRNA into siRNA. Only the Dicer-2/R2D2 complex, but neither Dicer-2 nor R2D2 alone, efficiently interact with duplex siRNA. Furthermore, the tandem dsRNA binding domains of R2D2 are required for siRNA binding. Therefore, although R2D2 is dispensable for siRNA production, it is required for incorporating siRNA onto the siRISC complex.

Generation of recombinant AGO2 protein is essential for in vitro reconstitution of the RNAi pathway. We believe that the unique poly glutamine repeat region of fly

AGO2 may be problematic for expression. Thus, a series of truncated AGO2 baculoviruses that remove some or all polyQ repeats of AGO2 were generated. Co-expression with AGO1 increases the expression level of AGO2 by at least 10 fold. Affinity purified full length and one truncated form of AGO2 show minimal RISC activity, i.e. could be programmed with single stranded siRNA and perform sequence specific cleavage of mRNA. Most interestingly, adding purified recombinant Dicer-2/R2D2 complex to recombinant Ago2 generated dsRNA and siRNA initiated RISC activity. Catalytic mutant of Ago2 is unable to reconstitute RISC activity with recombinant Dicer-2/R2D2 complex, showing that the RISC activity is specific. Therefore, the three component system, Dicer-2, R2D2, and Ago2, can reconstitute the RNAi pathway of *Drosophila*.

By a bioinformatics approach, a novel protein named Loquacious (Loqs) was identified with considerable sequence homology to R2D2. Loqs and Dicer-1 interact with each other by co-immunoprecipitation in S2 cell extract. Recombinant Loqs could enhance miRNA production by Dicer-1 by increasing its affinity for the pre-miRNA substrate. Furthermore, depleting Loqs or Dicer-1 by dsRNA knockdown resulted in reduction of the miRNA-generating activity and accumulation of pre-miRNA in S2 cells. To study the physiological function of *loqs* in flies, we obtained a piggyback (PB) fly strain in which the PB transposon was inserted into the first exon and before the translation start site of *loqs* gene. Pre-miRNAs accumulate in the $loqs^{PB}$ flies, indicating they are defective for miRNA biogenesis. However, while both siRISC and miRISC activities are greatly reduced in *dcr-1* null extract, these

activities are not affected in *loqs* null extract, indicating that loqs is not essential for miRISC assembly.

To test whether the known components are sufficient to reconstitute the miRNA pathway, recombinant AGO1 protein was expressed using the insect cell expression system. It is generally believed that siRISC slices, whereas miRISC represses translation of cognate mRNA in animals. However, recombinant AGO1 can be programmed by single stranded miRNA into a minimal miRISC and sequence specifically cleaves complementary mRNA *in vitro*. Furthermore, the catalytic activity of AGO1 is dependent on the consensus catalytic “DDH” motif. My present studies suggest that recombinant Dicer-1, Loqs and AGO1 are not sufficient to reconstitute the miRNA pathway, indicating that there are other unknown components to be discovered.

TABLE OF CONTENTS

PRIOR PUBLICATIONS

Xiang Liu, Joseph K. Park, **Feng Jiang**, Ying Liu, Dennis McKearin and Qinghua Liu (2007). Dicer-1, but not Loquacious, is critical for assembly of miRNA-induced silencing complexes. RNA 13, 2324-2329.

Xiang Liu, **Feng Jiang**, Savitha Kalidas, Dean Smith and Qinghua Liu (2006). Dicer-2 and R2D2 coordinately bind siRNA to promote assembly of the siRISC complexes**.** RNA 12(8), 1514-20.

Feng Jiang*, Xuecheng Ye*, Xiang Liu, Lauren Fincher, Dennis McKearin and Qinghua Liu**.** (2005). Dicer-1 and R3D1-L catalyze microRNA maturation in Drosophila. Genes Dev 19(14), 1674-1679. (* equal contribution)

LIST OF FIGURES

Chapter I

Chapter II

Chapter III

Chapter IV

LIST OF TABLES

Chapter I

LIST OF ABBREVIATIONS

CIRV	*Carnation ringspot virus*
DCL	Dicer like
DExDc	DEAD-like helicases superfamily
DGCR8	DiGeorge syndrome critical region gene 8
dsRBD	dsRNA binding domain
DSRM	Double-stranded RNA binding motif
dsRNA	double stranded RNA
DUF283	domain with unknown function 283 domain
endo-siRNA	endogenous siRNA
Exp5	exportin-5
HELICc	Helicase superfamily c-terminal domain
miRNA	microRNA
nt	nucleotide
Pasha	partner of Drosha
PAZ	Piwi, Argonaute and Zwille/Pinhead
piRNA	Piwi-interacting RNA
Piwi	P element induced wimpy testis
polyP	poly proline domain
polyQ	poly glutamine
pre-miRNA	microRNA precursor
pri-miRNA	primary microRNA transcript

PTGS	post-transcriptional gene silencing
rasiRNA	repeat-associated siRNA
RdRP	RNA dependent RNA polymerase
RISC	RNA induced silencing complex
RISC	RNA induced silencing complex
RNAi	RNA interference
RNase III	ribonuclease III domain
SDS-PAGE	sodium dodecyl sulfate polyacrylamide gel electrophoresis
siRNA	small interfering RNA
ssDNA	single stranded DNA
ssRNA	single stranded RNA
tasiRNA	trans-acting siRNA
WT	wildtype

Chapter I

Introduction: Molecular Mechanism of RNAi

The term RNA interference (RNAi) was first coined when Fire, Mello and coworkers discovered that double-stranded RNA were significantly more potent in interfering with endogenous gene expression than either strand individually when injected into the nematode C. elegans (Fire et al., 1998). The phenomenon of RNAi, termed post-transcriptional gene silencing (PTGS) in plants, was discovered even earlier when plant biologists Jorgensen et al introduced a pigment-producing transgene into petunia and get variegated or completely white flowers instead of the expected deep purple color (Napoli et al., 1990). Besides nematodes and plants, RNAi has since then been discovered in a wide variety of organisms including flies, humans, mice, zebrafish, trypanosomes, and fungi (Zamore et al., 2000).

Antisense small RNAs, ~25 nt in length and complementary to the endogenous mRNA, were discovered to be present in transgene induced PTGS in plants (Hamilton and Baulcombe, 1999). The first breakthrough in exploring the molecular mechanism of RNAi came from the establishment of an *in vitro* system which recapitulated dsRNA mediated mRNA degradation in *Drosophila* embryo extract (Tuschl et al., 1999). Using this *Drosophila in vitro* system, long dsRNA were found to be processed into small dsRNAs with 21-23 nt in length in an ATP-dependent manner (Zamore et al., 2000). The small RNA products were termed small interfering RNAs (siRNAs) (Zamore et al., 2000). A cell culture system that utilized dsRNA to regulate endogenous gene or exogenous introduced reporter expression was established in Drosophila S2 cells (Hammond et al., 2000). In the same study, the *in vitro* assay system for investigating the dsRNA-mediated nuclease was expanded to S2 cells

which renders large amount of material available for biochemical purification (Hammond et al., 2000). This ribonuclease complex was termed RNA induced silencing complex (RISC) and contained both protein and small RNA (Hammond et al., 2000).

To date, many classes of small RNAs have been discovered: siRNA, microRNA (miRNA), Piwi-interacting RNA (piRNA), trans-acting siRNA (tasiRNA), and endogenous siRNA (endo-siRNA). Since this dissertation study mainly focuses on siRNA and miRNA, detailed introduction of siRNA and miRNA pathway will be given, while other classes of small RNA action will be briefly described

siRNAs

Initially siRNAs were shown to be 21-23 nt intermediate products of long dsRNA-mediating silencing (Zamore et al., 2000). It was later shown that synthetic 21-22 nt RNA duplexes with 3’ overhang were able to trigger efficient sequence-specific target RNA cleavage (Elbashir et al., 2001b). The demonstration that synthetic 21 nt siRNA duplexes could be introduced in to *Drosophila* S2 cells and mammalian cells and target endogenous gene expression (Elbashir et al., 2001a) has proven RNAi to be an invaluable experimental tool to knock-down gene expression. siRNA duplexes are short enough to bypass the non-specific interferon response triggered by dsRNAs in mammalian cell culture (Bitko and Barik, 2001; Elbashir et al., 2001a). Further biochemical analysis of siRNA structure revealed that siRNA

duplexes have 5’ phosphate group, 3’ hydroxyl group and 2 nt 3’ overhang (Elbashir et al., 2001b; Elbashir et al., 2001c; Nykanen et al., 2001).

While siRNAs are generated as a duplex, once loaded, the active RISC only contains single-stranded siRNA (Martinez et al., 2002; Martinez and Tuschl, 2004). RISC uses the single-stranded siRNA as guide to cleave the target RNA in the middle of the complementary region, the nucleotide paired with the 10th nucleotide from the 5’ end of the guiding strand (Elbashir et al., 2001b).

miRNAs

MicroRNAs (miRNAs) represent a new class of non-coding genes, which are believed to sequence specifically control stability or translation of target mRNAs by binding to sites of antisense complementarity in the mRNAs (Bartel, 2004). The length of miRNAs is usually ~22nt, and they are typically excised from 60- to 70-nt stem-loop RNA precursor structures. The first miRNA *lin-4* was discovered in 1993, which mediates post-transcriptional regulation of the heterochronic gene *lin-14* during development in C.elegans (Lee et al., 1993; Wightman et al., 1993). But it was not widely noticed until the discovery of RNAi in 1998. After seven years of silence, *let-7*, another gene in the C.elegans heterochronic pathway, was discovered to encode a second 21nt regulatory RNA (Reinhart et al., 2000). Furthermore, let-7 RNA is evolutionally conserved in all three clades of bilaterian animals (Pasquinelli et al., 2000), from worm to fly to human. While miRNAs possess 5’ phosphate group and 3’

hydroxyl group similarly to siRNA, the mature miRNAs exist in a single-stranded form.

Since then, hundreds of miRNAs have been cloned or bioinformatically predicted in the genomes of C.elegans (Lau et al., 2001; Lee and Ambros, 2001), Drosophila (Aravin et al., 2003; Lai et al., 2003; Weber, 2005), zebrafish (Chen et al., 2005), mouse and human (Bentwich et al., 2005; Lagos-Quintana et al., 2001; Lagos-Quintana et al., 2003; Lagos-Quintana et al., 2002; Weber, 2005). Almost all of the cloned miRNAs are conserved in closely related animals, such as human and mouse (Lagos-Quintana et al., 2003), or C.elegans and C. briggsae (Lim et al., 2003a; Lim et al., 2003b). The clustering of miRNA genes and high homologies between species indicate that miRNAs have very important evolutionary and functional roles.

Other small RNAs

piRNAs are 24-30 nt in length and represent a new class of small RNAs that are crucial for germline development (Hartig et al., 2007). Repeat-associated siRNA (rasiRNA) is an alternative designation of piRNA (Aravin et al., 2003). piRNAs are genenrated from repeated or complex DNA sequence elements by a Dicer-independent mechanism and interact with a subset of Argonaute proteins, the Piwi-like Argonautes (Klattenhoff and Theurkauf, 2008). Distinct from siRNAs and miRNAs, piRNAs have a 2’-O-Methyl modification at their 3’-end. The nematode 21 nt RNAs beginning with U (21U RNAs) might be a functional analogue of piRNAs.

While the biological functions of piRNAs in the germline have been extensively studied, the molecular mechanism of piRNA biogenesis remains largely unknown (Hartig et al., 2007).

tasiRNAs are a class of endogenously expressed small RNAs discovered in plants that have the characteristics of both siRNAs and miRNAs (Vaucheret, 2005). They arise from dsRNA precursors and direct sequence specific cleavage of target mRNA. The biogenesis of tasiRNA requires components of both siRNA and miRNA pathways in plants (Vaucheret, 2005).

Very recently, a diversity of endo-siRNAs were discovered in mice and Drosophila (Okamura and Lai, 2008). They can be generated from transposable elements, or genomic regions that encode exons on both DNA strands, or mammalian pseudogene-gene pairs, or extended inverted repeats (hpRNAs). The biogenesis and biology of endo-siRNAs are still open questions because this is a relative new area (Okamura and Lai, 2008).

RNase III enzymes in RNAi

Ribonuclease III (RNase III) was first termed to describe an endonuclease specific for dsRNA substrates when partially purified from *E. coli* by Zinder and coworkers in 1968 (Robertson et al., 1968). RNase III is conserved in all studied prokaryotes and eukaryotes (Lamontagne et al., 2001). Catalysis by RNase III generates a characteristic dsRNA product consisting of a 5’ phosphate group, 3’

hydroxyl group and a 2 nt overhang at the 3' end (Lamontagne et al., 2001). There are three classes of RNase III enzymes based on domain composition, ranging from ~200 to ~2000 amino acids in length. Class 1 enzymes are the canonical RNase III, the simplest and smallest, containing a single ribonuclease domain and one dsRNA binding domain (dsRBD) (Fig. 1.1). They are ubiquitously found in bacteria, bacteriophage and some fungi including yeast (Lamontagne et al., 2001). Class 2 enzymes contain two ribonuclease domains and one dsRBD (Fig. 1.1). The founding member of this class, Drosha, contains a poly proline domain at the N terminus (Filippov et al., 2000). The class 3 enzymes are also known as the Dicer family of enzymes (Bernstein et al., 2001). They are the largest among the 3 classes, containing an N terminal DExD helicase domain, a domain of unknown function (DUF283), PAZ domain, two ribonuclease domains and one dsRBD (Fig. 1.1). The PAZ domain was termed after three proteins containing this similar 110-amino-acid .

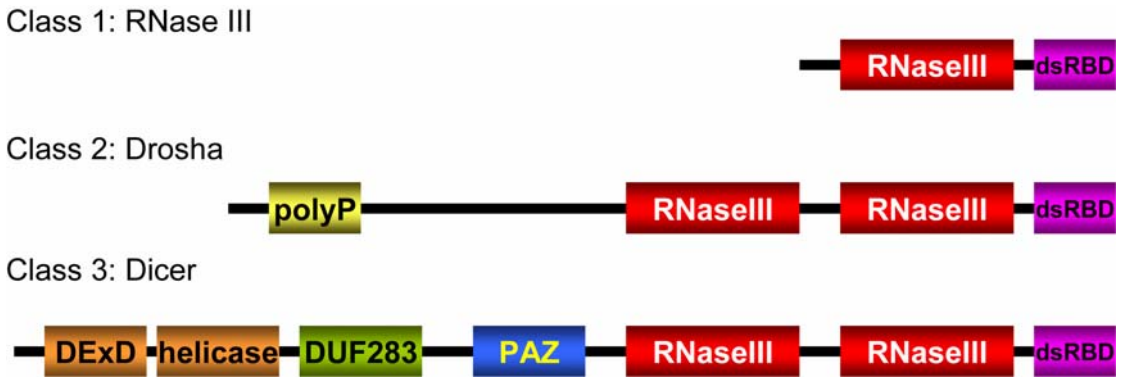

Figure 1.1. Schematic presentation of the three classes of RNase III enzymes. The diagrams were drawn relative to the length of the proteins. RNase III can be used to describe the class 1 enzymes or the robonuclease domain of the RNase III enzymes. Functional domains are colored as follows: ribonuclease III domain (RNase III), red; dsRNA binding domain (dsRBD), purple; poly proline domain (polyP), yellow; DExD helicase domain, brown; domain with unknown function 283 domain (DUF 283), green; PAZ domain, blue.

region: Piwi, Argonaute and Zwille/Pinhead (Cerutti et al., 2000)

The involvement of the RNase III enzymes in RNAi was revealed when Hannon and coworkers discovered that *Drosophila* Dicer was responsible for production of siRNA (Bernstein et al., 2001). The Dicer family of proteins is highly conserved in all studied eukaryotes with the exception of *S. cerevisiae*. In organisms including *S. pombe*, *C. elegans*, zebrafish and mammals, Dicer is encoded by a single-copy gene, but genomes of many other model organisms encode from two Dicers as seen in *Drosophila* and *Neurospora*, to four Dicer like (DCL) genes in *Arabidopsis*. Dicer was later discovered to process miRNA precursor (pre-miRNA) into mature miRNA (Hutvagner et al., 2001). Unlike dsRNA which contains perfect complementarity, hairpin structured pre-miRNA possess mismathches, bulges, or G:U wobble base pairs. Despite the chemical difference, the single Dicer in human is able to process both substrates and generates siRNA and miRNA (Zhang et al., 2004).

Structural anaylysis has demonstrated that bacterial RNase III functions as a homodimer with a single catalytic center (Blaszczyk et al., 2001). This dimerization occurrs between two ribonuclease domains, with each domain acting on one strand of the dsRNA substrate (Blaszczyk et al., 2001). Biochemical studies of human Dicer show that it functions as a pseudodimer, with the two RNase III domains in the same molecule interacting with each other (Zhang et al., 2004). The intramolecular dimer contains a single cleavage center, which processes dsRNA substrates at approximately 20 nt away from the 3’ end recognized by the PAZ domain (Zhang et al., 2004). Recently, a crystal structure of the human parasite *Giardia intestinalis* Dicer was

solved (Macrae et al., 2006). The Giardial protein may be considered a “minimal” Dicer with only the PAZ and tandem RNase III domains. The structure revealed that the ability of Dicer to generate products of discrete length stems from the distance of a long connector helix between the PAZ and RNase III domains (Macrae et al., 2006).

Drosha was first discovered to involve in the processing of human pre-ribosomal RNA (Wu et al., 2000). Through a candidate approach, it was identified as the core nuclease that process the long primary transcript of miRNA (pri-miRNA) (Lee et al., 2003). Drosha excises stem-loop precursors of miRNA (pre-miRNA) hairpins from the pri-miRNA in the nucleus (Lee et al., 2003). Dicer and Drosha represent the two classes of RNase III enzymes that play essential roles in RNAi. While dsRNA, pri-miRNA and pre-miRNA possess different chemical structure, the detailed mechanism of distinguishable substrate specificity of these RNase III enzymes awaits future high resolution structural studies of substrate-bound enzymes.

Argonaute proteins

Piwi (P element induced wimpy testis) was the first discovered member of the Argonaute family of proteins for its role in germline stem cell division (Lin and Spradling, 1997). The name Argonaute was first used to describe a mutant of *Arabidopsis ago1*, in which the morphology of the leaves resembled a small squid “the greater argonaute” (Bohmert et al., 1998). A biochemical approach to identify protein components of RISC in Drosophila S2 cell extract led to the discovery of

Argonaute 2 (AGO2) as an essential factor in RNAi (Hammond et al., 2001). Since then, the Argonaute proteins have been demonstrated to play pivotal roles in RNAi from multiple organisms. Members of the Argonaute family are defined by the presence of PAZ and PIWI domains and divided into three subgroups: Argonaute-like proteins, similar to Arabidopsis AGO1; Piwi-like proteins, similar to Drosophila Piwi; and a C. elegans-specific group (Hutvagner and Simard, 2008). Although organisms such as bacteria and archaea do not have RNAi function, they do have Argonaute proteins, indicating their ancient origin. The number of Argonaute genes encoded in each organism differs significantly, ranging from only one in *S. pombe* to at least 26 in *C. elegans* (Hutvagner and Simard, 2008). So far, only a subset of this family has been functionally characterized and the specific roles of each Ago is summarized in (Table 1.1) (Hutvagner and Simard, 2008).

PAZ and PIWI are two essential functional domains of Argonaute. The PAZ domain also exists in Dicers as described previously. Multiple crystal structures of PAZ domains of different Argonautes have shown that PAZ forms an oligonucleotide-binding fold (OB fold) and binds to single-stranded and double-stranded small RNAs with low affinity in a sequence-independent manner (Lingel et al., 2003; Ma et al., 2004; Song et al., 2003; Yan et al., 2003). These studies also demonstrated that the unique feature of PAZ lies in that it requires the 2 nt 3’ overhang for efficient complex formation. Since siRNAs and miRNAs are generated by RNase III enzyme Dicers, they bear the characteristic 2 nt 3’ overhang. Thus, by binding to the 3’ overhang, PAZ could distinguish these small regulatory RNAs from

Argonaute protein	Molecular function
Neurospora crassa	
QDE2	Quelling
SMS-2	Meiotic silencing of unpaired DNA
Schizosaccharomyces pombe	
Ago1	Heterochromatin silencing, TGS, PTGS
Tetrahymena	
Twi1	DNA elimination
Arabidopsis thaliana	
AGO1	miRNA-mediated gene silencing, tasiRNA
AGO4	piRNA, heterochromatin silencing
AGO6	piRNA, heterochromatin silencing
AGO7	tasiRNA, heteroblasty, leaf development
Caenorhabditis elegans	
RDE-1	Exogenous RNAi
ALG-1	miRNA-mediated gene silencing, TGS
ALG-2	miRNA-mediated gene silencing
ERGO-1	Endogenous RNAi
CSR-1	Chromosome segregation and RNAi
SAGO-1	Endogenous and exogenous RNAi
SAGO-2	Endogenous and exogenous RNAi
PPW-1	Endogenous and exogenous RNAi
PPW-2	Endogenous and exogenous RNAi
F58G1.1	Endogenous and exogenous RNAi
C16C10.3	Endogenous and exogenous RNAi
PRG-1	Germline maintenance
Drosophila melanogaster	
AGO1	miRNA-mediated gene silencing
AGO2	RNAi
AGO3	piRNA, transposon silencing
PIWI	piRNA, transposon silencing, germline stem-cell maintenance, RNAi
Aubergine	piRNA, transposon silencing, stellate silencing, RNAi
Zebrafish	
Ziwi	piRNA, germ-cell maintenance, transposon silencing
Murine/Human	
AGO1	Heterochromatin silencing
AGO2	RNAi, miRNA-mediated gene silencing, heterochromatin silencing
MIWI (mouse)	piRNA, spermatogenesis
MILI (mouse)	piRNA, spermatogenesis
RIWI (rat)	piRNA

Modified from (Hutvagner and Simard, 2008)

Table 1.1. Functions of Argonaute proteins in different species. The table summarizes the well charaterized Argonaute-like and Piwi-like proteins and their RNAi related or cellular functions. *Arabidopsis* has six more Argonaute-like proteins, *C. elegans* has 15 more Argonautes with undefined function(s), and mammals have two more Argonaute-like proteins and two more Piwi-like proteins.

degraded RNAs that are products of non-related pathways.

A significant advance was brought by structural analysis of full-length archaebacterium *Pyrococcus furiosus* Ago protein (Song et al., 2004). It revealed that the PIWI domain, at the C terminal of Argonaute, shows an RNase H-like structure, and the critical residues for the endonucleolytic activity of RNase H are conserved in the PIWI domain (Song et al., 2004). Mutagenesis analysis of the conserved residues in human Ago2 abolished the RNA cleavage activity targeted by small RNAs, supporting the model of Argonaute being the slicer in the RISC (Liu et al., 2004). Furthermore, the minimal RISC activity, the endonucleolytic cleavage activity programmed by a single-stranded siRNA, can be reconstituted with recombinant human Ago2 (Rivas et al., 2005). The same paper also defines the “DDH” motif which forms the catalytic center of the enzyme. These data indicate that human Ago2 functions as a slicer in RNAi.

The crystal structure of the eubacterium *Archaeoglobus fulgidus* Piwi protein (AfPiwi) associated with an siRNA-like small RNA has been solved (Ma et al., 2005; Parker et al., 2005). AfPiwi, utilized as a model for understanding the eukaryotic Ago-PIWI domain, was shown to bind to the 5' end of the guiding strand of the siRNA duplex. The crystal structure of another eubacterium Aquifex aeolicus Argonaute (Aa-Ago), a DNA-mediated RNA endonuclease, was solved (Yuan et al.,

2005) and a four step catalytic cycle model was proposed. According to this model, the 2 nt 3’ overhang of siRNA is locked in the PAZ domain in the beginning, but once target RNA starts to anneal to the 5’ end of siRNA, the 3’-end of the guiding strand is released from the PAZ domain, allowing full-length guiding strand:mRNA duplex to form. After the cleavage, the 2 nt 3’ overhang switchs back to the pocket of PAZ domain. However, a fully elaborated biochemical model of the small RNA-directed target RNA cleavage pathway awaits a crystallographic characterization of Argonaute from organisms furnishing genuine RNAi machinery.

In *Drosophila*, AGO1 (Kataoka et al., 2001), is dispensable for siRNA induced RNA cleavage, but is required for miRNA-mediated target RNA cleavage (Okamura et al., 2004). Fly embryos lacking AGO2, another member of the fly Argonaute-like proteins, are defective in siRNA-directed RNAi, but still capable of miRNA-directed target RNA cleavage (Okamura et al., 2004). In addition, AGO2 was reported to be the sole protein required for target RNA cleavage activity in RNAi (Rand et al., 2004). Depletion of AGO2, but not AGO1, from *Drosophila* S2 cells results in stabilization of multi-copied transgene mRNA with shortening of the mRNA poly(A) tail (Siomi et al., 2005).

In humans, while Ago2 is associated with both siRNA and miRNA and functions as a slicer (Liu et al., 2004; Meister et al., 2004b; Rivas et al., 2005), other Argonaute subfamily members including Ago1, Ago3, and Ago4, do not mediate such RNA cleavage, although all show high similarities to hAgo2 at peptide sequence levels and all associate with siRNA and miRNA (Liu et al., 2004; Meister et al., 2004b) (Sasaki

et al., 2003). In fact, human Ago1 and Ago4 lack a complete DDH motif, which explains their inability to slice (Liu et al., 2004). However, while possessing all three essential catalytic residues, human Ago3 has not been shown to be involved with any cleavage event. Therefore, not all Piwi domains possess a catalytic center and not all Argonautes are slicer-competent.

The siRNA pathway

siRNAs are processed by Dicer from exogenous dsRNAs by viral replication, aberrant transcription, or artificial introduction by humans (Bernstein et al., 2001). In *Drosophila*, there are two Dicer genes, Dcr-1 and Dcr-2. Dcr-1 preferentially process pre-miRNA and Dcr-2 catalyzes dsRNA processing (Lee et al., 2004b; Liu et al., 2003; Pham et al., 2004). The siRNA-generating enzyme was biochemically purified from *Drosophila* S2 cells and was found that it consisted of not only Dcr-2 but a dsRNA binding protein R2D2 (Liu et al., 2003). R2D2 is homologous to the *Caenorhabditis elegans* RNAi protein RDE-4. Further biochemical studies suggest that the Dcr-2/R2D2 complex also binds duplex siRNA, forms the RISC loading complex (RLC), and facilitates the transfer of siRNA onto siRISC (Hammond et al., 2001; Liu et al., 2003; Pham et al., 2004; Tomari et al., 2004b). AGO2 is the catalytic component of siRISC (Hammond et al., 2001; Rand et al., 2004). The Drosophila siRNA pathway is illustrated in Fig. 1.2.

While members of the Argonaute family of proteins are core components of RISC

and are required genetically for RNA silencing in every organism where their function has been studied (Hutvagner and Simard, 2008), it is unknown whether there are other essential components of siRISC. Genetic study and immunoprecipitation experiments show that proteins such as Armitage, Fragile X mental retardation 1 (dFMR1), and p68 RNA helicase (Dmp68) are associated with RISC (Ishizuka et al., 2002; Tomari et al., 2004a). To date, the exact roles of these proteins have not been elucidated.

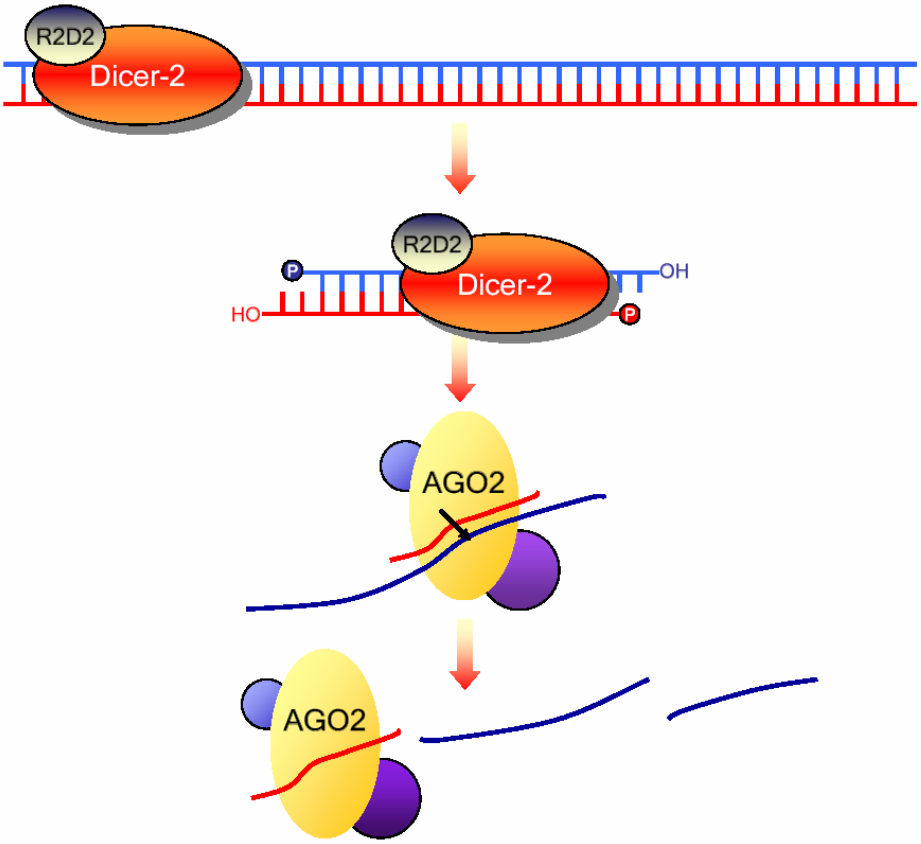

Figure 1.2. The molecular mechanism of the siRNA pathway in *Drosophila*. DsRNA is processed by Dcr-2/R2D2 complex into 21 nt siRNA duplexes with 5' phosphate group, 3' hydroxyl group and a 2 nt 3' overhang. Dcr-2/R2D2 complex binds to the siRNA duplex and facilitates siRNA loading onto the RNA induced silencing complex (RISC). The catalytic component of siRISC is Argonaute 2 (AGO2). Active siRISC uses one strand of siRNA as guide to sequence-specifically cleave target mRNA.

The miRNA pathway

MiRNA in animals are found in diverse genomic locations. The majority of miRNA genes are located in intergenic regions or in antisense orientation to annotated genes, indicating that they form independent transcription units (Lagos-Quintana et al., 2001; Lau et al., 2001; Lee and Ambros, 2001). Most other miRNA genes are found within introns of protein-coding genes, and introns and exons of mRNA-like non-coding genes (Rodriguez et al., 2004). The transcription of miRNA genes is mediated by RNA polymerase II (pol II) to generate long primary transcripts (pri-miRNAs) (Lee et al., 2004a). Pri-miRNAs are subsequently cleaved by nuclear Drosha into imperfect complementary stemloop structured pre-miRNA (Lee et al., 2003). This cleavage event predetermines mature miRNA sequence and generates optimal substrates for subsequent cleavage (Lee et al., 2003). Interestingly, recombinant Drosha alone cannot excise pre-miRNA hairpins accurately, but instead acts as a non-specific RNase that cleaves pri-miRNA indiscriminately (Gregory et al., 2004). The specificity of substrate recognition comes from a Drosha-interacting protein named DiGeorge syndrome critical region gene 8 (DGCR8) in humans (Han et al., 2004; Landthaler et al., 2004). The *Drosophila* homologue of DGCR8 is named Pasha (partner of Drosha) (Denli et al., 2004; Gregory et al., 2004). $Pasha^{fly}$/$DGCR8^{human}$ is a dsRNA-binding protein that confers substrate specificity and proper positioning of the Drosha ribonuclease center.

Pre-miRNA is exported out of the nucleus by exportin-5 (Exp5), member of the Ran-dependent nuclear transport receptor family (Bohnsack et al., 2004; Lund et al.,

2004; Yi et al., 2003). Pre-miRNA is subsequently cleaved by cytoplasmic RNase III enzyme Dicer (Dcr-1 in *Drosophila*) into ~22nt miRNA duplex (Bernstein et al., 2001; Hutvagner et al., 2001; Ketting et al., 2001). Notably, only one strand of this short-lived duplex remains as a mature miRNA, with the other strand being degraded (Bartel, 2004). Mature miRNAs associate with AGO1 in Drosophila (Okamura et al., 2004) while Ago1, Ago2, and Ago3 in mammals all interact with miRNAs (Liu et al., 2004; Meister et al., 2004b).

As post-transcriptional regulators of gene expression, miRNA works bi-modally. MiRNA specifies mRNA cleavage if the mRNA has perfect or near-perfect complementarity to the miRNA, or it represses translation if the mRNA only has suitable miRNA complementary sites (Tomari and Zamore, 2005). The complementary sites for the known animal miRNAs reside in the 3' untranslated regions (UTRs) (Brennecke et al., 2003; Lee et al., 1993; Poy et al., 2004; Reinhart et al., 2000; Yekta et al., 2004), while some known plant miRNA target sites exist in the protein coding region of mRNA (Chen, 2004; Llave et al., 2002; Xie et al., 2003). While plant miRNAs share near-perfect complementarity to their targets and direct sequence-specific cleavage (Rhoades et al., 2002), animal miRNAs share limited sequence complementarity with their targets and therefore mediate target translational repression (Bartel, 2004). The Drosophila cytoplasmic miRNA pathway is illustrated in Fig. 1.3.

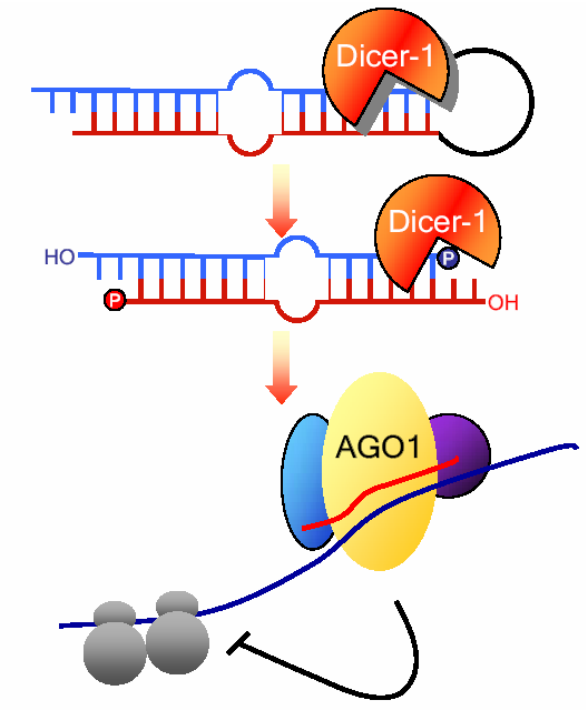

Figure 1.3. The molecular mechanism of the miRNA pathway in *Drosophila*. In the cytoplasm, miRNA precursor (pre-miRNA) is processed by Dcr-1 into miRNA duplex with 5' phosphate group, 3' hydroxyl group and a 2 nt 3' overhang. The miRNA duplex contains mismatches, bulges, and G:U wobbles, and only one strand will become mature miRNA. After loaded onto miRISC, since the mature miRNA does not share perfect sequence complementarity with the target mRNA, it will mediate translational repression. AGO1 is the core component of miRISC.

Chapter II

P19 inhibits RISC assembly

Abstract

The tombusvirus p19 protein is a plant viral silencing suppressor. It has been shown to bind 21-25nt duplex siRNA *in vitro* and *in vivo***.** Although much is known about how p19 binds siRNA, exactly how this binding inhibits RNAi machinery is not clear. By utilizing the heterologous *Drosophila in vitro* RNAi system, I was able to examine the molecular mechanism by which p19 suppresses RNAi machinery. Recombinant p19, but not binding defective mutants, inhibits both the siRNA and miRNA pathways in *Drosophila* S2 cell extract. In the siRNA pathway, while not affecting the enzymatic activity of Dcr-2, p19 competes with Dcr-2/R2D2 complex in siRNA binding and therefore interfere with siRISC assembly. However, once siRISC is formed, p19 no longer inhibits the cleavage activity. In the miRNA pathway, p19 stabilizes the miRNA duplex while not influencing Dcr-1's enzymatic activity. It inhibits the duplex miRNA initiated RISC activity at the assembly process while it has no impact on the endogenously formed miRISC. In summary, in both processes, p19 suppresses the formation of active RISC by sequestering the double-stranded small RNAs.

Introduction

Although RNAi was discovered in *C. elegans* in 1998, the phenomenon of RNA silencing was actually first discovered in plant eighty years before that (Baulcombe, 2004). RNAi pathways are found in most eukaryotic organisms, including fungi, plants and animal. In plants, transgene silencing and viral RNA silencing are under extensive study. Therefore, it is best illustrated in plants that RNAi serves as a general defense mechanism against foreign nucleic acids. Most known plant viruses contain single strand RNA (ssRNA) or single strand DNA (ssDNA) genome and replicate through double strand RNA (dsRNA) intermediates, which becomes a potent trigger for RNAi machinery (Silhavy and Burgyan, 2004). Viral expression is eventually silenced through sequence-specific cleavage and subsequent degradation of viral RNAs by host RNAi machinery. To counteract the host defense mechanism, most plant viruses have evolved to encode silencing suppressors. In fact, most viral suppressors have other established functions in the virus life cycle before they were discovered to be silencing inhibitors (Scholthof, 2007). The sequences of distinct viral silencing suppressors are highly diverse, while in the same virus family, the suppressor proteins are highly conserved (Burgyan, 2008). Consequently, it suggests that different suppressors inhibit RNAi at different steps. Studies of the inhibitory mechanisms of these viral suppressors may provide insights into endogenous mechanisms by which cells regulate the RNAi machinery.

The tombusvirus p19 protein is among one of the most studied viral suppressors.

p19 was shown to specifically bind 21-25nt duplex siRNA, but not ssRNA, *in vitro* and *in vivo*, preventing the virus induced systemic spreading of silencing beyond the site of local infection (Silhavy et al., 2002). The sequestering model was strongly supported by the three dimension structure of p19 bound to a 21nt siRNA (Vargason et al., 2003; Ye et al., 2003). The p19 homodimer functions as a "molecular caliper" to measure siRNA so as to bind best to the length of 20-22nt. The crystal structure of the *Carnation ringspot virus* (CIRV) p19-siRNA complex also revealed that both Trp39 and Trp42 were critical residues for interaction with the siRNA duplex end (Vargason et al., 2003). Mutation of Trp39 into glycine resulted in plant recovery from virus infection, suggesting defective inhibition of RNA silencing, while substituting arginine, a similarly charged residue, for both of Trp39 and Trp42 lead to mild symptoms and partial plant recovery (Vargason et al., 2003).

Although much is known about how p19 binds siRNA, exactly how this binding inhibits RNAi machinery is not clear. Does it affect Dicer activity? Or does it affect RISC activity? Will it inhibit siRISC as well as miRISC? At which exact step does it function? Does its suppressor activity correlate with siRNA binding strength? We want to address these questions using the heterogenous *Drosophila in vitro* system.

The molecular mechanism of RNAi is conserved in eukaryotes. The processing of long dsRNA or pre-miRNA is carried out by Dicer family of proteins, while the core component of RISC is Argonaute (Ago) family of proteins. In plants, there are at least four Dicer-like (DCL) genes and at least ten Argonaute-like (AGO) proteins, and not all of them have known functions (Eamens et al., 2008). Furthermore, in plants, there

are few biochemical assays established only in wheat germ extract (Tang et al., 2003). In contrast, in *Drosophila*, there are fewer genes encoding Dicer and Ago, the RNAi machinery is more biochemically defined, and the *in vitro* biochemical essays are well established. Therefore, by utilizing the heterologous *Drosophila in vitro* RNAi system, I am able to pinpoint the exact mechanism by which p19 suppresses RNAi machinery.

Material and Methods

Preparation of S100 from S2 cells

The Drosophila S2 cells (ATCC) were cultured in suspension in Drosophila-SFM media (Invitrogen), harvested at ~2 × 10^7 cells/ml, washed with PBS, and resuspended in three times pellet volume of buffer A (10 mM KOAc, 10 mM HEPES, pH7.4, 2 mM $Mg(OAc)_2$, 5 mM DTT) supplemented freshly with protease inhibitors including 1 mM Pefabloc SC, 5 μg/ml Leupeptine, and 0.7 μg/ml Pepstatin (Roche). After sitting on ice for 20 minutes, cells were broken with a douncer with 40 strokes followed by a 20,000g spin at 4 ºC for 30 minutes. The supernatant-S20 was further centrifuged at 100,000g for one hour at 4 ºC to make S100.

Purification of recombinant proteins

The plasmid constructs of recombinant GST tagged CIRV p19 wildtype, W39G, and W39/42R were generously provided by Dr. József Burgyán (Plant Biology Institute, Hungary). The constructs were transformed into E. coli strain BL21(DE3)

(Novagen). Each culture was grown in 1L LB with ampicillin and shaken at 37°C until an O.D.600 of ~0.6. Then IPTG was added to a final concentration of 1mM. The cultures were kept shaking at 37°C for another 3 hours. The bacteria pellets were collected by spinning at 1,000g in a Beckman J5.2 rotor for 20 minutes at 4°C. (The pellet can be stored at -80°C.) Each strain was lysed by sonication in 40ml of buffer T (20 mM Tris-HCl, pH 8.0, 50 mM NaCl, 5 mM b-mercaptoethanol) freshly supplemented with protease inhibitors described above. After spinning at 20,000g for 20 minutes at 4°C, each supernatant was collected and incubated with 1ml glutathione beads (GE) for at least 2 hours at 4°C. After washing with cold 50ml of buffer T containing 1M NaCl and 50ml of buffer T, the GST fusion proteins were eluted with 10ml of buffer T containing 10mM glutathione. Each protein elution was subject to 50 units of thrombin protease (GE) cleavage for 16 hours at 4°C. The cleavage products were separated by SP- Sepharose chromatography (GE). The peak fraction of p19 was stored in aliquots at –80ºC.

Polyhistidine-tagged recombinant Dcr-2, R2D2, Dcr-1, and Loquacious (Loqs) proteins were expressed in insect cells by the Bac-to-Bac baculovirus expressions system (Invitrogen). After adding virus for 44-60 hours, the infected Sf21 cells were harvested, washed in PBS, and the cells were broken with a douncer with 40 strokes in buffer T containing 20 mM imidazole with protease inhibitors. The S20 lysate was then incubated with Ni-NTA beads (Qiagen) for at least 2 hours at 4°C, loaded onto a column, washed sequentially with buffer T containing 1M NaCl and buffer T. After a buffer T with 50 mM imidazole wash, the His-tagged proteins were eluted in buffer T

containing 250 mM imidazole. The recombinant enzymes were further purified by SP- and Q-Sepharose chromatography and stored in aliquots at –80ºC in 10% glycerol. Freezing without glycerol will kill the enzymes.

RISC assays

The complementary sequence of let-7 was inserted into a GFP gene, and a 250bp long DNA sequence was amplified through PCR using a 5' primer containing T7 promoter site and a 3' primer containing 20 polyTs. The mRNA substrate was in vitro transcribed using Megascript T7 kit (Ambion). The mRNA was radiolabeled at the 5' G cap by guanylyl transferase (Ambion). In a 12 µl reaction, 4 µg RNA, 20 units of RNase Inhibitor (Ambion), and 6 µl α-^{32}P GTP (40 mCi/ml, MP) are incubated with 2 mM fresh prepared S-adenosyl methionine in 50 mM Tris, pH 8.0, 6 mM KCl, 1.2 mM $MgCl_2$, and 2.5 mM DTT. The reaction mixture was incubated for at least 2 hours at 37 ºC and the radiolabeled RNA was PAGE gel purified. In a 10 µl RISC reaction, S2 S100 extract was incubated with 4×10^4 cpm radiolabeled probe, 10 units of RNase Inhibitor, and 1 mM ATP at 30ºC for 30 minutes in 100 mM KOAc, 10 mM HEPES, pH 7.4 and 1 mM $Mg(OAc)_2$. The dsRNA, pre-let-7, let-7 siRNA, let-7/let-7*, or let-7 ssRNA triggers were respectively used at 1 nM, 250 nM, 25 nM, 10 nM and 250 nM final concentrations.

The reaction is stopped by addition of 200 µl 0.3 M NaOAc, phenol/chloroform extracted, ethanol precipitated with glycogen as a carrier, resolved on a 6% denaturing (7 M Urea) polyacrylamide gel (PAGE) and was directly exposed to X-ray film.

The RNAs used in the assays were custom ordered from Dharmacon, and phosphorated using cold ATP (Promega) by T4 polynucleotide kinase at the 5' ends. The sequences are as follows: synthetic 61 nt pre-let-7, 5'-UGAGGUAGUAGGUUGUAUAGUAGUAAUUAC ACAUCAUACUAUACAAUGUCUAGCUUUCUU-3'; synthetic 21 nt let-7 sense strand, 5'- UGAGGUAGUAGGUUGUAUAGU-3'; synthetic 21 nt anti-sense let-7, 5'-UAUACAACCUACUACCUCAUU-3'; synthetic 22 nt let-7*: 5'-UAUACAAUGUGCUAGCUUUCUU-3'.

The let-7 siRNA was generated by annealing equal amount of let-7 sense strand and anti-sense let-7. The biotinylated let-7 siRNA is the same in the sequence while the 3' ends of both stranded are biotinylated. The let-7/let-7* miRNA duplex was generated by annealing equal amount of let-7 sense strand and let-7*.

Gel mobility shift assay

let-7 siRNA was radiolabeled at the 5' end by T4 polynucleotide kinase (NEB) using γ-^{32}P ATP (10 mCi/ml, MP). In a 10 μl reaction, 5×10^4 cpm radiolabeled siRNA was incubated with S2 S100 extract or recombinant proteins at 30ºC for 30 minutes in 50 mM KOAc, 12 mM HEPES, pH 7.4, 0.8 mM $Mg(OAc)_2$, and 2.5 mM DTT. After addition of 1.5 μl 10× DNA loading dye, the mixture was resolved on a 5% native PAGE.

Antibodies

The anti-AGO2 antibody was raised in rabbits against a truncated AGO2 and further purified using the protocol provided by http://www.med.yale.edu/mbb/koelle/protocols/protocol_Ab_affinity_purif.html. The anti-Dcr-2 and anti-R2D2 antibodies have been described (Liu et al., 2003).

The pre-miRNA processing assay

Synthetic pre-let-7 was radiolabeled at the 5' end by T4 polynucleotide kinase (NEB) using γ-^{32}P ATP (10 mCi/ml, MP) followed by PAGE purification. In a 10 µl reaction, 5 × 10^4 cpm radiolabeled pre-let-7 was incubated with S2 S100 extract or 0.2 pmol recombinant Dcr-1/Loqs-PB complex at 30ºC for 30 minutes in 100 mM KOAc, 15 mM HEPES, pH 7.4, 10 mM $Mg(OAc)_2$, and 2.5 mM DTT. The reaction is stopped by addition of 200 µl 0.3 M NaOAc, phenol/chloroform extracted, ethanol precipitated with glycogen as a carrier, resolved on a 16% denaturing (7 M Urea) PAGE and was directly exposed to X-ray film.

Precipitation by streptavidin beads

A 400 µl RISC reaction was assembled with 25 nM biotinylated siRNA and 200 µl S2 S100 extract with or without p19. After 30 minutes at 30 ºC, 10 µl of streptavidin beads and 2 µl of 10% NP40 were added. After rotating for one hour at room temperature, the beads were washed five times with 0.5 ml wash buffer (100 mM KOAc, 10 mM HEPES, pH 7.4, 100 mM NaCl, 2 mM $Mg(OAc)_2$, 5 mM DTT, 0.1 % NP40) and boiled in 30 µl of 2x SDS sample buffer. The proteins associated

with streptavidin beads were resolved on a 6% SDS-PAGE and Western blotted for Dcr-2 and AGO2.

Results

p19 inhibits both siRISC and miRISC activity in S2 extract

To examine whether p19 functions as a potent inhibitor in the heterologous *Drosophila* RNAi system, I purified recombinant p19 and tested whether adding p19 to S2 extract would decrease the RISC activity *in vitro*. GST tagged WT p19 and W39G, W39/42R mutants were expressed and purified from BL21 cells. To eliminate the homodimerization effect from the GST tag, GST was cleaved from p19 by thrombin protease, and separated by SP-sepharose chromatography (Fig.2.1.A). All three forms of p19: WT, W39G and W39/42R expressed at similar level (Fig.2.1.A, lane 1, 4, and 7). When added to S2 cell extract, the long dsRNA initiated RISC activity was inhibited by only the WT p19 (Fig.2.1.B, lane 3 and 4), but not W39G (Fig.2.1.B, lane 5 and 6) and W39/42R (Fig.2.1.B, lane 7 and 8) mutants. And the inhibition by WT p19 was dose-dependent (Fig.2.1 B, compare lane 3 and 4). Similarly, WT p19 inhibited pre-miRNA initiated RISC activity in S2 cell extract (Fig.2.1.C).

These results suggest that the plant viral silencing suppressor p19 can function as a potent RNAi suppressor in a heterologous system, and that it can inhibit both siRISC

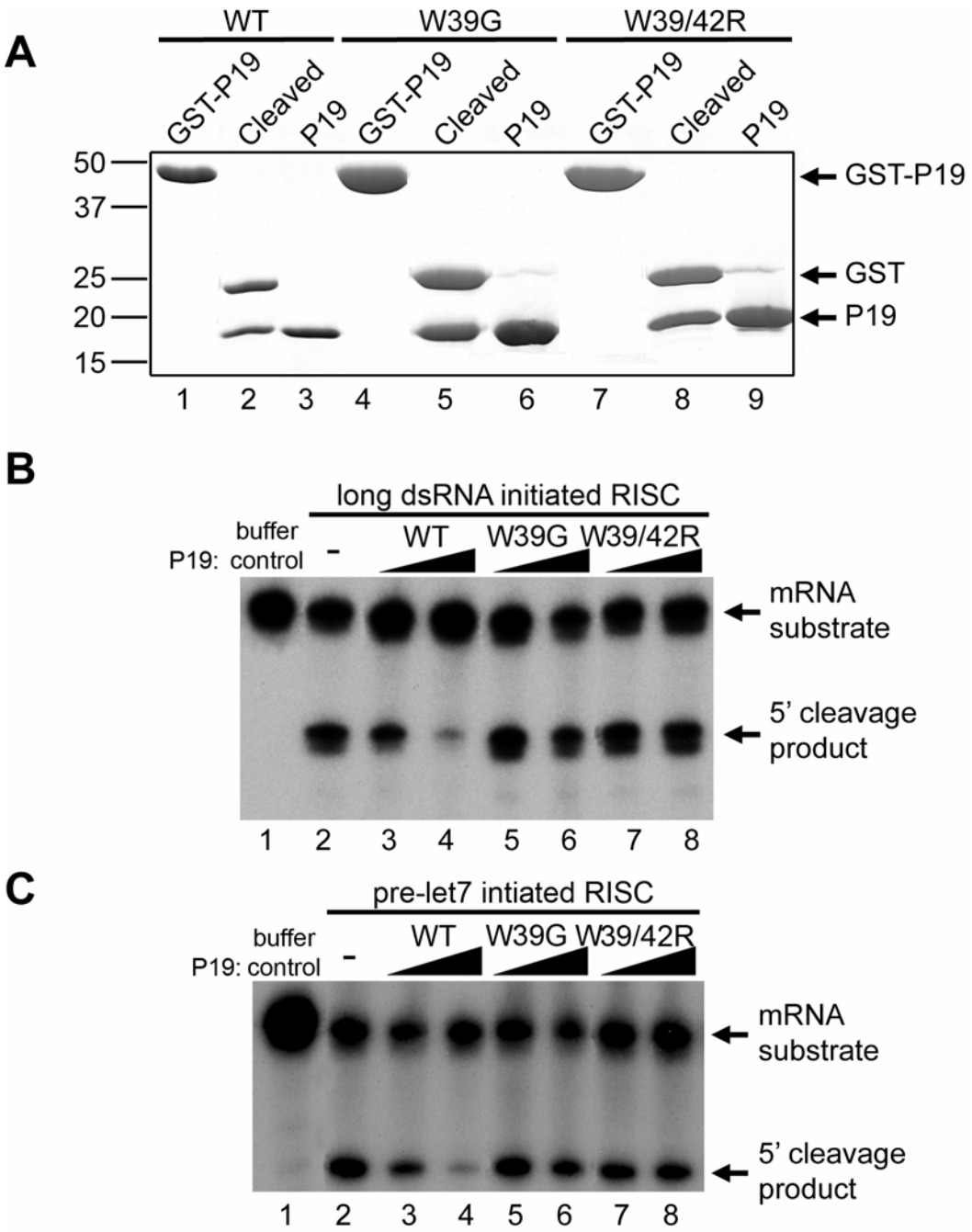

Figure 2.1. Recombinant p19 inhibits both dsRNA and pre-miRNA initiated RISC activity in S2 cell extract. (A) Coomassie blue stain of purified recombinant p19 proteins. GST tagged WT p19 and W39G, W39/42R mutants were expressed and purified from BL21 cells. The GST tag was cleaved by thrombin protease. GST and p19 were separated by SP-sepharose chromatography, and relatively pure preparation of p19 proteins were obtained. **(B)** Recombinant p19 inhibits the long dsRNA initiated RISC activity. Two different amount (1ng and 10ng respectively) of WT p19 (lane 3, 4), W39G (lane 5, 6) and W39/42R mutants (lane 7, 8) were added to S2 cell extract in long dsRNA initiated RISC reaction. **(C)** Recombinant p19 also inhibits pre-let7 initiated miRISC activity. Similar to panel B, same amount of WT p19 (lane 3, 4), W39G (lane 5, 6) and W39/42R mutants (lane 7, 8) were added to S2 cell extract in pre-let7 initiated RISC reaction.

and miRISC activity in S2 cell extract. This allowed me to further dissect the molecular mechanism of RNAi suppression by p19 in *Drosophila in vitro* assays.

p19 competes with Dcr-2/R2D2 complex for siRNA binding

To determine at what step p19 inhibits the siRNA pathway, I performed *in vitro* assays for individual steps of the RNAi pathway. I first examined the initiation step – siRNA biogenesis. Adding p19 to S2 cell extract or recombinant Dcr-2 catalyzed dsRNA processing reaction did not affect Dicer activity (data not shown), indicating that p19 does not interfere with the initiation step of RNAi. Dcr-2/R2D2 was previously discovered to be the main protein complex to bind siRNA (Liu et al., 2003), and I tested whether p19 could compete with Dcr-2/R2D2 for siRNA binding (Fig.2.2). About 0.05nmol of p19 out-competed most of the siRNA binding of 0.44nmol of Dcr-2/R2D2 (Fig. 2.2.A, lane 7). There is an almost 10 fold difference in the amount of protein binding siRNA between p19 and Dcr-2/R2D2, indicating p19 has almost 10 fold higher affinity toward siRNA compared to Dcr-2/R2D2.

To determine whether p19 could compete with endogenous Dcr-2/R2D2 complex to bind siRNA, the gel mobility assay was performed in S2 cell extract, and similar results were obtained. 0.05 nmol of WT p19 out-competed with most of the endogenous Dcr-2/R2D2 (Fig. 2.2.B, lane 7), while neither W39G nor W39/42R mutant showed any competition in siRNA binding. Even 100ng of the W39G mutant, 10 times more of the maximum amount of WT p19 used, showed very weak siRNA

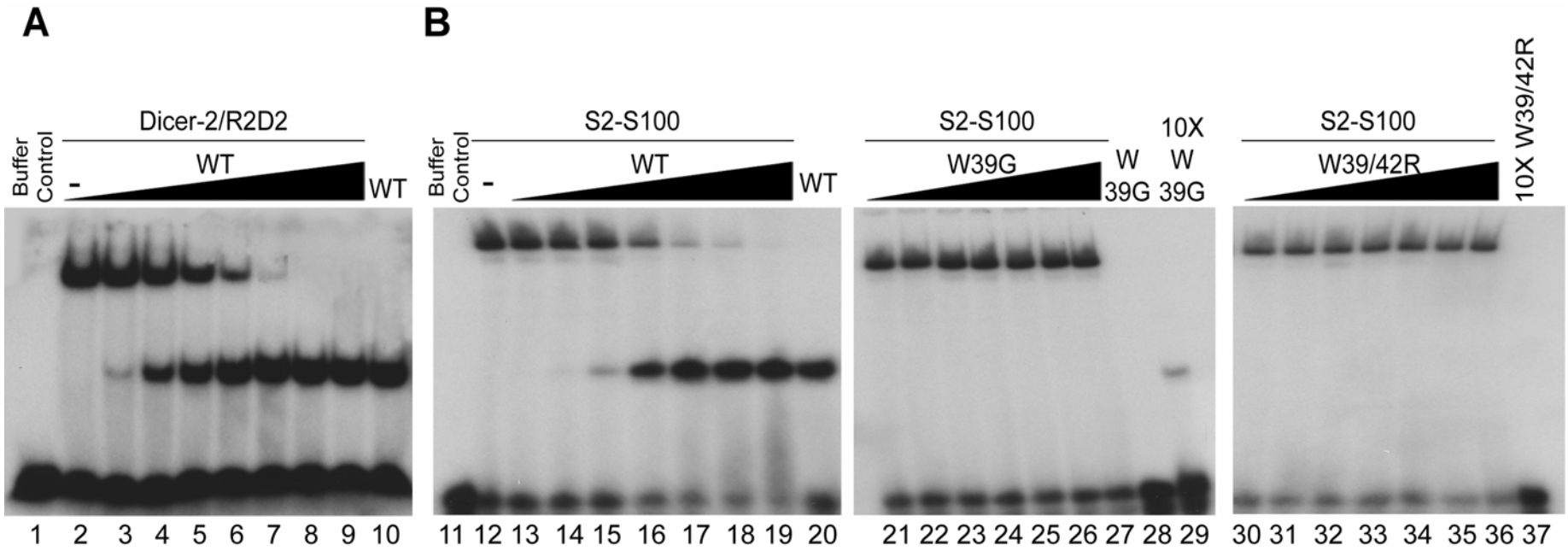

Figure 2.2. p19 competes with Dcr-2/R2D2 complex for siRNA binding. (A) Recombinant WT p19 competes with recombinant Dcr-2/R2D2 complex for siRNA binding in a dose-dependent manner. Each lane, except buffer control and p19 only, contains 100ng recombinant Dcr-2/R2D2 complex. The seven series of dilution of recombinant WT p19 are 0.01ng, 0.03ng, 0.1ng, 0.3ng, 1ng, 3ng, and 10ng respectively (lane 3 through lane 9). **(B)** Recombinant WT p19 (lane 11-20), but not W39G (lane 21-29) or W39/42R mutants (lane 30-37), competes with endogenous Dcr-2/R2D2 complex in S2 cell extract for siRNA binding in a dose-dependent manner. In lanes labeled as 10×W39G and 10×W39/42R (lane 19 & 27), 100ng of recombinant protein is used.

binding (Fig. 2.2.B, lane 19), while 100ng of the W39/42R mutant did not show any binding (Fig. 2.2.B, lane 27). These results indicates that the inability of the mutants to bind siRNA leads to their incompetence to compete with *Drosophila* Dcr-2/R2D2 complex, which is consistent with previous findings that p19 is a potent siRNA sequester.

p19 inhibits siRISC assembly

Since p19 does not affect siRNA biogenesis, it must target siRNA pathway at a downstream event – the effector step. Only WT p19 inhibited double-stranded siRNA initiated RISC activity (Fig. 2.3.A), consistent with previous results (Fig.2.1.B). In *Drosophila* extract, the formation of active RISC takes two steps: the first involves unwinding of the duplex siRNA leading to only one strand being incorporated to RISC, and the second involves recognition of the target mRNA leading to sequence specific cleavage of the mRNA by the nuclease AGO2 (Meister et al., 2004a; Rivas et al., 2005). When p19 was added in the RISC assembly step, it inhibited RISC activity (Fig. 2.3.B, lane 2 and 3). This indicates that p19 inhibits the assembly step by sequestering siRNA. Furthermore, p19 failed to inhibit the RISC activity when added after siRISC was assembled (Fig. 2.3 B, lane 4 and 5), indicating it has no effect against the cleavage activity of RISC.

To confirm that p19 blocks siRISC assembly, I examined the association of Dcr-2 and AGO2 – components of RISC, with 3'-biotinylated siRNA by precipitation using streptavidin beads. The biotinylated siRNA was as active as unmodified siRNA in

inducing RISC activities in S2 cell extract, and this RISC activity was inhibited by WT p19 (Fig. 2.3.C). Streptavidin beads only precipitated Dcr-2 (Fig. 2.3.D, lanes 1 and 2), AGO2 (Fig. 2.3.E, lanes 1 and 2) and R2D2 (data not shown), when biotinylated siRNA was used, suggesting that it was a specific interaction. I also performed streptavidin pull-down with WT p19, W39G, or W39/42R mutants. Consistently, almost no Dcr-2 or AGO2 was associated with biotinylated siRNA when WT p19 was added in the RISC reaction, indicating no active RISC was formed (Fig.2.3.D. and E.).

It was previously shown that p19 was unable to bind ssRNA (Vargason et al., 2003; Ye et al., 2003). Therefore, the most direct assay to show that p19 does not affect the cleavage activity of RISC would be single-stranded RNA initiated RISC assay. Even when 100ng of p19 – 10 times more than the amount causing significant inhibition of siRISC – was provided, the sslet-7 initiated RISC activity was not changed (Fig. 2.3.F lane 6), confirming that p19 targeting siRISC assembly was specific. Since p19 is a plant viral suppressor, it would be better if my findings in the *Drosophila in vitro* assays were confirmed in a plant system. Indeed, an *in vitro* assay system for RNA silencing in plants was established in wheat germ extract, and the activity of an endogenous RISC programmed by a miRNA was shown (Tang et al., 2003). Upon request, Dr. Guiliang Tang (University of Kentucky, Lexington, KY) generously gave us a batch of wheat germ extract that he had made, and I further explored the accessibility of his system. Though I could not detect any siRNA or long dsRNA initiated RISC activity, I successfully established the sslet-7 initiated RISC

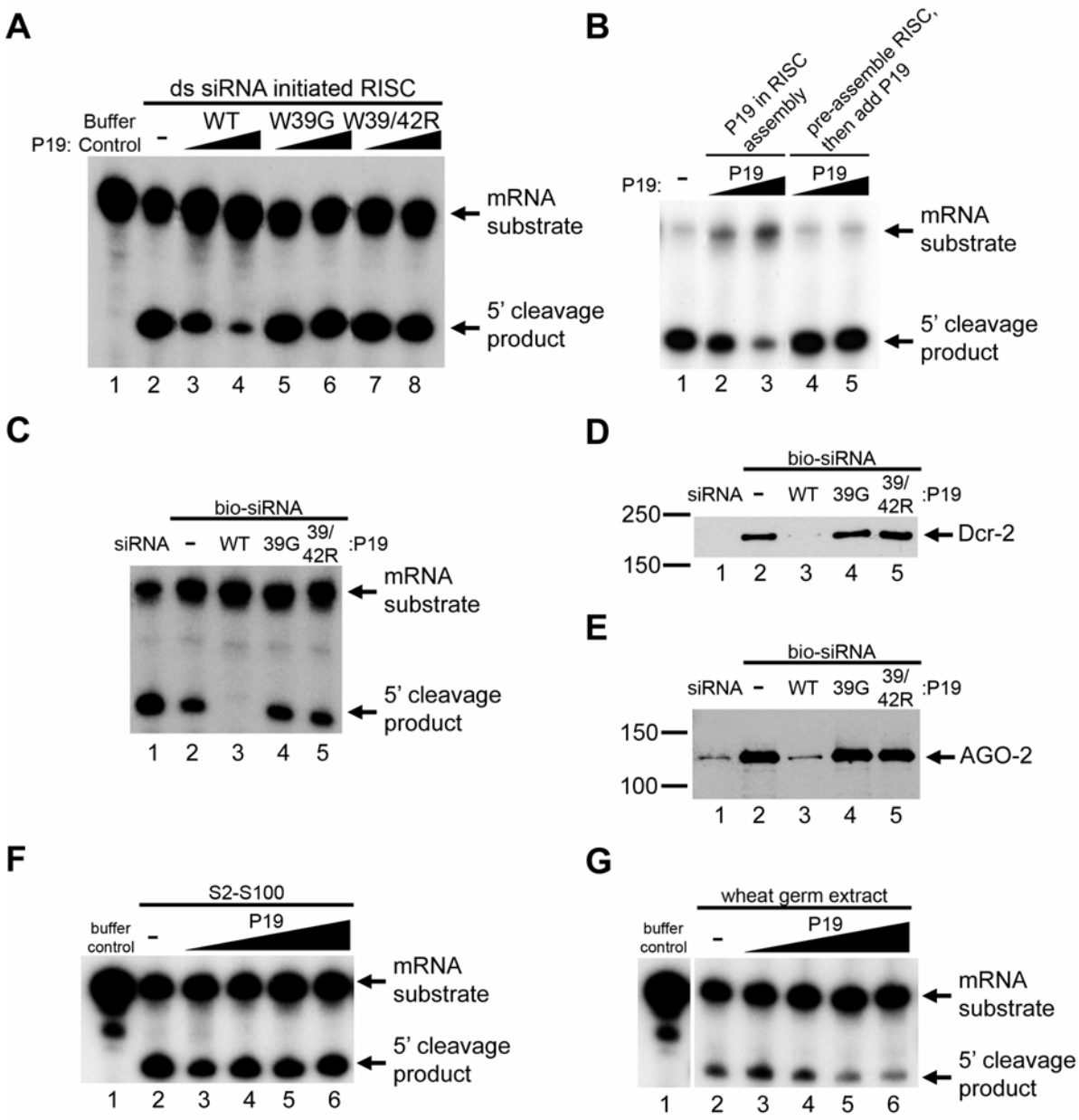

Figure 2.3. Recombinant p19 inhibits RISC assembly in the siRNA pathway, but it does not affect RISC cleavage. (A) Two different amount (1ng and 10ng respectively) of WT p19 (lane 3, 4), W39G (lane 5, 6) or W39/42R (lane 7, 8) mutants, were added to S2 cell extract in double-stranded siRNA initiated RISC assay. **(B)** RISC assay was done in a two-step fashion: first RSIC assembly step, with everything but mRNA substrate added, incubated for 30 minutes; second RISC cleavage step with mRNA substrate added, incubated for another 30 minutes. "p19 in RISC assembly" indicates p19 was added in the first RSIC assembly step (lane 2 and 3), while "pre-assemble RISC, then add p19" indicates p19 was not added until the second RISC cleavage step (lane 4 and 5). **(C-E)** RISC reactions were performed with unmodified siRNA (lane 1) or biotinylated siRNA (lane 2) in S100, with WT p19 (lane 3), W39G mutant (lane 4), or W39/42R mutant (lane 5). In lane 3-5, the amount of p19 used is 10ng in a 10μl reaction. **(C)** RISC assay showing the biotinylated siRNA functions as efficiently as unmodified siRNA. **(D & E)** The biotinylated

siRNA and associated proteins were precipitated by streptavidin beads, resolved by SDS-PAGE, and Western blotted for Dcr-2, shown in panel D. The same membrane was Western blotted for AGO2, shown in panel E. **(F)** Increasing amount (3ng, 10ng, 30ng, and 100ng respectively) of WT p19 was added to S2 cell extract in a 10µl sense let-7 initiated RISC reaction. **(G)** Four different doses (1ng, 3ng, 10ng, and 100ng respectively) of WT p19 were added to wheat germ extract in sense let-7 initiated RISC assay.

assay in the wheat germ extract (Fig. 2.3.G, lane 2). Though 100ng of p19 slightly decreased the activity (Fig. 2.3.G, lane 6), the effect was not as significant as the degree of inhibition seen in the siRNA initiated RISC activity. Therefore, the data from fly and plant extracts were generally consistent.

In summary, the combined results strongly support the hypothesis that p19 suppresses RNA silencing by sequestering double-stranded siRNA, thus preventing the active silencing effecter formation.

p19 inhibits miRISC assembly by preventing miRNA duplex from loading onto RISC

Compared to worm and mammalian RNAi machineries, the Drosophila system is unique because the existence of two Dicers instead of one, making the siRNA and miRNA pathways diverge at both the initiation and effector steps (Liu et al., 2003). In the initiation process, Dcr-1 generates miRNA, while Dcr-2 processes long dsRNA. I have shown that p19 also inhibits the pre-miRNA initiated RISC activity (Fig. 2.1.C), and I would like to determine at what step p19 inhibits the miRNA pathway.

I first examined the initiation step – miRNA biogenesis. Recombinant p19 increased the production of miRNA in S2 cell extract (Fig. 2.4.A, lane 2-6), while it

had no effect on recombinant Dcr-1/Loqs-PB catalyzed reaction (Fig. 2.4.A, lane 7-11), indicating the stability of miRNA was increased rather than the catalytic activity of the Dicer enzyme being enhanced. To directly test whether the stability of miRNA duplex was changed in the presence of p19, the remaining signals from radiolabeled let-7/let-7* duplex were compared after incubation in S2 cell extract with or without p19 at different time points (Fig. 2.4.B). The presence of p19 significantly enhanced the stability of let-7/let-7* duplex, changing from 30% remaining to 60% after 30 minutes incubation (Fig. 2.4.C).

The finding that p19 stabilized miRNA duplex suggests p19 may affect miRNA duplex initiated RISC activity. Indeed, I observed an inhibition pattern similar to siRNA initiated RISC activity (Fig. 2.4.D). To determine whether p19 targets miRISC assembly, the two step RISC reaction was performed again except using miRNA duplex as the trigger. Similar results were obtained: inhibition was observed only when p19 was added in the assembly process (Fig. 2.4.E), suggesting that p19 also prevents active miRISC formation, but not the cleavage step.

To further test if p19 inhibits miRISC at the cleavage step, I took advantage of the endogenously programmed miRISC. Bantam is one of the miRNAs that express in Drosophila S2 cells (Brennecke et al., 2003). When an mRNA that is perfectly matched to bantam was added to S2 cell extract, p19 failed to inhibit the cleavage activity from endogenous bantam RISC (Fig. 2.4.F), confirming that it does not affect the cleavage step. Next, I wanted to examine the effect of p19 in plant system. It has been shown that miR165 or miR166 was present in wheat germ extract.

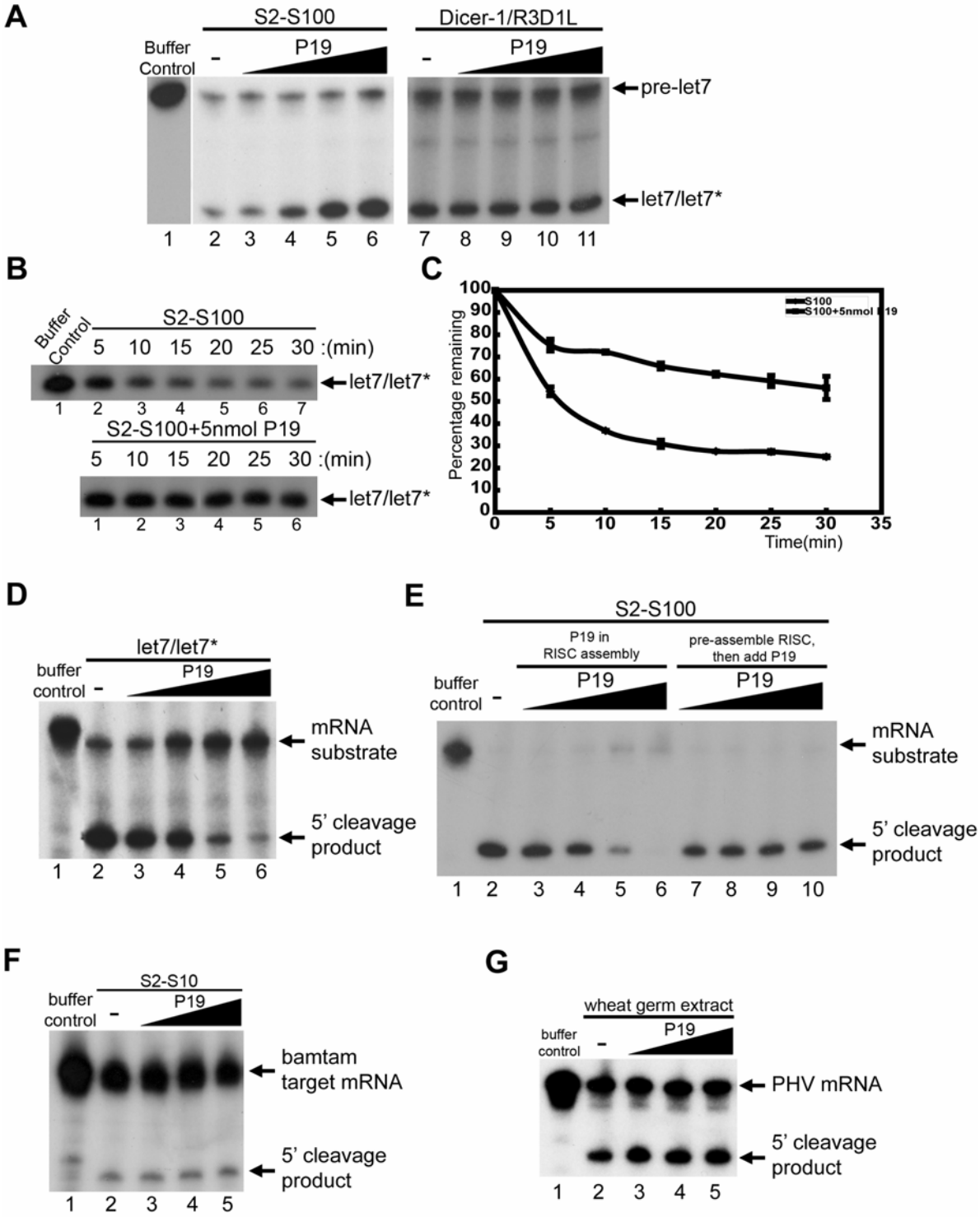

Figure 2.4. p19 inhibits miRISC assembly by preventing miRNA duplex from loading onto RISC. (A) Pre-miRNA processing assay in S2 cell extract or recombinant Dcr-1/Loqs-PB (R3D1L) complex. Increasing amount (3ng, 10ng, 30ng, and 100ng respectively) of p19 was added to a 10µl reaction. **(B & C)** The stability of let-7/let-7* duplex in S2 cell extract with or without 100ng of p19. Let-7 sense strand was radiolabeled at the 5' end and then annealed with let-7* to make a miRNA duplex. The duplex was incubated in S2 cell extract in the indicated time course, purified, and

resolved by urea-PAGE, shown in panel B. The experiment was done three times, each time quantitated by phosphor-imager, and the average values and standard deviations were obtained and plotted on a chart, shown in panel C. **(D)** RISC assay was done in S2 cell extract with p19 using let-7/let-7* duplex as trigger. Increasing amount (3ng, 10ng, 30ng, and 100ng respectively) of p19 was added to a 10μl reaction (lane 2-6). **(E)** RISC reaction was performed in a two-step fashion: first RSIC assembly step, with everything but mRNA substrate added, incubated for 30 minutes; second RISC cleavage step with mRNA substrate added, incubated for another 30 minutes. "p19 in RISC assembly" indicates p19 was added in the first RSIC assembly step (lane 2-6), while "pre-assemble RISC, then add p19" indicates p19 was not added until the second RISC cleavage step (lane 7-10). Same doses of recombinant p19 were added as in panel D. **(F)** Endogenous RISC programmed with bantam miRNA from S2 cell extract was assayed for cleaving an artificial mRNA containing perfect complementary sequence to bantam. Increasing amount (10ng, 30ng, and 100ng respectively) of p19 was added to a 10μl reaction (lane 3-5). **(G)** Endogenous RISC programmed with miR165/166 from wheat germ extract was assayed for cleaving PHV mRNA. Same doses of recombinant p19 were added as in panel F.

These two miRNAs only differ in a single C to U transition, and the difference was so small that it could not be distinguished by Northern hybridization (Tang et al., 2003). An endogenous miRISC programmed by miR165/166 from wheat germ extract can direct sequence specific cleavage of the Arabidopsis PHAVLUTA (PHV) mRNA (Tang et al., 2003). The DNA template for transcribing PHV RNA was generously given by Dr. Guiliang Tang (University of Kentucky, Lexington, KY). Comparably, p19 did not affect the cleavage activity of this endogenous miRISC in wheat germ extract (Fig. 2.4.G), supporting the finding in fly extract that p19 suppresses active miRISC assembly by preventing the loading of miRNA, and it does not inhibit the cleavage step of an endogenously pre- assembled miRISC.

Discussion

In this study, I examined the molecular mechanism of the plant viral suppressor

p19 in the *Drosophila in vitro* assay systems. The findings were consistent with the results from the available assays done in wheat germ extract. I discovered that p19, previously shown in plants to bind siRNAs both *in vivo* and *in vitro*, also mediates suppression of RNAi activity in *Drosophila* extracts. Through step by step examination of the siRNA pathways in Drosophila, I pinpointed the exact mechanism by which p19 suppresses siRNA machinery. I also provided direct evidence that p19 suppresses miRNA directed RISC activity. In both pathways, p19 prevents the active formation of RISC complexes, by targeting siRNA and miRNA duplexes, both of which are conserved intermediates in fly and plant RNAi pathways. Thus, p19 provides an example of utilizing a heterologous system to analyze the biochemical mechanism of suppressors that target the conserved elements of the RNAi machinery.

Mechanism of p19 mediated suppression of siRISC activity

p19 is a high affinity ds siRNA binding protein (Vargason et al., 2003; Ye et al., 2003). This led to a competitive inhibition hypothesis in which p19 interferes with active RISC formation by sequestering siRNAs (Lakatos et al., 2004). Taking advantage of various *in vitro* tools available in *Drosophila*, I tested this model using S2 cell extract and recombinant enzymes. As expected, p19 inhibits long dsRNA and siRNA induced RISC cleavage in S2 extract. Moreover, the inhibition mechanism lies in the RISC assembly process. By competitive binding of siRNA between p19 and Dcr-2/R2D2 complex, I discovered that the affinity of p19 to siRNA is almost 10 fold higher than Dcr-2/R2D2, showing the physiological advantage of virus over host

proteins.

Since some plant viral suppressors such as Cucumovirus 2b protein target more than one event to counteract RNAi activity (Scholthof, 2007), we would like to know whether p19 has other functions as well. However, my experiments demonstrate that p19 does not alter the enzymatic activity of both Dicers in *Drosophila*, nor does it interfere with ssRNA programmed RISC or endogenous RISC cleavage activity in both fly and plant extract. Therefore, at least in the fly system, p19 strictly targets a specific process – sequestration of siRNAs (Fig. 2.5).

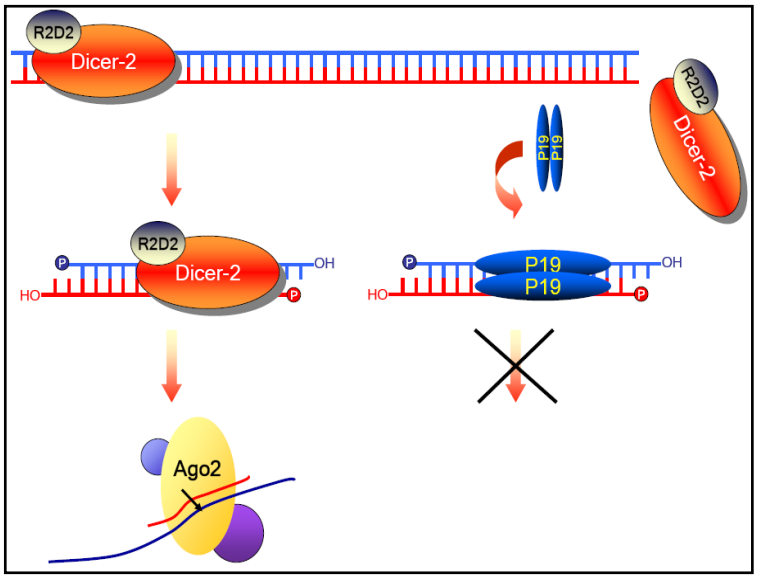

Figure 2.5. The sequestration model of p19 action in siRNA pathway. In Drosophila cells, the Dcr-2/R2D2 complex not only processes long dsRNA, but binds the siRNA product. p19 out-competes with Dcr-2/R2D2 complex so that no active siRISC is formed, thus, there is no RNAi activity.

Mechanism of p19 mediated suppression of miRISC activity

miRNAs are structurally similar to siRNAs. Both of them have a length of 21-25nt, and a 5' phosphate and 3' hydroxyl termini. However, different from siRNA, miRNA is generated from imperfect base paired hairpin precursors. Consequently, miRNA duplexes contain mismatches, bulges, or G:U wobble base pairs. It was not

previously known whether p19 would recognize imperfect complementary dsRNA. In S2 cells, miRNA duplexes are short-lived species, vulnerable to degradation in the abundant presence of nucleases. Stabilization of let-7/let-7* was observed in S2 cell extract with p19, suggesting p19 could also bind to miRNA duplex. This result is consistent with the Carrington group's finding that miRNA and miRNA* accumulate in transgenic Arabidopsis plants expressing p19 (Chapman et al., 2004). They have also shown a direct physical interaction between p19 and miRNAs by co-IP experiment (Chapman et al., 2004).

I have also discovered that p19 inhibited RISC activity when pre-miRNA was used as trigger. Carrington group has also reported that miRNA-guided cleavage of target mRNAs was decreased in transgenic Arabidopsis plants expressing p19 (Chapman et al., 2004). My observation suggests that p19 does not directly interfere with the enzymatic activity of the pre-miRNA processing machinery Dcr-1/Loqs-PB

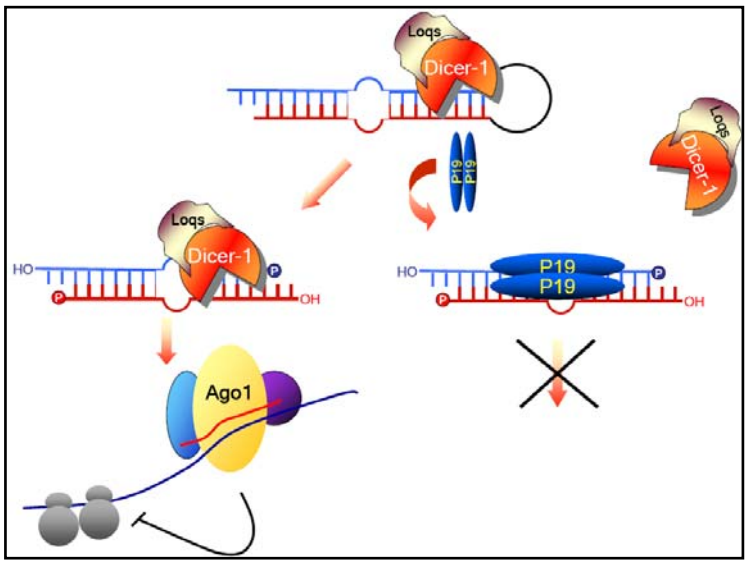

Figure 2.6. The sequestration model of p19 action in miRNA pathway. In *Drosophila* cells, the Dcr-1/Loqs complex not only processes pre-miRNA, but binds the product miRNA duplex. p19 replaces the Dcr-1/Loqs complex so that no active miRISC is formed.

or the RISC machinery, by sequestration of the miRNA duplex intermediate, it inhibits the assembly of active RISC (Fig. 2.6). This is similar to the parallel siRNA pathway.

In summary, the data obtained from *in vitro* studies in *Drosophila* system were in line with findings in plants, and could help us to understand the biochemical role played by p19 in compromising RNA silencing in plants. The sequestering mechanism may be applied to other dsRNA binding viral suppressors, such as p21 from Beet yellows virus (Reed et al., 2003). However, we must recognize the limitation of employing the fly system to study plant problems because there are significant differences between the two systems, such as lack of two distinct classes of siRNAs and RdRP mediated amplification of RNAi process. Another important lesson learned from this heterologous analysis is that as a potent ds small RNA binding protein, p19 could be explored as a useful tool to interfere with any regulatory pathways that involves ds siRNA like molecules in other organisms.

Chapter III

In vitro reconstitution of the siRNA pathway

Abstract

In vitro reconstitution allows for dissection of the RNAi machinery in a well-defined system and provides greater understanding of the mechanisms and regulations of the RNAi pathway. In *Drosophila*, the Dcr-2/R2D2 complex initiates RNAi by processing dsRNA into siRNA. Both proteins are required for incorporating siRNA onto the siRISC complex. Only the Dicer-2/R2D2 complex, but neither Dicer-2 nor R2D2 alone, efficiently interact with duplex siRNA. AGO2 is the main component of siRISC and generation of recombinant AGO2 is essential for *in vitro* reconstitution of the RNAi pathway. I have generated an active truncated AGO2 recombinant protein by removing some polyQ regions which are expressed at a higher level than the full length protein. Co-expression with AGO1 increased the expression level of AGO2 by at least 10 fold. Affinity purified full length and the truncated form of AGO2 showed minimal RISC activity, i.e. could be programmed with single-stranded siRNA and perform sequence specific cleavage of mRNA. Most interestingly, adding purified recombinant Dcr-2/R2D2 complex to recombinant AGO2 generates dsRNA and siRNA initiated RISC activity. Catalytic mutant of AGO2 is unable to reconstitute RISC activity with recombinant Dicer-2/R2D2 complex, suggesting that the RISC activity is specific. Therefore, I have shown that the three component system, Dcr-2, R2D2, and AGO2, are necessary and sufficient to reconstitute the RNAi pathway of *Drosophila*.

Introduction

In general, the siRNA pathway can be initiated by processing long dsRNA into small interfering RNA (siRNA). siRNAs are 21–25 nucleotide (nt) duplexes with 5' phosphate and 2 nt overhang at 3' hydroxyl termini (Tomari and Zamore, 2005). Nascent siRNA is incorporated into the RNA-induced silencing complex termed siRISC. The effector RISC complexes contain single-stranded siRNA as guide RNA for sequence-specific cleavage of complementary mRNA (Martinez et al., 2002).

siRNAs are generated by Dicer, a family of large multidomain RNase III enzymes (Bernstein et al., 2001). Our group has previously purified this siRNA-generating enzyme from *Drosophila* S2 cells and found that it consisted of Dcr-2 and a previously unknown protein that we named R2D2 (Liu et al., 2003). R2D2 contains tandem dsRNA-binding domains (R2) and forms a heterodimeric complex with Dcr-2 (D2). R2D2 is homologous to the *Caenorhabditis elegans* RNAi protein RDE-4. Recent biochemical studies suggest that the Dcr-2/R2D2 complex also binds duplex siRNA, forms the RISC loading complex (RLC), and facilitates the transfer of siRNA onto Ago2, the catalytic component of siRISC (Liu et al., 2003; Pham et al., 2004; Tomari et al., 2004b). We previously employed an *in vitro* fractionation and reconstitution assay in partially purified extract to demonstrate that recombinant Dcr-2/R2D2 complex enhances incorporation of siRNA into the effector siRISC complex (Liu et al., 2003). Furthermore, photocross-linking experiments suggest that R2D2 preferentially binds the more stable end of siRNA, whereas Dcr-2 is often found at the less stable end (Tomari et al., 2004b). Thus, R2D2 could serve as

the sensor for the thermodynamic asymmetry of siRNA, thereby orienting Dcr-2 to the end that is easier to unwind.

In our previous study, we had difficulty in obtaining recombinant R2D2 alone because it was insoluble when expressed in insect cells (Liu et al., 2003). By gaining soluble maltose-bind protein (MBP)-R2D2 fusion protein, I was able to examine the detailed mechanism of R2D2 in the process of loading siRNA onto the siRISC complex through gel mobility shift assays. The function of predicted tandem dsRNA-binding domains of R2D2 was also examined.

One main component in the RISC complex was discovered to be Argonaute family of proteins (Hammond et al., 2001). Structural analysis revealed that the PIWI domain of Ago resembles the structure of RNase H. However, different from RNase H, it utilizes RNA instead of DNA as the guiding strand (Song et al., 2004). Recombinant human Ago2 functions as a minimal RISC that can be programmed with a single-stranded siRNA and cleave the target mRNA (Rivas et al., 2005). In *Drosophila*, both biochemical and genetic studies have shown that AGO2 is the catalytic component of siRISC (Hammond et al., 2001; Miyoshi et al., 2005; Okamura et al., 2004; Rand et al., 2004). Both strands of siRNA get loaded onto RISC and the passenger strand is cleaved in an AGO2-dependent manner, thereby liberating the single-stranded guide (Matranga et al., 2005; Miyoshi et al., 2005; Rand et al., 2005). This passenger strand cleavage event is only one of the mechanisms for loading siRNA onto AGO2 because siRNA bearing non-cleavable passenger strand is still able to trigger RISC cleavage (Matranga et al., 2005; Rand et al., 2005).

So far, all studies of siRISC assembly process were carried out in cell extracts or with immunoprecipitated endogenous complexes and the activity could only be correlated with the associated proteins. Without total *in vitro* reconstitution, the exact molecular mechanism remains unclear. The minimal reconstituted system will also enable us to identify regulators of the RNAi pathway by "biochemical supplementation". To reconstitute the siRNA pathway *in vitro*, generation of recombinant AGO2 is essential. Though previous efforts to generate full-length Ago2 were not successful (Rand, T. unpublished data), I was able to develop an expression and purification system to obtain recombinant AGO2. Here I show that it is possible to *in vitro* reconstitute the Drosophila siRNA pathway entirely from recombinant proteins.

Materials and Methods

Purification of recombinant Dcr-2 and R2D2 proteins

Polyhistidine-tagged recombinant Dcr-2 and Dcr-2/R2D2 complex were produced and purified from insect cells as previously described in Chapter II. The R2D2 open reading frame (ORF) was cloned as an NcoI-NotI fragment into pMBP-parallel vector. The maltose-binding protein (MBP)-R2D2 fusion protein was produced in *E. coli* BL21 strain. After the BL21/pMBP-R2D2 culture reached OD600 of ~0.8 at 37 ºC, IPTG was added to 1 mM to induce expression of MBP-R2D2 for 5 hour at 25ºC. Cells were lysed by sonication in Buffer T (100 mM Tris-HCl, pH 8.0, 50 mM NaCl, 5 mM-mercaptoethanol) freshly supplemented with complete protease

inhibitor cocktail (Roche). MBP-R2D2 proteins were purified using an Amylose-Agarose column (NEB) followed by SP- and Q-Sepharose chromatography. Mutant MBP-R2D2 constructs were generated by Quikchange mutagenesis (Stratagene) and the proteins were expressed and purified as described above.

Cleavage of MBP-R2D2 by thrombin protease

Biotinylated human thrombin, cleavage buffer, streptavidin agarose beads, and spin filters were supplied by the Thrombin Cleavage Capture Kit (Novagen). 1 mg of MBP-R2D2 was incubated with 10 units of biotinylated thrombin in a total volumn of 500 μl at 4ºC overnight. Because some protein precipitated during the incubation, the mixture was spun at 13,000 rpm at 4ºC for 15 minutes. After washing 100 μl streptavidin beads with cleavage buffer for three times, the supernatant was added to beads, and the mixture was rotated at 4ºC for 1 h. The mixture was transferred onto a spin filter and was spinned at 5000 rpm at 4 ºC for 3 minutes. The flow through was collected and it contained free MBP and R2D2 proteins.

Poly I:C agarose beads pull down

Poly (inosine) (I): poly (cytosine) (C) dsRNA-conjugated agarose beads (GE) were washed three times with binding buffer (100 mM KOAc, 15 mM HEPES, pH 7.4, 2 mM $Mg(OAc)_2$, and 5 mM DTT). 32.5 μg of MBP-R2D2 WT or mutants was incubated with 20 μl of poly I:C beads at 4 ºC for 2 hrs. After washing the beads with binding buffer for three times, the beads were resupended in 2×SDS loading buffer

and loaded onto a SDS-PAGE.

The gel was stained by Coomassie Brilliant Blue (Bio-Rad).

Cloning of recombinant AGO2

Total RNA was isolated from 4 × 10^6 S2 cells by TRIzol (Invitrogen). RT-PCR reactions were performed using the SuperScript III reverse transcriptase (Invitrogen). In brief, the RT-PCR reaction was set up as follows: 1 μg RNA was used in a 20 μl reaction of reverse transcription, and 1 μl of the RT product was used in a 25 μl PCR reaction. The Expand High Fidelity PCR System (Roche) was used. The cDNAs of full length and truncated AGO2 were amplified using the same reverse primer 5'-GCGGCCGCTCAGACAAAGTACATGGGGTTTTTC-3'. The forward primers include: 5'-CATATGGGAAAAAAAGATAAGAACAAG-3' for full length PB isoform (3.65 kb); 5'- CATATGCACTTTCCAATTACCACCCCAG-3' for full length PC isoform (3.65 kb); 5'-CTCGAGCAGCAAGGAGGCCAACAGCAAAAATC-3' for truncated A form (3.4 kb); 5'-CTCGAGCAACAACAAGGTGGCCATG-3' for truncated B form (2.8 kb); 5'- CTCGAGCAACCAAACCAAACCCAGAGCC-3' for truncated C form (2.45 kb).

D965A mutant AGO2 was generated by Quikchange (Stratagene) using the following two primers: 5'-CATGTACATTGGAGCCGcTGTGACCCATCCCTCTC-3' and 5'-GAGAGGGATGGGTCACAGCGGCTCCAATGTACATG-3'.

All sequences were cloned as SalI-NotI fragments into pFastBac-HT C vector (Invitrogen). To produce N terminal His/Flag double tagged AGO2 constructs, an annealed oligo pair encoding 3× Flag peptide sequence was phosphorylated by T4 polynucleotide kinase (NEB) and ligated to NcoI-StuI-cut pFB-HT constructs. The two primers used are: 5'-CATGGACTACAAAGACGATGACGACAAGGGCGGAG-3', and 5'-CTCCGCCCTTGTCGTCATCGTCTTTGTAGTC-3'.

Cloning of heat shock proteins

The RT-PCR was done as described in the preceding paragraph. The primers used for amplifying Hsc70-4 are: 5'- CATATGTCTAAAGCTCCTGCTGTTG-3' and 5'-GCGGCCGCTTAGTCGACCTCCTCGATGGTG-3'. The primers used for amplifying Hsp83 are: 5'- CATATGCCAGAAGAAGCAGAGACCTTTG-3' and 5'-GCGGCCGCTTAATCGACCTCCTCCATGTGGGAAGC-3'.

Expression test of baculoviruses

In each well of 24-well plate, 0.6 × 10^6 Sf9 cells (Invitrogen) were plated with 0.4 ml of Sf-900 II SFM medium (Invitrogen) with 1:200 antibiotic-antimycotic (Invitrogen). 2 μl of AGO2 viruses (full length or truncated) and 1 μl of all other viruses including Dcr-2, R2D2 and AGO1 viruses were added into each well. The cells were infected for 45-60 hrs and then lysed in 400 μl of 1×SDS sample buffer.

Antibodies

The commercial antibodies used were: monoclonal anti-His (Sigma), polyclonal anti-GST (GE), monoclonal anti-Flag (Sigma), respectively.

Expression and purification of recombinant AGO2

Sf9 cells were grown to 2.5 $\times$ 10^6 density before baculovirus infection. For one preparation, at least 2 L of cells were needed. Cell pellet must be prepared within two-week after harvest. His-tagged or His/Flag-tagged AGO2 (full length or truncated) virus was added to Sf9 cells at 1:100 ratio. For co-expression, Dcr-2 virus was added at 1:300 ratio, R2D2 virus was added at 1:600 ratio, and GST tagged AGO1-M virus was added at 1:400 ratio. After 57-63 hrs infection, the Sf9 cells were harvested, washed in PBS, and lysed by 40 strokes with a douncer in buffer T containing 20 mM imidazole with protease inhibitors. Each S20 lysate was incubated with 0.5 ml Ni-NTA beads (Qiagen) at 4°C for at least 4 hrs or up to overnight. The mixture was then loaded onto an empty chromatography column (Bio-Rad), and washed sequentially with buffer T containing 20 mM imidazole (NO salt allowed!). After a buffer T with 50 mM imidazole wash, His-tagged AGO2 was eluted in 2 ml buffer T containing 250 mM imidazole. The elution was stored in aliquots at –80ºC in 10% glycerol.

For His/Flag double tagged AGO2 proteins, the 2 ml Ni elution was incubated with 100 μl of Flag beads (Sigma) at 4°C for at least 4 hours. The Flag beads were washed five times with buffer T (NO salt allowed!) and then eluted in 200 μl buffer T

with 500 ng/μl 3× Flag peptide (Sigma). The Flag elution was stored in aliquots at –80ºC in 10% glycerol. Notably, protein prep stored at –80ºC for more than one month lost RISC activity.

Viral Plaque Assay

1×10^6 Sf9 cells were plated with 2 ml of Sf-900 medium with 1:200 antibiotic-antimycotic into each well of 6-well plates. Let the cell adhere for 1 h in the 28ºC incubator, during which time serial dilutions of virus were made. The parental viral pool was diluted to 10^{-5}, 10^{-6} and 10^{-7} concentrations in 5ml of Sf-900 medium with 1:200 antibiotic-antimycotic. Following the 1 h incubation to adhere cells, except the negative control well, medium was removed from the wells and replaced with 1 ml of virus dilution. For each dilution, two duplicate wells were used. Let the virus infect cells for 1 h in the 28ºC incubator. During the 1 h incubation, 4% Agarose Gel (Invitrogen) was microwaved to melt and then cooled to 40ºC in a 40ºC water bath, during which time Sf-900 medium (1.3×) was warmed to 40ºC. Plaquing medium was made by mixing 1 volume of the melted 4% Agarose Gel with 3 volumes of Sf-900 medium (1.3×) and kept at 40ºC.

Following the 1 h incubation, plaquing medium was placed in a little beaker filled with water/ice until it reached ~room temperature. Starting from the highest dilution, the virus was removed from the wells and replaced with 2 ml of plaquing medium. The step must be done quickly to avoid dessication of the cell monolayer and solidification of plaquing medium. The plates were left in the hood to let plaquing

medium solidify. 0.2 ml of Sf-900 medium with 1:200 antibiotic-antimycotic was added to each well to prevent agarose from drying.

The plates were incubated in the 28ºC incubator for 7-10 days until plaques were visible. The positions of each plaque were marked under microscope and the plaques were taken up by glass Pasteur pipettes and resuspended in 1 ml of Sf-900 medium. After spinning at 5,000 rpm for 2 minutes, each supernatant was transferred to a 6-well plate with 1×10^6 Sf9 cells and 1 ml Sf-900 medium in each well. After incubation in the 28ºC incubator for ~7 days until the cells were mostly lysed, the viral clones were harvested.

RISC assays and gel mobility shift assays

The assays were done as previously described in Chapter II.

dsRNA processing assay

Uniformly radiolabeled dsRNA substrates were transcribed using α-^{32}P GTP (40 mCi/ml,MP), A/C/UTPs and Riboprobe® System-T7 Kit (Promega). In a 10 µl reaction, 1×10^5 cpm of α-^{32}P-labeled dsRNA and 1 mM ATP was incubated with extract in 100 mM KOAc, 15 mM HEPES, pH 7.4, 2 mM $Mg(OAc)_2$, and 5 mM DTT at 30 ºC for 30 minutes. The reaction is stopped by addition of 200 µl 0.3 M NaOAc, phenol/chloroform extracted, ethanol precipitated with glycogen as a carrier, resolved on a 16% denaturing (7 M Urea) PAGE and was directly exposed to X-ray film.

Glycerol Gradient Centrifugation

A 3 ml 10–30% glycerol gradient was prepared by Gradient Mixer. 300 µL of Ni elution of recombinant AGO2 was gently added on top of the gradient. The contents were centrifuged at 55,000 rpm at 4°C for 3.5 hours using an SW60Ti rotor (Beckman). Twelve fractions (275µL/fraction) were carefully taken from the top of the tube without disturbing the gradient and subsequently used for Coomassie blue staining or Western blotting to detect the presence of AGO2, or RISC assays.

Results

Dcr-2 and R2D2 coordinately bind the siRNA duplex

Previous biochemical studies have suggested that the Dcr-2/R2D2 complex binds the siRNA duplex, forms the RISC loading complex (RLC), and facilitates incorporation of siRNA into the siRISC complex (Liu et al., 2003; Pham et al., 2004; Tomari et al., 2004b). However, we could not determine if either R2D2 or Dcr-2 alone could bind the siRNA, because R2D2 was not soluble when expressed alone in insect cells. To get recombinant R2D2 without co-expression of Dcr-2, I expressed and purified recombinant MBP-R2D2 fusion protein alone in *E. coli* (Fig. 3.1.A, left lane). Fig3.1B shows the His-tagged recombinant Dcr-2 alone and Dcr-2/R2D2 complex from insect cells. Native gel mobility shift assays were performed by incubating the 5' radiolabeled synthetic siRNA duplex with recombinant R2D2, Dcr-2, or the Dcr-2/R2D2 complex proteins. As shown in Figure 3.1.C, although S100 and recombinant Dcr-2/R2D2 complex from insect cells showed binding of the probe

(lane1 and 2), neither Dcr-2 nor MBP-R2D2 alone could efficiently interact with siRNA in this assay. A distinct mobility shift was observed only when Dcr-2 and MBP-R2D2 were combined in the reaction (Fig. 3.1.C, lane 5). To determine whether it was the MBP-tag that the siRNA shift generated by Dcr-2/MBP-R2D2 was slightly higher than that of the Dcr-2/R2D2 complex (Fig. 3.1.C, lane 5), the MBP tag was cleaved by thrombin protease (Fig. 3.1.A, right lane). After cleavage, the shift generated by Dcr-2 plus R2D2 ran at the same position as that of the Dcr-2/R2D2 complex (Fig. 3.1.C, lane 6). These results suggest that Dcr-2 and R2D2 coordinately bind the siRNA duplex to promote assembly of the siRISC complex. Indeed, both Dcr-2 and R2D2 can be efficiently photocross-linked to radiolabeled siRNA by ultraviolet light (Liu et al., 2003; Tomari et al., 2004b).

Both dsRNA-binding domains of R2D2 are critical for siRNA binding

R2D2 contains two putative dsRNA-binding domains (dsRBDs) at the amino (N) terminus. To further analyze these domains, three mutant R2D2 proteins were generated by replacing two highly conserved alanine (A) residues with lysines (K) in the first (m1), second (m2), or both (dm) dsRBDs of R2D2 (Fig. 3.2.A). These mutant forms of R2D2 were also produced and purified as MBP fusion proteins from *E. coli*. To determine if these R2D2 mutants could bind long dsRNA, I used poly (inosine) (I):poly (cytosine) (C) dsRNA-conjugated agarose beads to pull down purified wild-type or mutant MBP–R2D2 proteins. As shown in Figure 3.2.B, while mutant 2 (M2) was precipitated as efficiently as wild-type R2D2, neither mutant 1 (M1) nor

double mutant (DM) could interact with long dsRNA. These results indicated that the

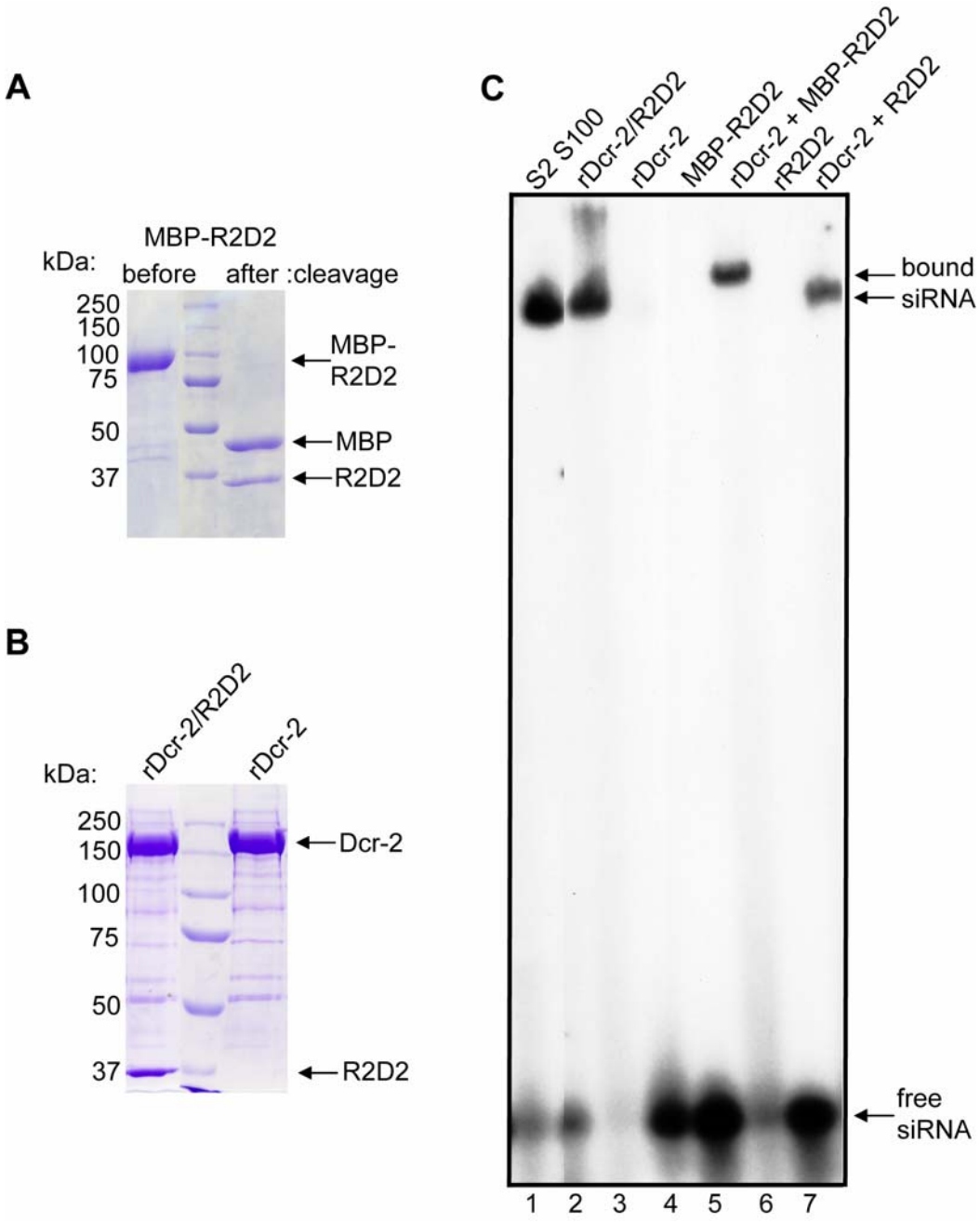

Figure 3.1 Dcr-2 and R2D2 Dcr-2 and R2D2 coordinately bind siRNA duplex. (A) A coomassie-stained SDS-PAGE gel showing purified recombinant MBP-R2D2 from *E. coli* (left) and free MBP and R2D2 after thrombin cleavage (right). **(B)** A coomassie-stained SDS-PAGE gel showing purified recombinant His-tagged Dcr-2/R2D2 complex (left) and Dcr-2 (right) proteins from insect cells. (C) The gel-shift assays were performed by incubating 5' radiolabeled siRNA duplex and 10 µg S2 S100 extract (lane 1), 10-pmol recombinant Dcr-2/R2D2 complex (lane 2), Dcr-2 (lane 3), MBP-R2D2 (lane 4), Dcr-2 + MBP-R2D2 (lane 5), R2D2 (lane 6), and Dcr-2 + R2D2 (lane 7). The arrowhead points to free siRNA. Two arrows refer to the Dcr-2/MBP-R2D2/siRNA and Dcr-2/R2D2/siRNA complexes, respectively.

first, but not the second, dsRBD of R2D2 was capable of binding long dsRNA. Alternatively, the second dsRBD of R2D2 might be covered by the C-terminal region of unknown function, thereby rendering it inaccessible to long dsRNA. However, the latter scenario was unlikely because the same results were obtained after removing the C-terminal 107 amino acids from wild-type and mutant MBP–R2D2 (data not shown).

To determine if either or both dsRBDs of R2D2 was necessary for siRNA binding, I performed siRNA gel mobility shift assays using wild-type or mutant MBP–R2D2 proteins alone or in combination with recombinant Dcr-2. Mutations in either dsRBD abolished the ability of MBP–R2D2 to cooperate with Dcr-2 for siRNA binding (Fig. 3.2.C, lanes 7-12). It should be noted that Dcr-2 interacted with mutant R2D2 proteins as efficiently as with wild-type control (data not shown) (Liu et al., 2003). Together, these results indicate that both dsRBDs of R2D2 are critical for the Dcr-2/R2D2 complex to bind and load siRNA onto the siRISC complex.

Generation of active recombinant AGO2

Drosophila AGO2 is distinct from other proteins of the *Drosophila* Argornaute/PIWI family in that it contains a unique poly glutamine (polyQ) repeat regions at the amino (N) terminus (Fig. 3.3). PolyQ regions have been implicated in neurodegenerative disease proteins such as Hungtingtin, where they trigger protein mis-folding and aggregation (Ross and Poirier, 2004). We hypothesize that the unique polyQ repeat region of fly Ago2 may be problematic for expression. After comparing the sequences among the N terminal polyQ regions of AGO2 orthologs from different *Drosophila*

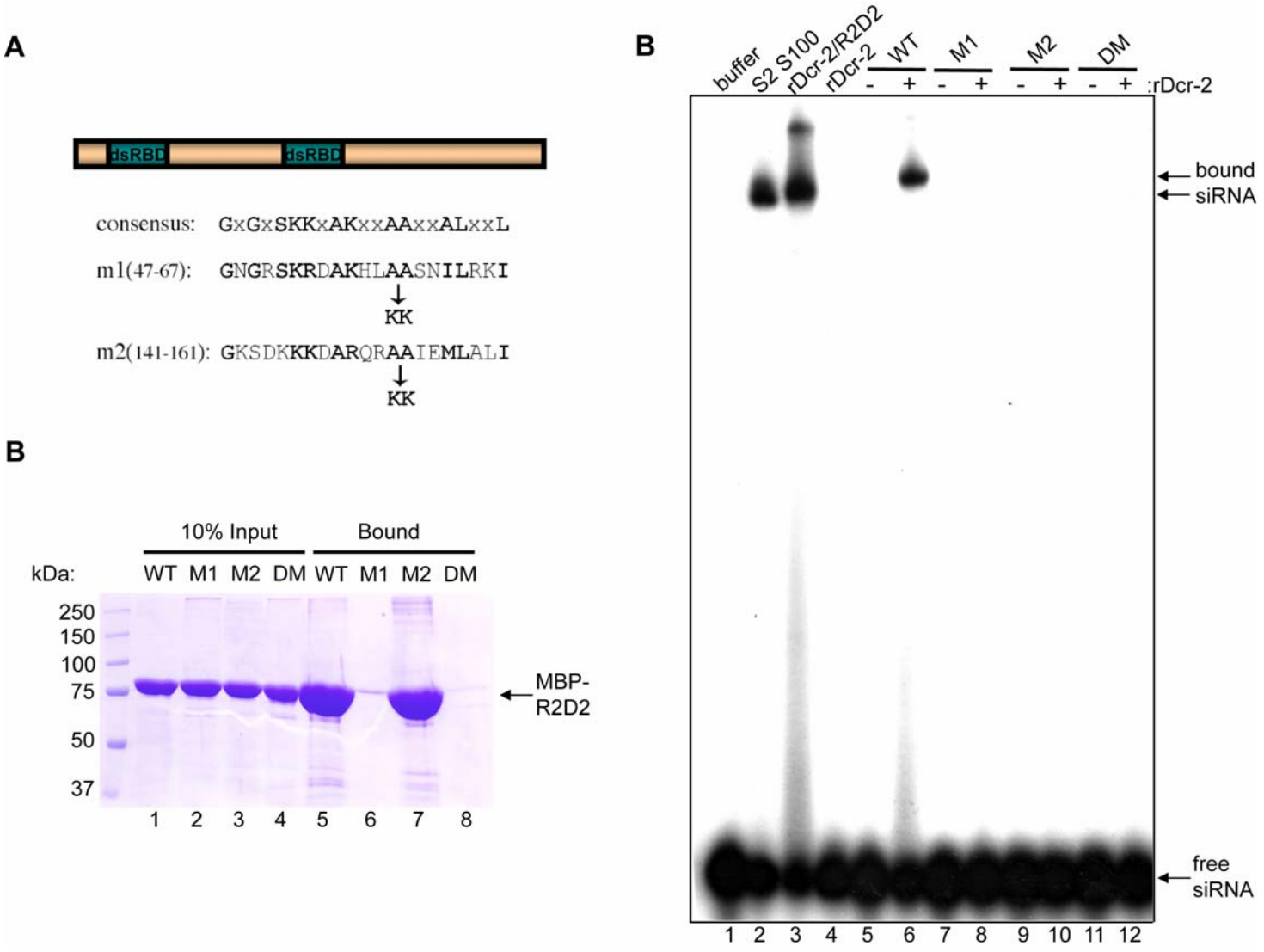
A
dsRBD
dsRBD
consensus: GxGxSKKxAKxxAAxxALxxL
m1(47-67): GNGRSKRDAKHLAASNILRKI
KK
m2(141-161): GKSDKKKDARQRAAIEMLALI
KK
B
10% Input
Bound
kDa:
WT M1 M2 DM WT M1 M2 DM
250
150
100
75
50
37
MBP-R2D2
1 2 3 4 5 6 7 8
B
buffer
S2 S100
rDcr-2/R2D2
rDcr-2
WT
M1
M2
DM
- + - + - + - + :rDcr-2
bound siRNA
free siRNA
1 2 3 4 5 6 7 8 9 10 11 12

Figure 3.2. Both dsRNA-binding domains (dsRBDs) of R2D2 are required for binding siRNA and promoting siRISC assembly. (A) A schematic diagram of R2D2 domain structure. Part of the consensus dsRBD motif was shown below. Two highly conserved alanine (*A*) residues were replaced by lysines (*K*) in the first (m1, A59–60K), second (m2, A153–154K), or both (dm, A59–60K, A153–154K) dsRBD of R2D2. **(B)** The poly (*I*): poly (*C*) long dsRNA-conjugated beads were used to precipitate purified wild-type (WT) and mutant MBP-R2D2 recombinant proteins. 10% input (lanes 1–4) and 100% bound proteins (lanes 5–8) were resolved by SDS-PAGE followed by coomassie staining. **(C)** The gel-shift assays were performed in buffer alone (lane *1*), 10 μg S2 S100 extract (lane 2), 10-pmol recombinant Dcr-2/R2D2 complex (lane 3), Dcr-2 (lane 4), 12.5-pmol wild-type MBP-R2D2 alone or with 3.5-pmol recombinant Dcr-2 (lane 5, 6), MBP-R2D2 mutant 1 alone or with Dcr-2 (lane 7, 8), MBP-R2D2 mutant 2 alone or with Dcr-2 (lane 9, 10), and MBP-R2D2 double mutant alone or with Dcr-2 (lane 11, 12).

species, it was found that *D. melanogaster* AGO2 contains the most extensive polyQ region (Meyer et al., 2006). Thus, I have generated a series of truncated Ago2 baculoviruses that remove some or all polyQ repeats of Ago2 according to cross species conservation (Meyer et al., 2006). Truncated A form starts before the long polyQ repeats and is missing the short polyQ repeats (Fig. 3.3). Truncated B form starts with the eighth long polyQ repeat, while truncated C form does not contain any polyQ region and starts from a highly conserved sequence “PAG…” according to Meyer et al., 2006 (Fig. 3.3). In the mean time, I also generated full length PB and PC alternatively spliced isoforms of AGO2, which only differ in the very end of N terminus, with first six amino acids specific for the PB form and first nine amino acids specific for the PC form (Fig. 3.3).

All five baculoviral forms of His-tagged AGO2 were produced and tested for expression. As shown in Fig. 3.4.B, the expression of full length and truncated forms were all detected by Western blot using an antibody against His, with truncated forms

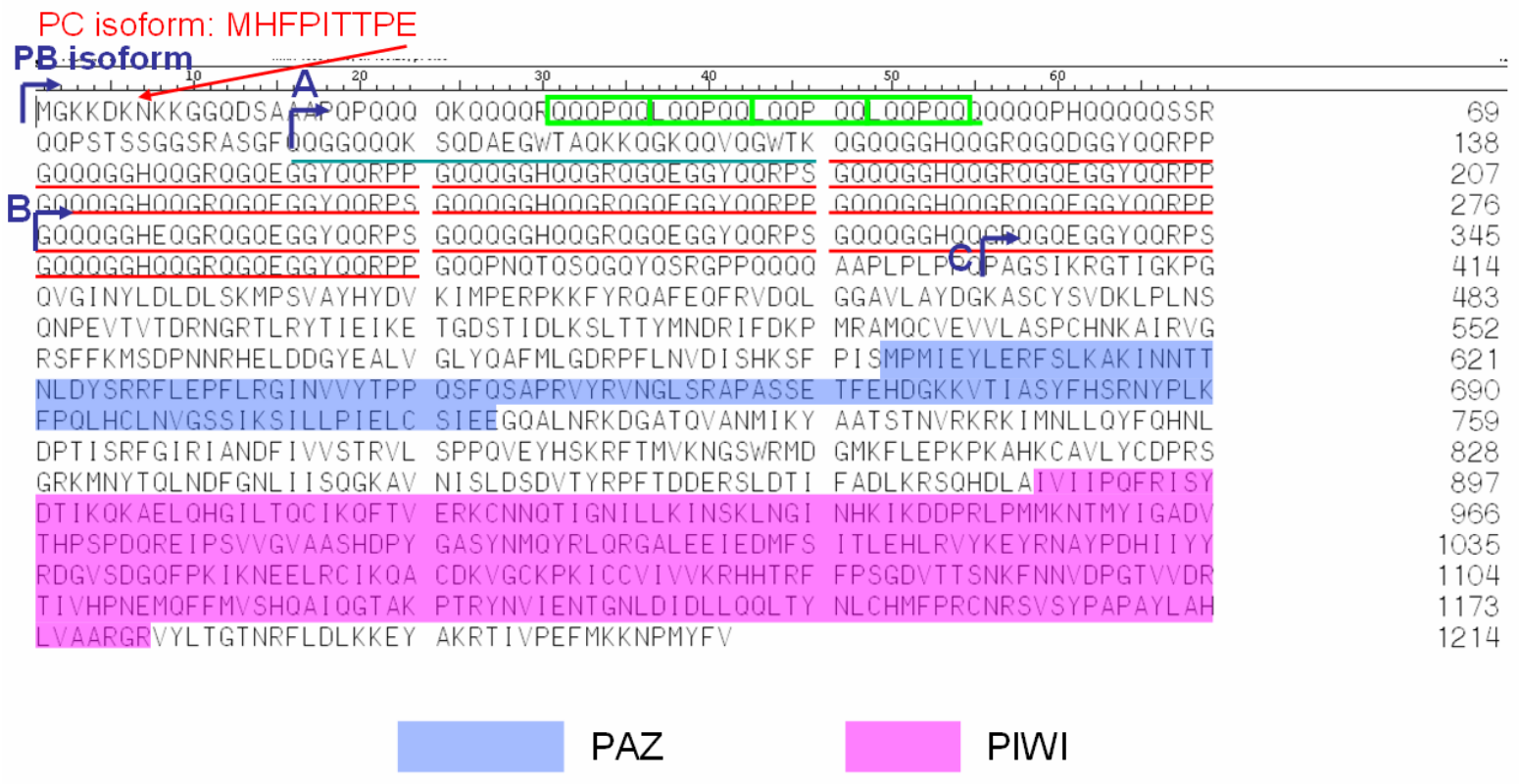

Figure 3.3. The protein sequence of *Drosophila* AGO2. The protein sequence of the PB isoform of AGO2 is shown with the PAZ domain in shaded blue and PIWI domain in shaded pink region. The PC isoform is essentially the same as the PB isoform except at the very end of the N terminus, replacing the first six amino acids of the PB form for the nine amino acids highlighted in red. The N terminus of AGO2 is composed of a short poly-glutamine (polyQ) region and a long polyQ region. The short poly Q region is highlight by green rectangle with 4 repeats of L(Q)QQPQQ sequence. The layout of the sequence is arranged in 23-character sequence blocking so that the 11 repeats (underlined in red) comprising the long polyQ repetitive sequence GQ(QG)QQGGHQ(E)QGRQGQEGGYQQRPP(S) can be best visualized. The letters A, B and C with arrows mark the translational start sites where the three truncated forms of AGO2 begin.

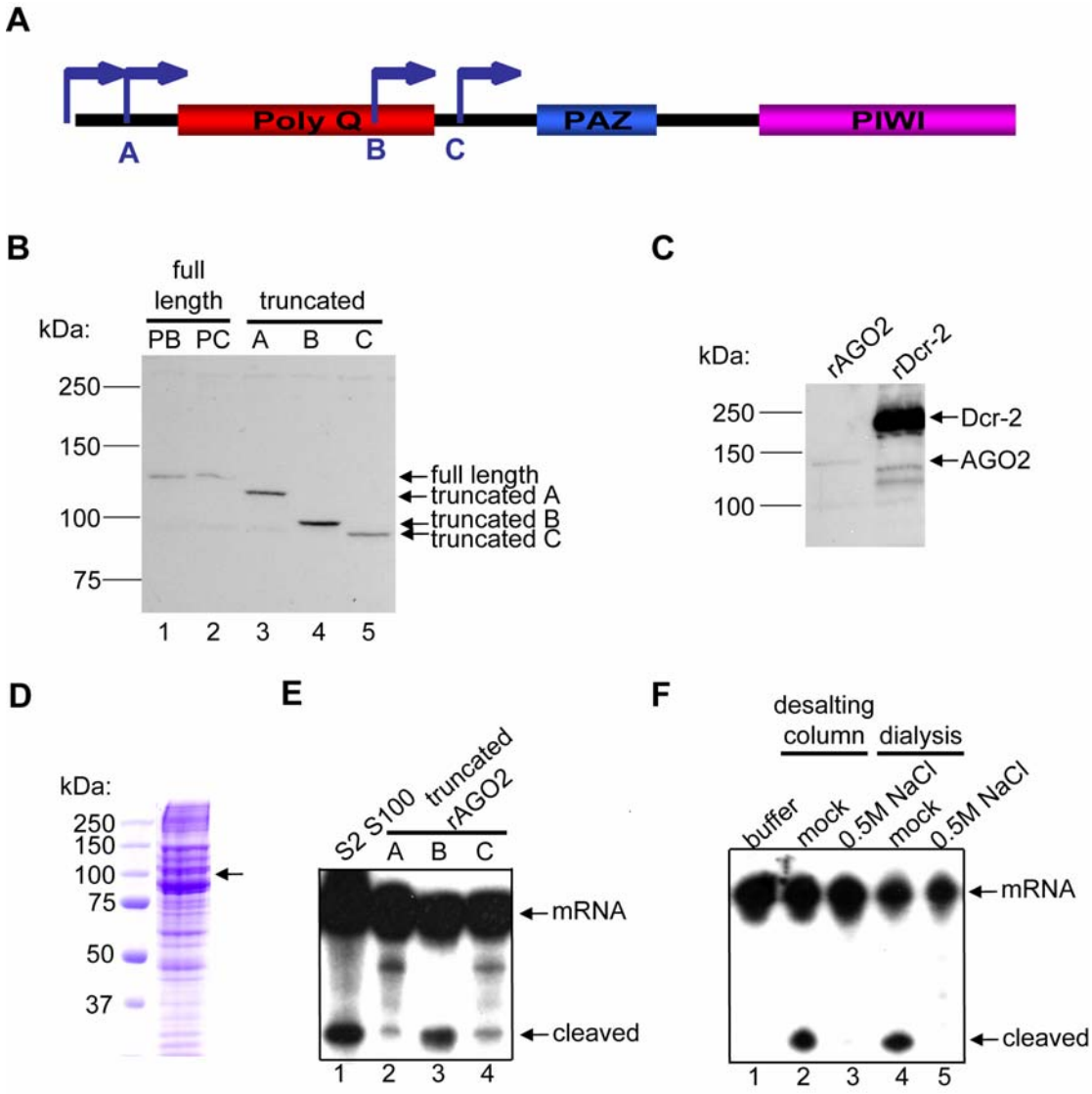

Figure 3.4. Difficulties in generating recombinant AGO2. (A) A schematic diagram showing the relative start positions of the truncated A, B, and C forms of AGO2. **(B)** Western blot using anti-His antibody to detect expression of various forms of His-tagged recombinant AGO2 in baculovirus Sf9 cell lysate. **(C)** Comparison of the expression level of recombinant full length PB form of AGO2 and Dcr-2, both of which are His-tagged, in Sf9 cell lysate. **(D)** A coomassie blue stained SDS-PAGE showing affinity purified recombinant truncated B form of AGO2. The arrow points to the relative molecular weight of the truncated AGO2 based on Western blot shown in panel B. **(E)** The single-stranded siRNA initiated RISC assays were performed with S2 S100 extract (lane 1), or 5 µl of affinity purified truncated A (lane 2), B (lane 3) or C (lane 4) form of AGO2. **(F)** Salt sensitivity of purified recombinant truncated B form of AGO2. The single-stranded siRNA initiated RISC assays were performed with no (lane 2) or high salt (lane 3) added recombinant AGO2 run through desalting column (Bio-Rad), or with no (lane 4) or high salt (lane 5) added recombinant AGO2 dialyzed. 5 µl of recombinant AGO2 was used.

expressing at higher level than full length (Fig. 3.4.B). However, when compared with Dcr-2, another His-tagged protein, the expression level of AGO2 was significantly lower and barely detected (Fig. 3.4.C).

Despite the low expression level, I expressed and purified the three truncated forms of AGO2 to test whether they possess slicer activity. From previous observation that high salt treatment irreversibly damaged pre-loaded siRISC (Rand et al., 2004), I did not use high salt wash during affinity purification of the recombinant proteins. Shown as an example in Fig. 3.4.D, the protein preparation of truncated B form of AGO2 was not pure and contained no distinguishable protein band at the predicted molecular weight of the recombinant protein (Fig. 3.4.D, arrow). Despite that, when a single-stranded siRNA was used as trigger in RISC reaction, a minimal RISC activity was detected in truncated B form of AGO2, while truncated A and C forms showed significantly lower activity (Fig. 3.4.E). The truncation in A and C form may disrupt protein folding and therefore interfere with activity. For simplicity, unless specified, truncated AGO2 refers to the B form. Though AGO2 has been implicated to be involved with the slicer activity of siRISC through partial biochemical purification and genetic studies (Hammond et al., 2001; Matranga et al., 2005; Okamura et al., 2004; Rand et al., 2004; Rand et al., 2005), this is the first time that recombinant AGO2 is obtained and shown to possess slicer activity *in vitro*.

To determine whether the salt-labile component of siRISC is AGO2, I performed salt sensitivity test for small aliquots of truncated recombinant AGO2. When 500 mM of NaCl was added and immediately removed via desalting column or dialysis, the

recombinant protein lost activity, while mock treated protein sustained activity (Fig.3.4.F, compare lanes 2 and 3, 4 and 5), indicating that the irreversible damage of RISC activity was brought by salt, not desalting procedure. Therefore, AGO2 is the salt sensitive component of siRISC.

Co-expression of AGO1 enhances the expression level of AGO2

An advantageous feature of the baculovirus expression system is that multiple proteins can be easily expressed at the same time by co-infection with multiple viruses. I tested whether co-expression of other known RNAi components would affect the expression level of AGO2. As shown in Fig. 3.5.A, co-expression of siRNA pathway components R2D2 and Dcr-2/R2D2 complex enhanced AGO2 expression (lanes 2 and 3). To our surprise, co-expression of miRISC component AGO1 enhanced AGO2 expression the most. Co-expression of other miRNA pathway components Dcr-1 and Loqs (please refer to Chapter IV for detailed discussion on Loqs) had no effect (data not shown). Because AGO1 also functions as a slicer (please refer to Chapter IV for detailed discussion on AGO1), to eliminate the slicer function contributed by AGO1, I tested the effect of catalytic dead mutant of AGO1 on AGO2 expression. Consistently, co-expression of AGO1 mutant (AGO1-M) increased AGO2 expression to a higher degree, possibly owing to a higher expression level of the mutant than WT (Fig. 3.5.B, compare lanes 2 and 3). GST-tagged AGO1-M improved expression to a similar degree as His-tagged one (Fig. 3.5.B, lane 4). Co-expression of AGO1 enhanced the expression of truncated AGO2 in a similar manner as full length

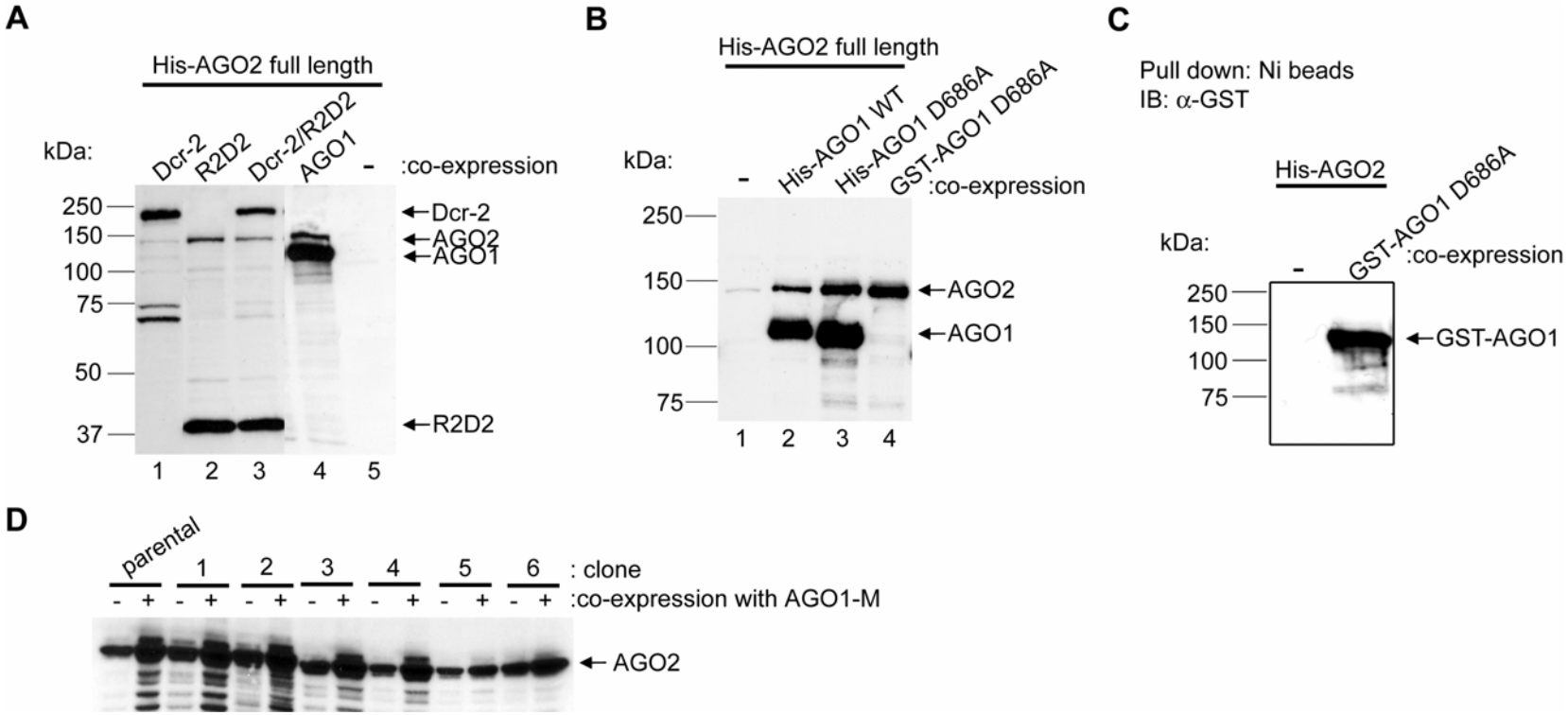

Figure 3.5. Co-expression of AGO1 enhances the expression level of AGO2. (A) The expression levels of full length AGO2 were compared when co-expressed with Dcr-2 (lane 1), R2D2 (lane 2), both Dcr-2 and R2D2 (lane 3), or AGO1 (lane 4). All recombinant proteins are His-tagged, and Western blot was performed with an antibody against His. **(B)** The expression levels of full length AGO2 were compared when co-expressed with His tagged AGO1 wildtype (WT) (lane 2), His tagged AGO1 D686A catalytic mutant (lane 3), or GST-tagged AGO1 D686A mutant (lane 4). Western blot was performed with an antibody against His. **(C)** His-tagged truncated AGO2 was expressed alone or with GST-tagged AGO1 mutant, affinity purified using Ni beads, and Western blotted with an antibody against His GST. **(D)** The expression levels of truncated AGO2 from the parental heterogeneous baculovirus pool or different homogenous virus clones. The expression levels were also compared when GST-AGO1 mutant was co-expressed. Western blot was performed with an antibody against His.

protein (data not shown).

To understand the mechanism of AGO1 enhancing AGO2 expression, I co-expressed truncated AGO2 with GST-tagged AGO1-M, affinity purified proteins using Ni beads, and performed Western blot against GST. GST-AGO1-M was detected in the Ni pull-down (Fig. 3.5.C), suggesting AGO1 associates with AGO2. Thus, co-expression of AGO1 may stabilize AGO2, leading to a higher expression level. Further studies are needed to find out the interacting regions in these two proteins.

It was previously shown that by viral plaque assay, an individual viral clone was isolated with higher expression level than parental pool (Deisenhofer Lab, unpublished data) (Rudenko et al., 2002). It is possible that though initially transfected viral genome is the same, through packaging in different cells, the behavior of individual viral clones may vary. I isolated more than ten clones for both truncated and full length AGO2, (6 of which are shown in Fig. 3.5.D), and none of them showed increased expression level compared to the parental virus pool, while some showed decreased expression. Thus, plaque assay was not able to identify higher expression clones.

Reconstitution of the siRNA pathway by recombinant AGO2 and Dcr-2/R2D2

After sufficient amount of recombinant AGO2 was obtained by co-expressing AGO1-M, the next important experiment would be to determine whether *Drosophila* siRNA pathway could be reconstituted *in vitro* by combining AGO2 and Dcr-2/R2D2

recombinant proteins. The long dsRNA initiated RISC reaction is the *in vitro* assay for detecting entire RNAi machinery activity. As shown in Fig. 3.6.A, while Dcr-2/R2D2 (lane 4) or truncated AGO2 alone (lane 9) or Dcr-2 plus AGO2 (lane 10) was not able to cleave target mRNA when programmed with dsRNA, a cleavage product was generated by adding three proteins together (lane 11). AGO2 with R2D2 was not able to slice either (data not shown). This result suggests that Dcr-2, R2D2 and truncated AGO2 are necessary and sufficient to reconstitute the entire RNAi machinery. Recombinant full length AGO2 also reconstituted RNAi activity with Dcr-2/R2D2, but the activity was lower because of lower expression than truncated protein, (data not shown). Thus, from here on, unless mentioned, the data shown were mostly done with truncated AGO2. Though the polyQ regions of AGO2 were reported to be involved in early embryogenesis (Meyer et al., 2006), my result suggests that it is not completely required for in vitro RNAi activity because the truncated form is missing the entire short polyQ region and 7 long polyQ repeats.

When co-expressed with His-tagged Dcr-2 and R2D2, the purified AGO2 complex also displayed RNAi activity (Fig. 3.6.A, lane 8), demonstrating another method of reconstitution. Notably, without co-expression with AGO1-M, the amount of purified recombinant AGO2 is too low to show RISC activity when combined with exogenously added Dcr-2/R2D2, proving the co-expression step to be crucial (Fig. 3.6.A, lane 7).

Similarly, the siRNA induced RISC activity was only detected by combining recombinant Dcr-2/R2D2 and truncated AGO2 (Fig. 3.6.B, lane 5) or co-expressed

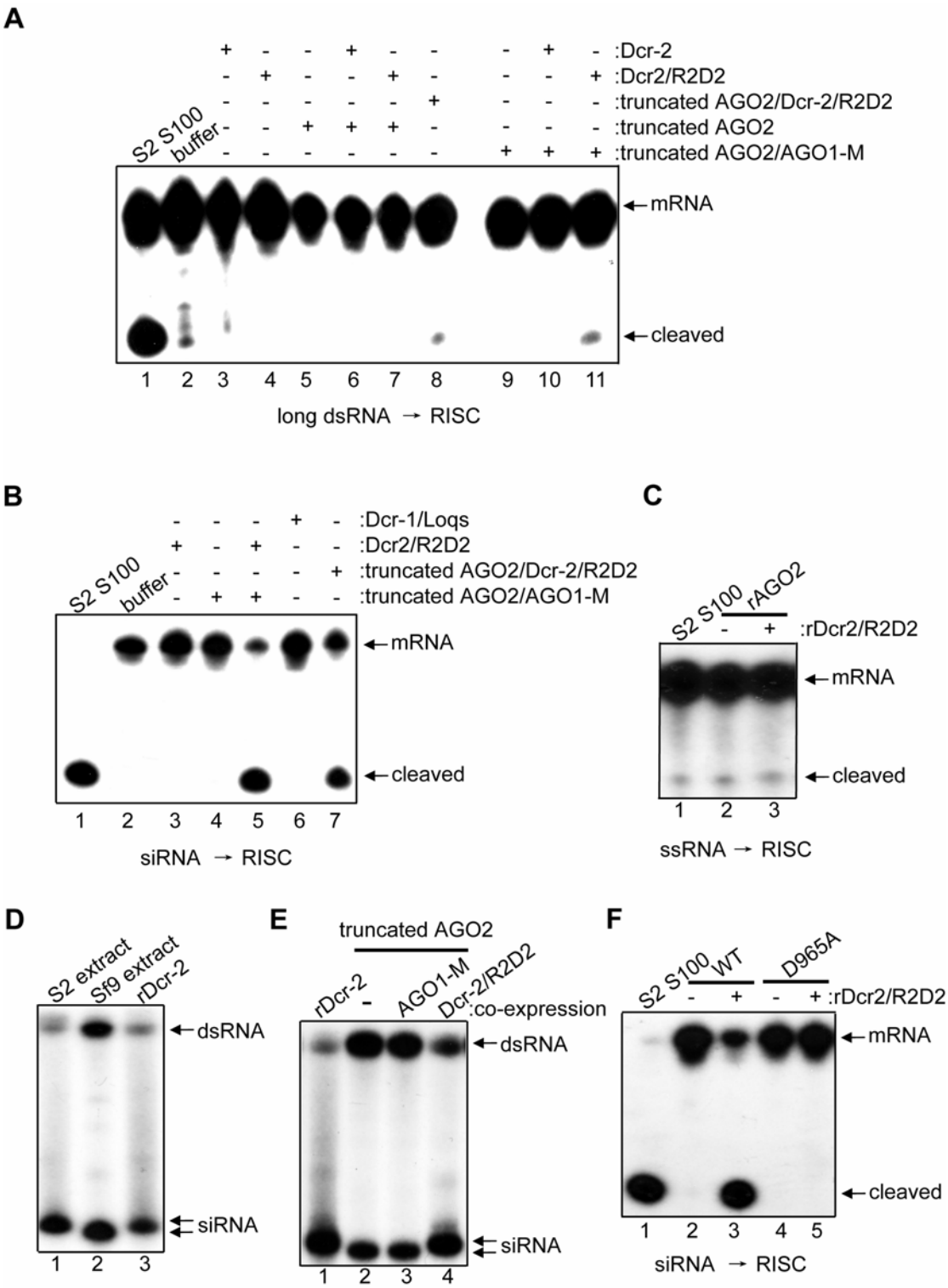
A
:Dcr-2
:Dcr2/R2D2
:truncated AGO2/Dcr-2/R2D2
:truncated AGO2
:truncated AGO2/AGO1-M
S2 S100
buffer
mRNA
cleaved
1 2 3 4 5 6 7 8 9 10 11
long dsRNA → RISC
B
:Dcr-1/Loqs
:Dcr2/R2D2
:truncated AGO2/Dcr-2/R2D2
:truncated AGO2/AGO1-M
S2 S100
buffer
mRNA
cleaved
1 2 3 4 5 6 7
siRNA → RISC
C
S2 S100
rAGO2
:rDcr2/R2D2
mRNA
cleaved
1 2 3
ssRNA → RISC
D
S2 extract
Sf9 extract
rDcr-2
dsRNA
siRNA
1 2 3
E
truncated AGO2
rDcr-2
AGO1-M
Dcr-2/R2D2
:co-expression
dsRNA
siRNA
1 2 3 4
F
S2 S100
WT
D965A
:rDcr2/R2D2
mRNA
cleaved
1 2 3 4 5
siRNA → RISC

Figure 3.6. Recombinant AGO2 and Dcr-2/R2D2 reconstitute the *Drosophila* siRNA pathway. (A) The **long dsRNA** initiated RISC assays were performed in various combinations of recombinant proteins. The assay done in S2 S100 extract served as a size marker. The assays were done with 5 μl of truncated AGO2 alone (lane 5) or in combination with 50ng of Dcr-2 (lane 6) or 50ng of Dcr-2/R2D2 complex (lane 7), truncated AGO2 co-expressed with Dcr-2 and R2D2 (lane 8), or truncated AGO2 co-expressed with AGO1-M alone (lane 9) or in combination with 50ng of Dcr-2 (lane 10) or 50ng of Dcr-2/R2D2 complex (lane 11). The assays were also performed with 50ng of recombinant Dcr-2 (lane 4) and 50ng of Dcr-2/R2D2 (lane 5) to serve as negative controls. **(B)** The **double-stranded siRNA** initiated RISC assays were performed with truncated AGO2 co-expressed with AGO1-M alone (lane 4) or in combination with 50ng of Dcr-2/R2D2 complex (lane 5) or 50ng of Dcr-1/Loqs complex (lane 6), or truncated AGO2 co-expressed with Dcr-2 and R2D2 (lane 7). The assay done in S2 S100 extract served as a size marker while the assay done with Dcr-2/R2D2 complex served as a negative control. **(C)** The **single-stranded siRNA** initiated RISC assays were performed with truncated AGO2 co-expressed with AGO1-M alone (lane 2) or in combination with 50ng of Dcr-2/R2D2 complex (lane 3). **(D)** The **dsRNA processing** assays were performed in 10 μg S2 cell extract (lane 1), Sf9 cell extract (lane 2), or recombinant Dcr-2 enzyme (lane 3). **(E)** The dsRNA processing assays were performed with recombinant Dcr-2 enzyme (lane 1), truncated AGO2 expressed alone (lane 2), co-expressed with AGO1-M (lane 3) or Dcr-2 and R2D2 (lane 4). **(F)** The **double-stranded siRNA** initiated RISC assays were performed with truncated AGO2 WT alone (lane 2) or in combination with 50ng of Dcr-2/R2D2 complex (lane 3), or D965A catalytic mutant alone (lane 4) or in combination with 50ng of Dcr-2/R2D2 complex (lane 5). Both recombinant Ago2s were co-expressed with AGO1-M.

and co-purified AGO2/Dcr-2/R2D2 complex (Fig. 3.6.B, lane 7), while Dcr-2/R2D2 complex alone (Fig. 3.6.B, lane 3) or AGO2 alone (Fig. 3.6.B, lane 4) was unable to load siRNA and cleave target mRNA. These data directly show the critical roles played by Dcr-2 and R2D2 in RISC assembly. Another control included in this experiment was Dcr-1/Loqs complex, the miRNA biogenesis machinery. The observation that Dcr-1/Loqs complex together with AGO2 did not reconstitute siRISC suggests the specificity of the siRISC machinery (Fig. 3.6.B, lane 6).

In addition, the single-stranded siRNA initiated RISC activity of AGO2 was not affected by addition of Dcr-2/R2D2 complex (Fig. 3.6.C), indicating the minimal

RISC activity involves AGO2 alone and Dcr-2/R2D2-dependent RISC assembly process involves a double-stranded RNA feature. The weak minimal RISC activity contrasts with robust slicer activity shown in Fig. 3.6.B, suggesting that there is significant coupling between the unwinding of double-stranded siRNA and the formation of active slicer.

Since high salt wash was not applied during protein purification, the preparation was not clean (Fig. 3.4.D) and possibly contained the endogenous RNAi machinery from insect cells through interaction with *Drosophila* AGO2. To test this possibility, I performed dsRNA processing assays and discovered that Sf9 cells possess Dicer activity and the siRNAs generated by Sf9 Dicer are smaller in size than *Drosophila* Dcr-2 (Fig. 3.6.D). Thus, if insect cell Dicer co-purified with AGO2, its Dicer activity can be distinguished from *Drosophila*'s. As shown in Fig. 3.6.E, recombinant AGO2 prep indeed contained insect cell Dicer (lanes 2 and 3). When AGO2 was co-expressed and co-purified with Dcr-2 and R2D2, the activity from Dcr-2 became predominant (Fig. 3.6.E). Thus, it raises a question whether the reconstitution system represents specific activity from recombinant Drosophila proteins or RNAi machinery from insect cells.

To test the concern that the reconstitution may come from co-purified insect cell RNAi machinery, a catalytic mutant of AGO2 was produced. The catalytic center of Drosophila AGO2 is highly homologous to human Ago2, with the conserved "DDH" motif present (Fig. 4.9). Aspartic acid 965 is among one of the residues in the "DDH" motif of Drosophila AGO2, and was mutated to alanine. The mutant expressed at a

similar level as WT (data not shown). Presumably a single mutant that resides in the inferior portion of a protein possibly retains overall structure and regular interaction with other proteins. Catalytic mutant AGO2 did not reconstitute siRISC in combination with Dcr-2/R2D2 complex (Fig. 3.6.F, lanes 4 and 5). It also lost dsRNA induced RISC and minimal RISC activity (data not shown), indicating the RISC activity observed in WT AGO2 is dependent on AGO2 but not associating RNAi machinery from insect cells.

Further purification of recombinant AGO2 through native fractionation methods

To improve the purity of recombinant AGO2 prep, native fractionation methods such as glycerol gradient and gel filtration column were utilized. Glycerol gradient centrifugation separates protein complexes due to different sedimentation constant through a gradient of the viscous component – glycerol. By Coomassie blue staining, compared to input, each fraction showed improved purity (Fig. 3.7.A, top). While Western blot revealed that AGO2 was widely spread from fraction #4 through #12 (Fig. 3.7.A, bottom), the siRISC activity had a clear peak in fractions #5, 6 and 7 when combined with Dcr-2/R2D2 for assaying (Fig. 3.7.B), suggesting that not all AGO2 had the same conformation and the active conformation only comprise a small portion of the total amount.

The fractions that contained the peak siRISC activity were combined and loaded onto Superose 6 gel filtration column. Gel filtration chromatography separates

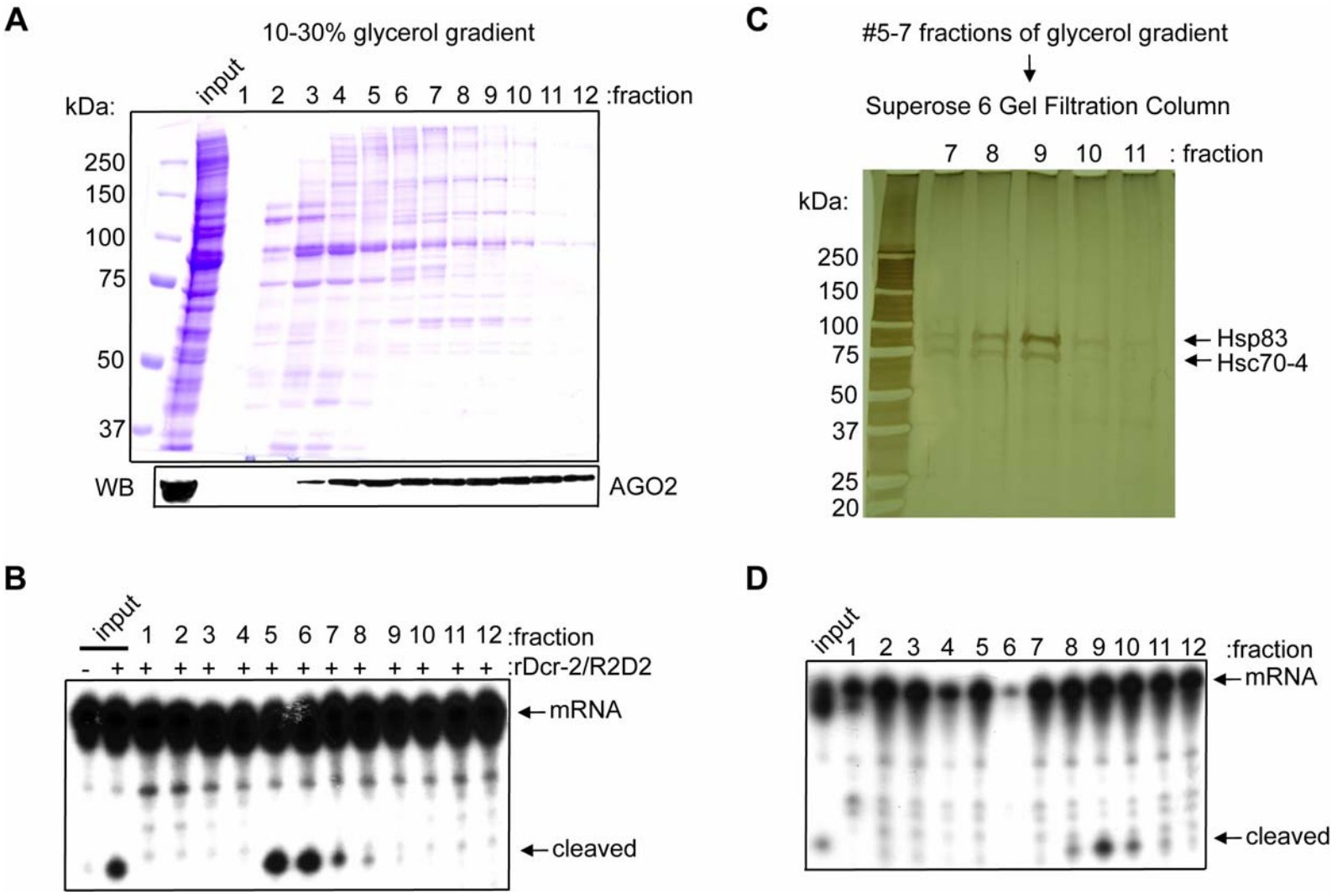
A
10-30% glycerol gradient
input
1 2 3 4 5 6 7 8 9 10 11 12 :fraction
kDa:
250
150
100
75
50
37
WB
AGO2
C
#5-7 fractions of glycerol gradient
Superose 6 Gel Filtration Column
7 8 9 10 11 : fraction
kDa:
250
150
100
75
50
37
25
20
Hsp83
Hsc70-4
B
input
1 2 3 4 5 6 7 8 9 10 11 12 :fraction
- + + + + + + + + + + + + :rDcr-2/R2D2
mRNA
cleaved
D
input
1 2 3 4 5 6 7 8 9 10 11 12 :fraction
mRNA
cleaved

Figure 3.7. Purified recombinant truncated AGO2 complex contains heat shock protein 83 (Hsp83) and heat shock protein cognate 4 (Hsc70-4). (A) A coomassie-stained SDS-PAGE showing partially purified His-tagged recombinant truncated AGO2 using 10-30% glycerol gradient centrifugation. In the bottom of this panel, Western blot with an antibody against His showed AGO2 spread out in fractions #4 through #12. **(B)** The double-stranded siRNA initiated RISC assays were performed in 5 μl glycerol gradient fractions. 50ng of recombinant Dcr-2/R2D2 complex was added in every reaction except the first lane, which served as a negative control. The siRISC activity peaked in fractions #5-7. **(C)** Fractions 5, 6 and 7 of glycerol gradient were pooled together and loaded onto Superose 6 gel filtration column. A silver-stained SDS-PAGE showing the protein bands present in the activity peak according to panel D. The mass spectrometry results of the two major bands in fraction #9 were insect cell Hsp83 (top) and Hsc70-4 (bottom) respectively. **(D)** The double-stranded siRNA initiated RISC assays were performed in 5 μl Superose 6 fractions. 50ng of recombinant Dcr-2/R2D2 complex was added in all reactions. The siRISC activity peaked in fractions #8-10.

proteins on the basis of molecular size. After the two-step purification, the amount of protein in each fraction became so low that protein bands could only be visualized by sliver staining (Fig.3.7.C). Despite the absence of detectable signal of AGO2 from Western blot (data not shown), an activity peak came out of Superose 6 at fractions #8 to #10 (Fig. 3.7.D), which runs between the molecular weight markers 158 kDa and 44 kDa. Based on the 100 kDa of the truncated AGO2 molecular weight, recombinant AGO2 possibly exists in a monomeric form. However, on the silver stained SDS-PAGE, there were only two visible bands in the activity peak fractions, none of which had the molecular weight of ~100 kDa (Fig. 3.7.C). Mass spectrometry revealed that the ~90 kDa band contained Hsp83, and the ~70 kDa band contained Hsc70-4, both of which are insect cell proteins. Thus, heat shock proteins from insect cells associate with recombinant AGO2.

To determine whether the interaction between AGO2 and heat shock proteins has any functional consequence; i.e. whether Hsp83 and Hsc70-4 specifically enhance the

expression of AGO2 or influence the RISC activity, or whether they are just general molecular chaperones in the insect cell that helps protein folding, I cloned and expressed *Drosophila* Hsp83 and Hsc70-4. Co-expression of Hsp83 (Fig. 3.8.A, lane 4), Hsc70-4 (Fig. 3.8.A, lane 3) or both (Fig. 3.8.A, lane 5) did not affect the expression level of AGO2. Moreover, adding Hsp83, or Hsc70-4 or both did not change the RISC activity from AGO2 alone or in combination with Dcr-2/R2D2 complex (Fig. 3.8.B, cf lanes 3 and 4 to 5 and 6, 7 and 8, 9 and 10). Therefore, the discovered association between heat shock proteins and AGO2 is likely due to a general molecular chaperone mechanism.

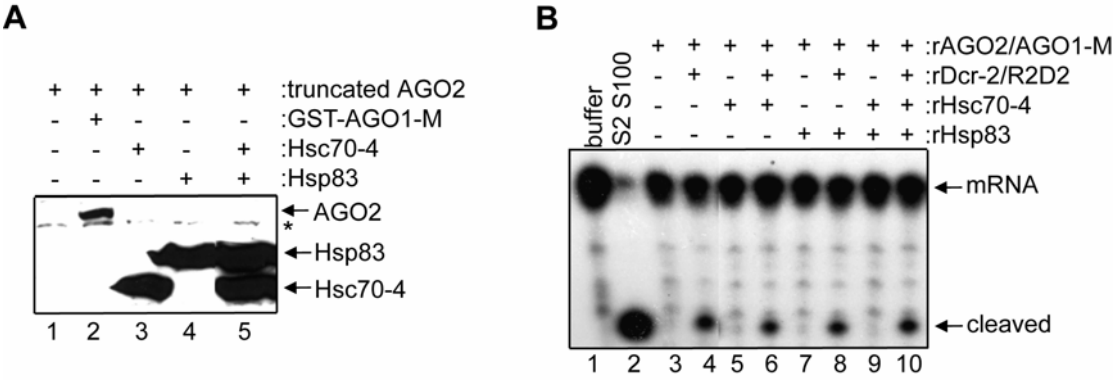

Figure 3.8. Hsp83 and Hsc70-4 do not affect expression level or activity of truncated AGO2. (A) The expression levels of truncated AGO2 were compared when expressed alone (lane 1), co-expressed with GST-tagged AGO1-M (lane 2), Hsc70-4 (lane 3), Hsp83 (lane 4), or both Hsc70-4 and Hsp83 (lane 5). All recombinant proteins were His-tagged except AGO1, and Westenr blot was done with an antibody against His. The asterisk refers to a cross reacting band to His antibody. **(B)** The double-stranded siRNA initiated RISC assays were performed with truncated AGO2 alone, in combination with 50ng of Hsc70-4, Hsp83, or both Hsc70-4 and Hsp83, in the absence (lanes 3, 5, 7, and 9) or presence of 50ng of Dcr-2/R2D2 (lanes 4, 6, 8, and 10).

Further purification of recombinant AGO2 through tandem tag purification

Another method to improve purity of recombinant AGO2 prep is through tandem affinity purification by constructing two epitope tags at the N terminus. I inserted a 3

× Flag tag between the N terminal His tag and AGO2 ORF. Tandem purification with Ni beads first and Flag beads second significantly improved AGO2's purity, with only one major band corresponding to AGO2, confirmed by Mass Spectrometry (Fig.3.9.A). As Flag elution sustained long dsRNA initiated RISC activity when combined with Dcr-2/R2D2 (Fig. 3.9.B), we were more confident in concluding that these three proteins reconstitute Drosophila siRNA pathway in vitro.

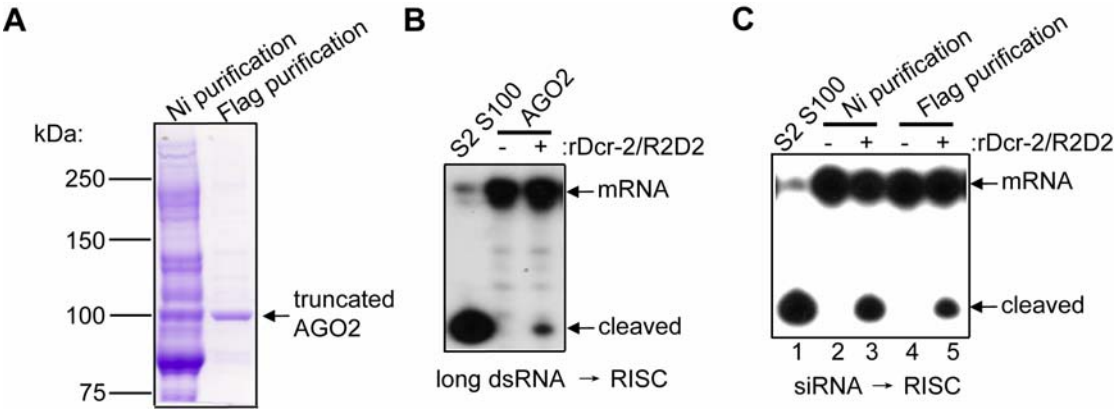

Figure 3.9. Tandem purification produced much purer and yet active recombinant AGO2. (A) A coomassie-stained SDS-PAGE comparing the purity of AGO2 after one step Ni beads purification (left lane) and two step Ni and Flag beads purification (right lane). **(B)** The long dsRNA initiated RISC assays were performed with tandem purified truncated AGO2 alone or with 50ng of Dcr-2/R2D2. **(C)** The double-stranded siRNA initiated RISC assays were performed to compare siRISC activity between single-step (lanes 2 and 3) and tandem-step (lanes 4 and 5) purified recombinant AGO2.

A technical problem I encountered during the Flag purification is that the efficiency of binding was too low. By comparing input and flow-through of Flag beads using Western blot against AGO2, significant amount of AGO2 still remained in the flow-through (data not shown). While the volume from Ni elution to Flag elution was decreased to one tenth, the AGO2 concentration was even lower in the final Flag elution, though in principle it should be 10 fold higher (data not shown). This may

explain why lower siRISC activity was observed in recombinant AGO2 after tandem purification compared to single purification (Fig. 3.9.C, cf lanes 3 and 5). While purifying other Flag tagged recombinant proteins such as Flag-Dcr-1 yielded considerable amount of protein, the capacity of Flag beads was not saturated for binding AGO2. There is as yet no clear solution to this, but it can be speculated that the folding of AGO2 somehow interferes with the exposure of the Flag epitope.

Conserved residues in the DExDc, HELICs, DUF 283 and RNase III domains of Dcr-2 are not essential for siRISC assembly

The question immediately follows reconstitution is that how two strands of siRNA are separated that allows one stand to be loaded onto AGO2 protein. Whether or not there is a helicase to unwind the double stranded siRNA remains an open question in the field. Since we reconstituted the whole pathway with only 3 proteins, it is reasonable to think that the helicase activity is performed by these 3 proteins. Among them, Dcr-2 is the best candidate, because it possess a putative DEAD box-like helicase domain (DExDc) and a putative Helicase c-terminal domain (HELICc). I made mutations in both domains. In DExDc, lysine is a critical residue for ATP binding and hydrolysis. In mutant 1, the lysine was mutated to arginine, which is still able to bind ATP, but not able to hydrolyze it (Fig. 3.11.A). In mutant 2, the lysine was mutated to asparagine, which is not able to bind ATP (Fig. 3.11.A). In HELICc, the tandem aspartic acid and glutamic acid are essential residues in the catalytic center. In mutant 3, the tandem DE residues were both mutated to alanines

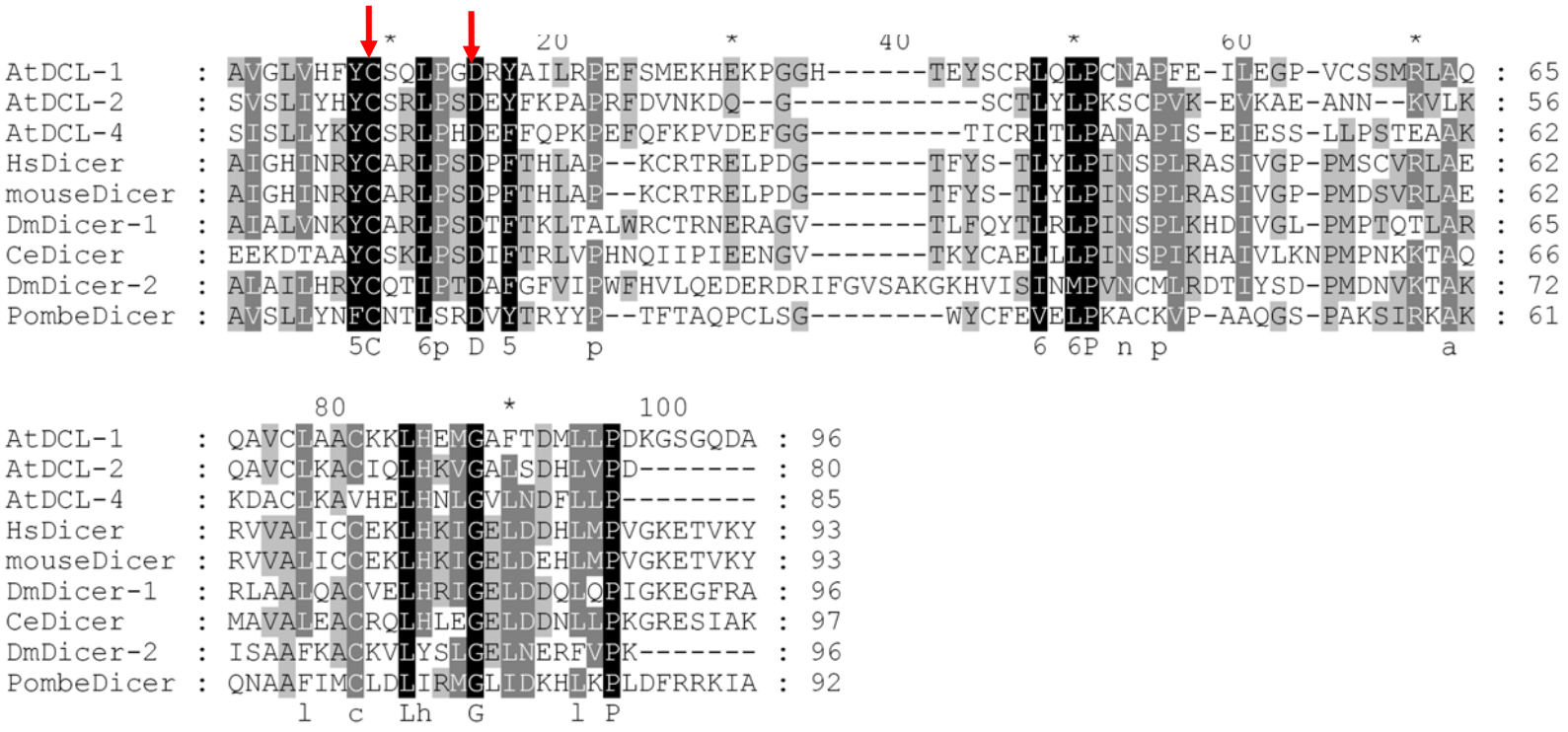

Figure 3.10. Sequence alignment of domains of unknown function 283 (DUF283) among Dicer genes. DUF283 is a conserved domain found in Dicer protein family, with 3 possible zinc ligands. Because cysteine is an essential residue for zinc finger domain to coordinate a zinc ion, I chose to mutate the highly conserved cysteine (pointed by the left red arrow) (poistion at 579th residue in Drosophila Dcr-2) to alanine. Due to crucial roles played by acidic residues in the catalytic center of nucleases, I also mutated the highly conserved aspartic acid (pointed by the right red arrow) (poistion at 585th residue in Drosophila Dcr-2) to alanine.

(Fig. 3.11.A).

There is also a domain with unknown function (DUF283) residing in Dicer-2, which is predicted to contain 3 possible zinc ligands. I aligned DUF283 domains of Dicers from common species, and chose a conserved cysteine due to general association of cysteine with zinc binding in zinc finger domains, and a conserved aspartic acid due to general critical role played by aspartic acid in the catalytic center of nucleases (Fig. 3.10). The corresponding mutants, M4 and M5, were made (Fig. 3.11.A). Moreover, a catalytic dead Dcr-2, M6, was generated, with four point mutations in the two RNase III domains (Fig. 3.11.A).

All the above six mutants were expressed with R2D2 in insect cells and purified as complexes (Fig. 3.11.B). Dicer activity was first examined. While mutations in RNase III abolished activity as expected (Fig.3.11.C, lanes 20-22), mutants of DEXDc or HELICc were unable to process dsRNA (Fig.3.11.C, lanes 5-13). Mutations in the DUF283 did not cause any activity change (Fig.3.11.C, lanes 14-19). The experiment was done with a titration so that activity between WT and mutants could be fairly compared. In summary, together with RNase III domains, DExDc and HELICc domains of Dcr-2 are critical for dicer activity.

Next, to determine the siRNA binding ability of each mutant, gel mobility shift assays were performed. While there were two complexes with similar intensity formed between WT or M1 Dcr-2/R2D2 and siRNA, some mutants formed predominantly one complex, with M2, M3 and M5 forming mainly the lower complex and M4, M6 forming mainly the higher complex (Fig. 3.11.D). This experiment was

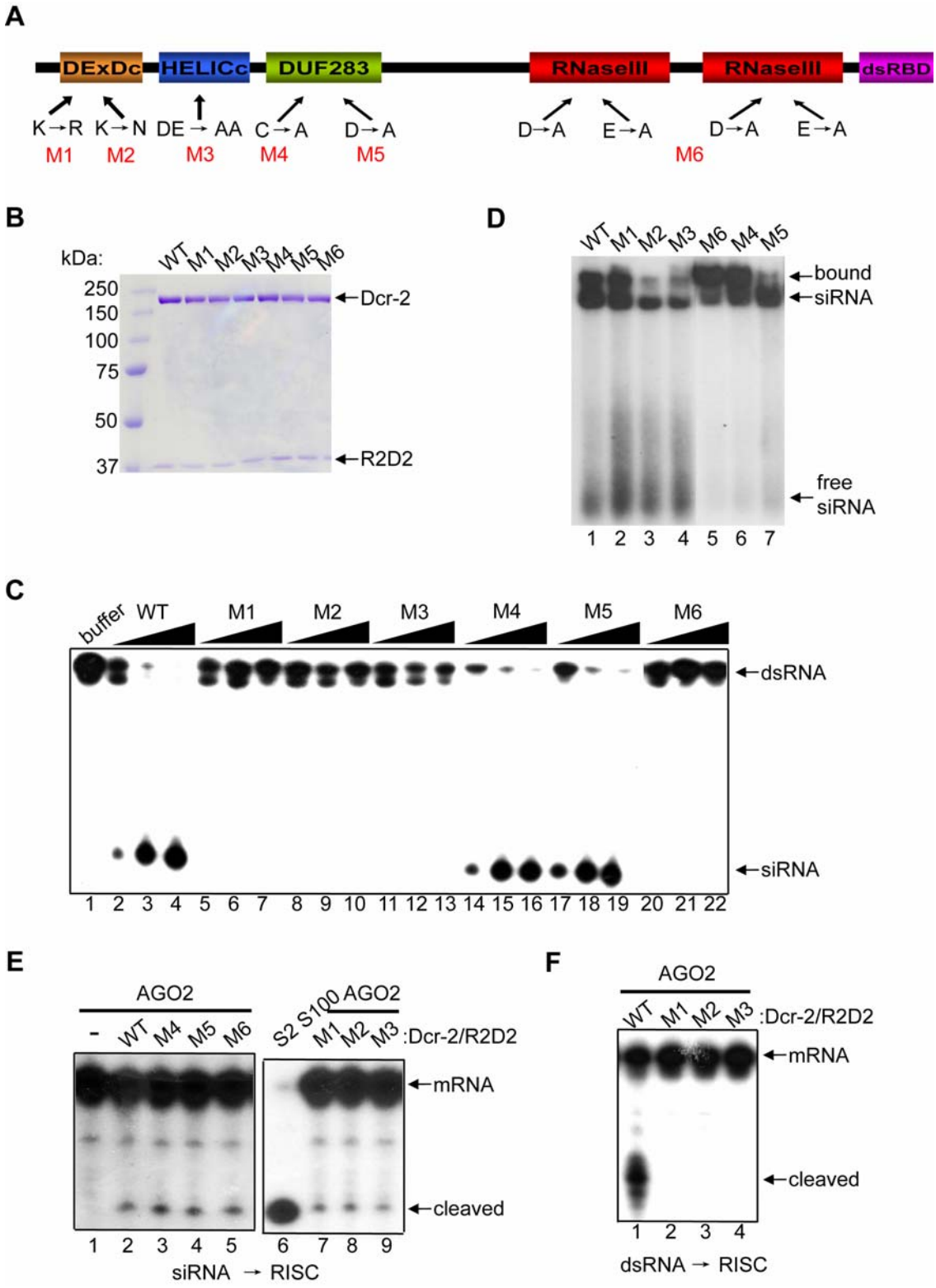

Figure 3.11. Conserved residues in the Helicase, ATPase, DUF 283, and catalytic domains of Dcr-2 are not essential for siRISC assembly. (A) A schematic diagram representing the overall domain structures of Drosophila Dcr-2. The domain abbreviations stand for: DExDc - DEAD-like helicases superfamily; HELICc - Helicase superfamily c-terminal domain; dsRBD -dsRNA binding domain. Six point mutants of Dcr-2 were made and the residue(s) being mutated in each mutant is

shown with arrow pointing to its residing domain. **(B)** A coomassie-stained SDS-PAGE showing 1 μg of recombinant protein of each mutant was expressed, purified and equalized to the same concentration as wildtype (WT). **(C)** The dsRNA processing assays were performed to determine whether the mutations affect Dicer activity. Each recombinant protein was used at 3 amounts: 1ng, 10ng and 100ng. The lanes for each form are: WT (lanes 2-4), mutant 1 (lanes 5-7), mutant 2 (lanes 8-10), mutant 3 (lanes 11-13), mutant 4 (lanes 14-16), mutant 5 (lanes 17-19), and mutant 6 (lanes 20-22). **(D)** Gel mobility shift assays were performed with WT (lane 1) and mutants (lanes 2-7) of Dcr-2. Notably, there were two protein bound complexes present in WT Dcr-2 and currently it could not be explained. **(E)** The ds siRNA initiated RISC assays were performed with 5 μl of tandem purified truncated AGO2 alone (lane 1) or in combination with 50ng of WT (lane 2) or mutant Dcr-2 complexed with R2D2 (lanes 3-5 and 7-9). **(F)** The long dsRNA initiated RISC assays were performed with 5 μl of tandem purified truncated AGO2 in combination with 50ng of WT (lane 1) or mutant Dcr-2 complexed with R2D2 (lanes 2-4).

repeated multiple times and the patterns were reproducible. Previously we have only observed one complex formed by Dcr-2/R2D2 complex with siRNA (Liu et al., 2003; Liu et al., 2006), the appearance of two complexes may be due to too much protein used in the assay. I have not yet determined the qualitative difference between the two complexes, but based on the observation that all of the mutants formed at least one complex with siRNA, we can summarize that none of those mutations completely abolish the siRNA binding ability of Dcr-2/R2D2.

To our surprise, the double-stranded siRNA initiated RISC assays showed that none of those mutations affects siRISC activity (Fig. 3.11.E), indicating those residues in the DExDc, HELICc, DUF283 and RNase III domains are not involved in loading siRNA onto Ago2. This result suggests that the dicing and RISC loading are separated functions of Dcr-2. The long dsRNA initiated RISC assays showed that mutants 1-3 were not able to reconstitute RNAi with AGO2 (Fig. 3.11.F), which is consistently with previous data that they were not able to process dsRNA (Fig.

3.11.C).

Discussion

The current study established the first *in vitro* reconstitution system of *Drosophila* RNAi machinery. It also strengthens the previous model that Dcr-2/R2D2 complex bridges the initiation step (siRNA production) and the effector step (siRNA loading onto siRISC) of the *Drosophila* RNAi pathway (Liu et al., 2003). By removing the potentially problematic N terminal polyQ region, I successfully obtained small amount of recombinant AGO2 through making truncation in the polyQ region and co-expression with *Drosophila* AGO1. Though no salt is allowed in purification, the purity was improved significantly by tandem purification through two epitope tags. The slicer activity from recombinant AGO2 is specific because mutation in one of DDH catalytic motif caused loss of activity. Dcr-2, R2D2 and AGO2 are necessary and sufficient to reconstitute the minimal RNAi machinery. This is supported by that only the Dcr-2/R2D2 complex, but neither Dcr-2 nor R2D2 alone, could efficiently interact with the siRNA duplex.

How do Dcr-2 and R2D2 bind siRNA?

Only the Dcr-2/R2D2 complex, but neither Dcr-2 nor R2D2 alone, could efficiently interact with siRNA duplex in the gel mobility shift assays, indicating that Dcr-2 and R2D2 bind siRNA coordinately. R2D2 contains tandem dsRNA-binding domains (dsRBDs). I have shown that the first, but not the second, dsRBD of R2D2 is capable of binding long dsRNA. However, both dsRBDs of R2D2 are necessary for

siRNA binding by the Dcr-2/R2D2 complex. Thus, the second dsRBD of R2D2 is critical for binding to siRNA rather than long dsRNA. It is possible that, without the second dsRBD, the first dsRBD of R2D2 only possesses low affinity for the 21–22-nt siRNA duplex.

We and others have previously shown that R2D2 as well as Dcr-2 could be efficiently cross-linked to radiolabeled siRNA by ultraviolet (UV) light (Liu et al., 2003; Tomari et al., 2004b). Thus, both Dcr-2 and R2D2 are in close contact with siRNA strands. Since neither Dcr-2 nor R2D2 bind siRNA alone, it is possible that siRNA is bound at the interface between Dcr-2 and R2D2. It is also possible that association of Dcr-2 and R2D2 triggers conformational change in either or both proteins, allowing them to bind siRNA cooperatively.

Generation of recombinant AGO2

In other proteins, polyQ regions are associated with protein aggregation (Ross and Poirier, 2004). Thus, the extensive polyQ regions at the N terminus of AGO2 may be problematic for expression. Truncation of part of the polyQ region leads to higher expression level than wildtype protein. The biggest breakthrough originates from the significant increase in AGO2 expression when co-expressed with AGO1. Indeed, without co-expression, the level of purified AGO2 was too low to show slicer activity (Fig. 3.6.A). Initially we had concern about possible contamination of insect cell RNAi machinery in recombinant AGO2 preparation. However, by tandem purification and native fraction procedures, I have significantly improved the purity of

recombinant AGO2. Through mutagenesis of the AGO2 catalytic DDH motif, I have also shown that the slicer activity of AGO2 is specific. These results suggest that I have indeed successfully made the functional recombinant AGO2.

However, there are still some unsolved mysteries about AGO2. Where does the salt sensitivity come from? In the process of spliceosome assembly, some complexes such as U1 snRNP have been discovered to contain salt-sensitive subunits (Gottschalk et al., 1998). The exact nature of the salt-sensitive association as yet remains to be determined. Perhaps one definitive approach to understand this problem is through structural analysis. Furthermore, the recombinant AGO2 is extremely labile in that the pellet of insect cells expressing AGO2 can not be stored at -80ºC for over two weeks and purified recombinant AGO2 can not be stored at -80ºC for over one month. Otherwise, the activity will be lost. At the same time, most other recombinant enzymes that we have purified retain activity for at least one year, and the S2 cell extract sustains RISC activity after more than two-year storage. There is no clear mechanism discovered either, though we can speculate that it may contribute to the aggregative nature of the polyQ region of AGO2.

Reconstitution of RNAi by recombinant Dcr-2, R2D2 and AGO2

Although extensive studies through genetic or immunoprecipitation approach have discovered many proteins involved in RNAi, such as Aubergine (Kennerdell et al., 2002) and Armitage (Tomari et al., 2004a), the exact biochemical function of any particular protein or complex remains largely unknown because most investigations

were carried out in the crude extract or immuno-purified endogenous complexes. Here I have described an *in vitro* system to reconstitute *Drosophila* siRNA pathway from recombinant Dcr-2, R2D2 and AGO2. The reconstituted complex has the ability to recognize and process long dsRNA, load one strand of siRNA onto AGO2, and form an active RSIC that cleaves the target mRNA in a sequence-dependent manner.

It has been reported that Dcr-2 is required for siRNA-initiated RISC assembly in vivo (Lee et al., 2004b; Pham et al., 2004). Our group has obtained genetic evidence that R2D2 is also required for loading siRNA onto the siRISC complex *in vivo* (Liu et al., 2006). Here I have shown that Dcr-2 and R2D2 coordinately bind siRNA and possibly constitute the gateway for siRNA loading and RISC activation. The reconstitution of RNAi by Dcr-2, R2D2 and AGO2 directly demonstrated that Dcr-2/R2D2 complex is necessary and sufficient for siRNA loading. There is significant coupling between siRNA loading and formation of active slicer because the reconstituted complex showed much stronger activity in the double-stranded siRNA initiated RISC assay than single-stranded siRNA (Fig. 3.6, cf B and C).

The minimal reconstituted system will become an invaluable tool to identify novel regulators of the RNAi pathway by "biochemical supplementation", i.e. use the system as a base to purify a fraction from S2 cell extract that can enhance or inhibit the RISC activity. It will also enable us to define the mechanism played by those novel regulators.

How is siRNA loaded onto AGO2?

1) Helicase model.

It is possible that the Dcr-2/R2D2 complex helps recruit the siRNA duplex to AGO2 for siRISC assembly (Liu et al., 2003; Tomari et al., 2004b). However, it remains unclear exactly how the Dcr-2/R2D2 complex facilitates incorporation of siRNA into the siRISC complex. While newly synthesized siRNA is double-stranded, siRNA exists as a single-stranded form in an active siRISC complex (Martinez et al., 2002). Thus, the nascent siRNA duplex must be unwound during siRISC assembly. It is reasonable to speculate that the Dcr-2/R2D2 complex facilitates unwinding of the siRNA duplex, thereby promoting incorporation of single-stranded siRNA into the siRISC complex. Dcr-2 is a candidate for the siRNA-unwinding helicase because it carries putative DEXDc and HELICc helicase domains and physically contacts the siRNA end that is easier to unwind (Tomari et al., 2004b).

However, two mutations in the dcr-2 helicase domain were able to reconstitute the double-stranded siRNA-initiated RISC activity with AGO2, while they lost dsRNA processing activity. This result suggests that a DExDc and HELICc helicase domains are possibly involved in ATP hydrolysis and unwinding long dsRNA, but not required for Dcr-2 to promote siRISC assembly. In addition, recombinant Dcr-2 or Dcr-2/R2D2 complex cannot unwind the siRNA duplex in vitro (Tomari et al., 2004b). An explanation can be offered that Dcr-2/R2D2 may not possess helicase activity in the absence of AGO2. Alternatively, the helicase domain that is responsible for unwinding siRNA may reside in regions other than the 190 kDa Dcr-2 protein.

2) Passenger strand cleavage by Ago2 model.

Recent studies suggest an alternative model for separation of siRNA strands and activation of the siRISC complex (Matranga et al., 2005; Rand et al., 2005). Both studies above used tissue extract or cell extract instead of purified protein, therefore, it remains unclear whether AGO2 directly mediates cleavage-assisted dissociation of siRNA. My observation (Fig. 3.6.B) that AGO2 alone is unable to perform double-stranded siRNA initiated RISC cleavage indicates that AGO2 can not recognize double-stranded siRNA and the recruitment of duplex siRNA to AGO2 by Dcr-2/R2D2 complex is essential. Only after siRNA loading will the PIWI domain of AGO2 cleave the passenger strand and facilitate the formation of an active siRISC complex containing only the guide strand. It is likely that the orientation of siRNA binding by the Dcr-2/R2D2 complex allows AGO2 to access and cleave only one of the two siRNA strands. Therefore, the Dcr-2/R2D2 complex determines which strand of siRNA duplex becomes the guide strand and AGO2 slices the opposite strand.

The two mechanistic models of siRISC assembly are not mutually exclusive. Since siRNAs bearing uncleavable passenger strand was still able to induce RISC cleavage (Matranga et al., 2005; Rand et al., 2005) , it indicates the possible existence of unwinding mechanism for conversion of siRNA duplex into single-stranded state. In either model, the Dcr-2/R2D2 complex plays a critical role in facilitating the strand separation of the duplex siRNA. Future studies are needed to identify the helicase that unwinds siRNA and to assess the passenger cleavage mechanism in the reconstitution system.

Chapter IV

Biochemical Analysis of the miRNA pathway in *Drosophila*

Abstract

By a bioinformatics approach, we identified a novel protein, Loqs/R3D1, with considerable sequence homology to R2D2 and RDE-4. Loqs gene encodes two protein isoforms, Loqs-PA and Loqs-PB, by alternative splicing. Immunoprecipitation experiments showed that endogenous Loqs and Dcr-1 associate with each other in vivo. Recombinant Loqs-PB isoform enhances the catalytic activity of Dcr-1 to generate miRNA by increasing its affinity for the pre-miRNA substrate. Depleting Loqs or Dicer-1 by RNAi results in reduction of the miRNA-generating activity and accumulation of pre-miRNA in S2 cells. The *loqs*^{PB} mutant flies are defective for miRNA biogenesis in both males and females. Though Loqs functions in concert with Dcr-1 in catalyzing miRNA maturation, it is not required for miRISC assembly. To understand the molecular mechanism of miRISC action, recombinant AGO1 was generated. Recombinant AGO1 can be programmed by single stranded miRNA into a minimal miRISC and sequence specifically cleaves complementary mRNA *in vitro*. Furthermore, the catalytic activity of Ago1 is dependent on the consensus catalytic "DDH" motif. My present studies suggest that recombinant Dicer-1, Loqs and Ago1 are not sufficient to reconstitute the miRNA pathway, indicating that there are other unknown components to be discovered.

Introduction

Both siRNA and miRNA are produced by Dicers, a family of large multidomain RNase III enzymes (Bernstein et al., 2001). Although species such as *Caenorhabditis elegans* and humans, contain a single Dicer gene, two Dicers, Dcr-1 and Dcr-2, have been found in *Drosophila* (Bernstein et al., 2001). Genetic studies have suggested that Dcr-1 and Dcr-2 are responsible for miRNA and siRNA production, respectively (Lee et al., 2004b). Previously, our group has purified the dsRNA processing enzyme from S2 cell extracts and found that it consists of Dcr-2 and a novel dsRNA-binding protein R2D2 (Liu et al., 2003). Dcr-2 and R2D2 form a heterodimeric complex named the RISC loading complex (RLC) (Tomari et al., 2004b). Although R2D2 does not regulate siRNA production, it is required for incorporating siRNA onto siRISC (Liu et al., 2003). Moreover, the orientation of RLC on the duplex siRNA, with R2D2 binding the most stable double-stranded end, determines which siRNA strand gets assembled onto RISC (Tomari et al., 2004b).

Biogenesis of miRNA occurs in a two-step process. In the nucleus, the primary miRNA (pri-miRNA) is transcribed by RNA polymerase II (Pol II) processed by another RNase III enzyme named Drosha into 60–70nt hairpin-structured pre-miRNA (Lee et al., 2003). Drosha requires the company of the dsRNA-binding protein Pasha in fly (or DGCR8 in human) for processing pri-miRNA (Denli et al., 2004; Gregory et al., 2004; Han et al., 2004; Landthaler et al., 2004). Once generated, pre-miRNA is exported by Exportin 5/RanGTP to the cytoplasm (Bohnsack et al., 2004; Lund et al.,

2004; Yi et al., 2003), and is further cleaved by Dcr-1 in fly (or Dicer in human) into 21-24nt mature miRNA (Hutvagner et al., 2001; Lee et al., 2004b).

Both Drosha and Dicer in human contain tandem RNase III domains that form a single catalytic center to make a pair of cuts at the double-stranded stem of pre-miRNA hairpin, creating products bearing characteristic ends of 5'-phosphate, 3'-hydroxyl, and 2nt 3' overhang (Han et al., 2004; Zhang et al., 2004). Drosha cleaves at the base of the pre-miRNA stemloop to release it from pri-miRNA and to generate one end of miRNA (Han et al., 2004). Dicer cuts near the loop of pre-miRNA at a 21-24nt distance from the Drosha cleavage site to excise miRNA from its precursor (Cullen, 2004).

Based on previous discoveries that an RNase III enzyme often works with a dsRNA-binding partner, such as Dicer-2/R2D2 in the siRNA pathway (Liu et al., 2003) and Drosha/Pasha in the miRNA pathway (Denli et al., 2004; Gregory et al., 2004; Han et al., 2004; Landthaler et al., 2004), we hypothesized that Dcr-1 might also functions in concert with an unknown dsRNA-binding protein in the miRNA pathway. Through a bioinformatics approach, we identified an open reading frame (ORF, CG6866) in the fly genome that showed considerable homology with R2D2 and RDE-4, an R2D2 homolog in C. elegans (Liu et al., 2003; Tabara et al., 2002). The sequence alignment was done using Clustal X (Fig. 5.1.A). Furthermore, PSI-Blast ranked this ORF as the best hit among R2D2-like proteins in FlyBase, and vice versa. In our original publication, we named this protein R3D1 because it contained three putative dsRNA-binding domains (R3) and was later found to

associate with Dicer-1 (D1) (Fig. 4.1.A). Due to name conflict (Forstemann et al., 2005; Saito et al., 2005), this gene is now called loquacious (loqs). The loqs gene encodes two alternatively spliced proteins, Loqs-PB (long; 465 amino acids) and Loqs-PA (short; 419 amino acids) (Fig. 4.1.B). The exon 4 that is missing in Loqs-PA encodes a 46 amino-acid long peptide that resides in the region between the last two dsRNA-binding domains (Fig. 4.1.C).

It is unclear how siRNA or miRNA is transferred from Dicer to Argonaute to form the effector RISC complexes. Our previous studies on R2D2 have shown that while R2D2 does not regulate siRNA production, it cooperates with Dcr-2 to bind siRNA and facilitate siRNA loading onto the effector siRISC complexes (Liu et al., 2003; Liu et al., 2006). If loqs belongs to the growing family of dsRBPs that play important roles in the RNAi pathway, it would be interesting to know whether loqs has similar function in the miRNA pathway as R2D2 in the siRNA pathway.

In vitro reconstitution allows dissecting the RNAi machinery in a well-defined system and provides greater understanding of the mechanisms and regulations of the RNAi pathway. The minimal reconstituted system will enable us to identify regulators of the RNAi pathway by “biochemical supplementation”. To reconstitute the miRNA pathway *in vitro*, the generation of recombinant AGO1 is essential because AGO1 is among one of the main components of miRISC (Okamura et al., 2004). The Ago family of proteins contains two signature domains, PAZ and PIWI. The PIWI domain resembles the structure of RNase H and functions as the slicer of RISC that cleaves the target mRNA (Liu et al., 2004; Song et al., 2004). Among the four human Ago

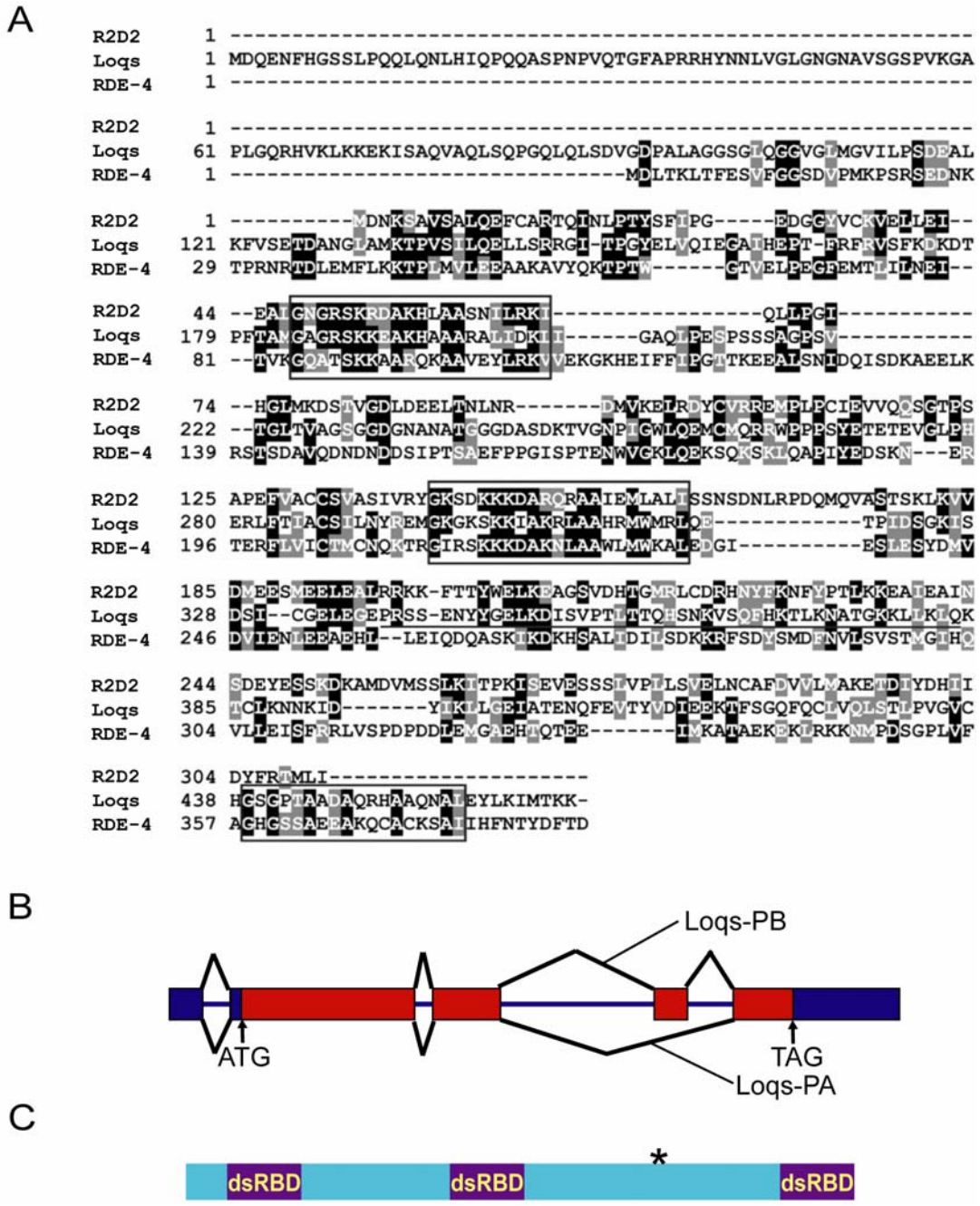

Figure 4.1. The discovery of Loqs. (A) Sequence alignment of Loqs-PB, R2D2, and RDE-4. Boxes refer to the most conserved motifs of three putative dsRNA-binding domains. The underlined region represents 46 amino acids encoded by exon 4 that is alternatively spliced and present only in Loqs-PB. **(B)** A schematic diagram showing alternative splicing of Loqs-PB and Loqs-PA. Exons are shown as boxes with blue color representing untranslated region (UTR) and red color representing protein coding region. **(C)** A diagram showing the predicted dsRNA-binding domains in loqs. The star represents the relative position where exon 4 encoding peptide locates.

proteins, the slicer activity has only been demonstrated for AGO2 (Liu et al., 2004; Meister et al., 2004b; Rivas et al., 2005). In Chapter III, I have shown that *Drosophila* AGO2 possesses slicer activity and recombinant AGO2, together with recombinant Dcr-2/R2D2 complex, could reconstitute the *Drosophila* siRNA pathway in the test tube. Thus, questions remain to be answered whether *Drosophila* AGO1 also functions as a slicer and whether recombinant AGO1 plus recombinant Dcr-1/Loqs complex would reconstitute the miRNA pathway *in vitro*.

Materials and methods

Cloning, expression, and purification of recombinant proteins

Total RNA was isolated from 4 $\times$ 10^6 S2 cells by TRIzol (Invitrogen). RT-PCR reactions were performed using the SuperScript III reverse transcriptase (Invitrogen). In brief, the RT-PCR reaction was set up as follows: 1 μg RNA was used in a 20 μl reaction of reverse transcription, and 1 μl of the RT product was used in a 25 μl PCR reaction. The cDNAs of Dcr-1, loqs and AGO1 were amplified using primers including 5'-CATATGGCGTTCCACTG GTGCGACAAC-3' and 5'-AAGCTTGTCTTTTTTGGCTATCA -3' for Dcr-1 (6.75 kb), 5'-ATGGACCAGGAGAATTTCCACGGC -3' and 5'-GCGGCCGCCTACTTCTTGGTCAT GATCTTCAAG -3' for loqs (1.4 kb), and 5'-CATATGTCCACGGAGCGTGAGCTGGC-3' and 5'-CTCGAGGGCAAAGTACATGACCTTCTTG-3' for AGO1 (2.85 kb). All PCR

products were resolved by 1.2% agarose gel electrophoresis. The cDNAs were cloned into modified pFastBac (with 6× His added by oligo) (Invitrogen). Polyhistidine (His)-tagged recombinant proteins were expressed in insect cells by using the Bac-to-Bac baculovirus expression system (Invitrogen) as described in Chapter II. Loqs-PB, Loqs-PA and AGO1 were His-tagged at the N terminus, whereas Dcr-1 was double His-tagged at both ends.

Antibodies and co-IP

The anti-Dcr-2, anti-R2D2 and anti-AGO2 antibodies have been described in Chapter II. The anti-Loqs antibody was raised in rabbits against full-length recombinant Loqs-PB and further affinity purified as described in Chapter II. The anti-Dcr-1 antibody were a generous gift from Dr. Gregory Hannon (Cold Spring Harbor Laboratory, Cold Spring Harbor, NY) (used for IPs), and purchased from Abcam (used for Western blots). The anti-GFP and anti-AGO1 antibodies were from Molecular Probes and Abcam respectively. Co-IP experiments were carried out in 500 μL volume by incubating 2 mg of S100, 10 μL of affinity-purified antibodies, and 10 μL protein A-Sepharose beads (Santa Cruz) for 2 hrs in RISC buffer (110 mM KOAc, 10 mM HEPES at pH 7.4, 2 mM $Mg(OAc)_2$, 5 mM DTT, 0.05% NP-40). The beads were washed six times with 1 mL RISC buffer containing 50 mM NaCl, and boiled in 2x SDS sample buffer prior to Western blot analysis.

RNAi in S2 Cells

In a 24-well dish, 1×10^6 S2-GFP cells were soaked in 0.5 mL serum-free media (SFM) (Invitrogen) containing 10–15 μg dsRNA for 36 hrs, followed by a second dose for another 36 hrs. Following RNAi treatment, whole cell lysates were prepared in 2% SDS buffer for Western blotting. For Northern blotting, a 6-well dish was used instead, and the number of cells and the amount of dsRNA were 4 fold as much as were used in a 24-well. Total RNA was isolated using TRIzol (Invitrogen) for Northern blotting.

The primers used to make DNA templates for dsRNA include:

(T7= 5'-GTAATACGACTCACTATAGG-3')

dsGFP (550 bp): 5'-T7-GGCGACGTAAACGGCCACA-3' and 5'-T7-GGCAGGACCATGTGATCGCG-3'

dsAGO1 (900 bp): 5'-T7-GACAGCGGTGCATTAAAAAG-3' and 5'-T7-GTCAATTCGTGTTGCAGGAC-3'

dsDcr-1 (600 bp): 5'-T7-CGTAGTCCACTGCTGCACT-3' and 5'-T7-CTATCAAGCCCTGCTTTT-3'

dsDcr-2 (600 bp): 5'-T7-CGGAGAACGCAAAGCTCTC-3' and 5'-T7-CGTCGCATTTGCTTAGCTG-3'

dsLoqs (1.15 kb): 5'-T7-GCACTATAATAACCTTGTCG-3' and 5'-T7-GAACTGGCCAGAGAAGGTCT-3'

dsR2D2 (900 bp): 5'-T7-ATAACAAGTCAGCCGTATC-3' and 5'-T7-AATCAACATGGTGCGAAAA-3'

Northern blot

Total RNA was isolated from S2 cells, wild-type, heterozygous, and homozygous loqs^{PB} young adult flies by using TRIzol (Invitrogen), resolved by 12% denaturing (7 M urea) polyacrylamide gels, and transferred onto Zeta-probe membrane (Bio-Rad). While 20 μg total RNA from S2 cells were loaded per lane (Fig. 1), 30 μg of total RNA were used for whole flies. After transfer, the membranes were UV cross linked at 120 mjoules and then baked in an 80°C oven connected to a vacuum. Northern hybridization and washes were all carried out at 40°C. The membranes were pre-hybridized in 0.2 M sodium phosphate (pH 7.0) plus 7% SDS for 1 hr and then hybridized in the same solution with radioactive probes added for 16 hrs. Following two washes in 2× SSC plus 0.1% SDS for 20 min, the final wash was in 0.5× SSC plus 0.1% SDS for 20 min.

All probes for Northern blotting were custom ordered oligos from IDT, and they were radiolabeled at the 5' end by T4 polynucleotide kinase using γ-32P ATP (10 mCi/ml, MP). The sequences are: a DNA oligo, 5'-GGCCGACAAAATCAGCTTTCAAAATGATCTCACTTGT-3', for bantam in S2 cells; a DNA oligo, 5'-TAC AACCCTCAACCATATGTAGTCCAAGCA-3', for 2SrRNA; and an RNA oligo, 5'-UCGUACCAGAUAGUGCAUUUUCA-3', for miR277 in flies.

Gel mobility shift assays

The assay was performed as the pre-miRNA processing assay (as described in

Chapter II) except for using 1×10^5 cpm pre-let7 in the presence of 0.2 mM Mg^{2+} and 2.5 mM EDTA. let-7/let-7* duplex was radiolabled at the 5' end by T4 polynucleotide kinase (NEB) using γ-^{32}P ATP (10 mCi/ml, MP). In a 10 µl reaction, 5×10^4 cpm radiolabeled let-7/let-7* duplex was incubated with recombinant proteins at 30ºC for 30 minutes in 50 mM KOAc, 12 mM HEPES, pH 7.4, 0.8 mM $Mg(OAc)_2$, and 2.5 mM DTT. After addition of 1.5 µl 10× DNA loading dye, the reaction mixture was resolved on a 5% native PAGE.

RISC assays

pre-bantam initiated RISC assay was performed as all other RISC assays as described (Chapter II) except for using 200 nM pre-bantam in 10 mM HEPES, pH 7.4 and 10 mM $Mg(OAc)_2$. Synthetic 60 nt pre-bantam was custom ordered from Dharmacon, and phosphorated using cold ATP (Promega) by T4 polynucleotide kinase at the 5' end. The sequence of pre-bantam is: 5'-CCGGUUUUCGAUUUGGUUUGACUGUUUUUCAUAC AAGUGAGAUCAUUUUGAAAGCUGAUU-3'.

Generation of loqs or dcr-1 null egg extracts

To generate loqs null egg extract, mosaic germlines were generated by crossing virgin female flies of yw [hsFLP]; *loqs*^{KO} [FRT]40A/CyO (Park et al., 2007) with male flies of ovo^{D1-18} [FRT]40A/MS(2)M^1 Sp/CyO (BL# 2121). The parents were flipped into fresh bottles every 3–4 days and the progenies were heat shocked in a

38°C water bath for 1.5 hrs/day for two consecutive days. After enclosing, we sorted F1 virgin mosaic females with the genotype yw [hsFLP]/+; *loqs*^{KO} [FRT]40A/ ovo^{D1-18} [FRT]40A. Similarly, we used virgin female flies of yw[hsFLP]; [FRT]40A/Cyo to generate wild-type control eggs. For *dcr-1* null extract, virgin female flies of yw [hsFLP]; [FRT]82B *dcr-1*^{Q1147X}/TM3 (Lee et al., 2004b) were crossed with male flies of w*; [FRT]82B ovo^{D1-18}/βTub85D^{D}/TM3 (BL# 2149). We sorted F1 virgin mosaic females with the genotype yw[hsFLP]/w*; [FRT]82B *dcr-1*^{Q1147X} /[FRT]82B ovo^{D1-18}.

Because ovo^{D1-18} is a dominant sterile marker, mature oocytes can only develop from germline stem cells (GSCs) that lack ovo^{D} and are homozygous for *loqs*^{KO} or *dcr-1*^{Q1147X} mutation, which are generated by the Flipase (FLP)/FRT-mediated mitotic recombination (Fig. 4.2). Thus, the F1 virgin mosaic females could produce 100% of

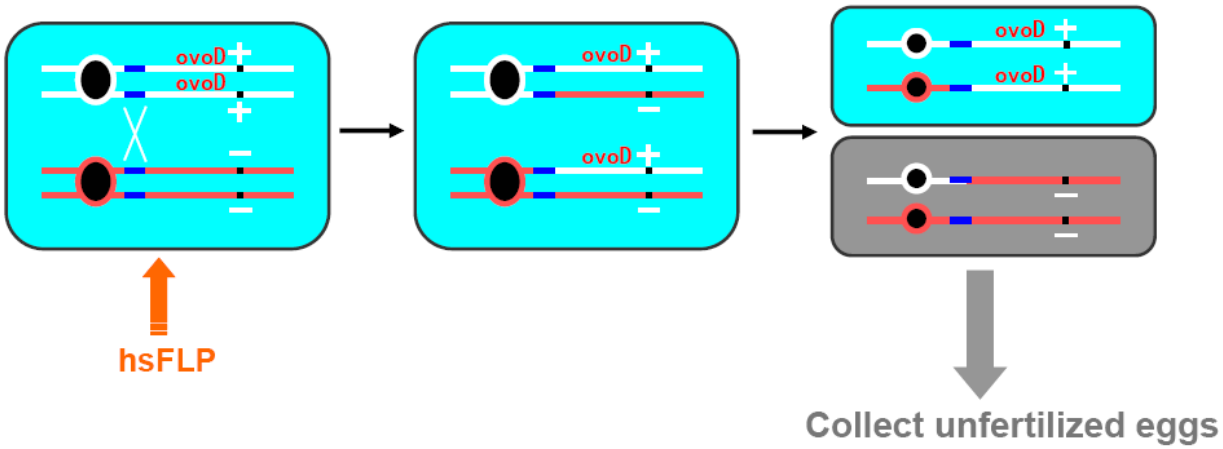

Figure 4.2. The schematic presentation of FLP/ovo^{D} system. To bypass the lethality of homozygous *dcr-1* or *loqs* animals and *dcr-1* or *loqs* obtain null extract, the FLP/ovo^{D} system was used. During mitosis, upon induction of Flipase (FLP) expression by heat shock, the chromosome arms exchange position at the site of FRT. After segregation of sister chromatids, one daughter cell may result in carrying two copies of the mutant gene and may give rise to mature oocyte during differentiation. Mature oocytes will not develop from germline stem cells (GSCs) that contain ovo^{D} because ovo^{D1-18} is a dominant sterile marker. Thus, all the eggs laid contain two copies of mutant gene.

loqs^{KO} or *dcr-1*^{Q1147X} mutant eggs. Only a small time window allowed for mutant egg collection because Dcr-1 and Loqs were both required for self-renewal of GSCs (Jin and Xie, 2007; Park et al., 2007). This procedure was optimized to generate thousands of F1 mosaic virgin females and collect *loqs* or *dcr-1* mutant eggs every 24 hrs on apple juice plates with wet yeast paste.

The harvested unfertilized eggs were treated with 50% bleach for 1 min followed by washing twice with PBS and once with buffer A (10 mM KOAc, 10 mM HEPES at pH 7.4, 10 mM Mg(OAc)2, and 5 mM DTT). Subsequently, dechorinated eggs were resuspended in three volumes of buffer A that were freshly supplemented with protease inhibitors (Roche). After sitting on ice for 15 min, the eggs were dounced 30 times followed by centrifugation at 13,000 rpm for 20 min at 4°C. The supernatant was *dcr-1* or *loqs* null extracts and was stored in a –80°C freezer.

Partial purification of endogenous miRISC

All purification steps were carried out at 4ºC. Q-Sepharose column was purchased from GE. 1 ml of S100 (~ 15 mg/ml)was diluted to 5 ml in buffer A, filtered by 0.22 μm syringe filter (Nalgene), and then loaded to 1 ml Q-Sepharose column. The column was washed with 10 ml buffer A and eluted in buffer A containing 1M NaCl. The two protein peak fractions were pooled together and dialyzed in buffer A overnight. 2 μl of input, Q column flow-through (FT), or Q bound was used in each RISC reaction.

0.5 ml of S100 was precipitated by ammonium sulfate (AS) at 10%, 20%, 30%

or 40% saturation. After a 30-min rotation at 4ºC and a 30-min 20,000g spin, the pellet was dissolved in buffer A and the supernatant was dialyzed in buffer A overnight. In each RISC reaction, 2 μl of each fraction was used.

Results

Loqs-PB interacts with Dcr-1 and AGO1

To test physical association of endogenous Dicer-1 and Loqs, I performed coimmunoprecipitation (co-IP) experiments by using anti-Dcr-1 or anti-Loqs antibodies in the cytosolic (S100) extracts of S2 cells. Loqs-PB (~55 kDa) was present in the IPs of anti-Dcr-1 but not anti-Dcr-2 antibodies (Fig. 4.3.A). We could not detect the presence of Loqs-PA (~50 kDa) probably because it was either absent or masked by the Immunoglobin (IgG) heavy chain (Fig. 5.3.A). Reciprocal IP using anti-Loqs antibody brought down Dcr-1 but not Dcr-2, whereas anti-R2D2 antibody only brought down Dcr-2 (Fig. 4.3.B). In addition, both Dcr-1 and Loqs interacted with AGO1 (Fig. 4.3.A & B), a critical component of miRISC (Okamura et al., 2004). These studies indicate that endogenous Loqs-PB specifically associates with Dcr-1 and AGO1, which are key components of the initiation and effector complexes of the miRNA pathway.

Loqs-PB enhances miRNA production by Dicer-1

Using Bac-to-Bac expression system, we successfully expressed and purified

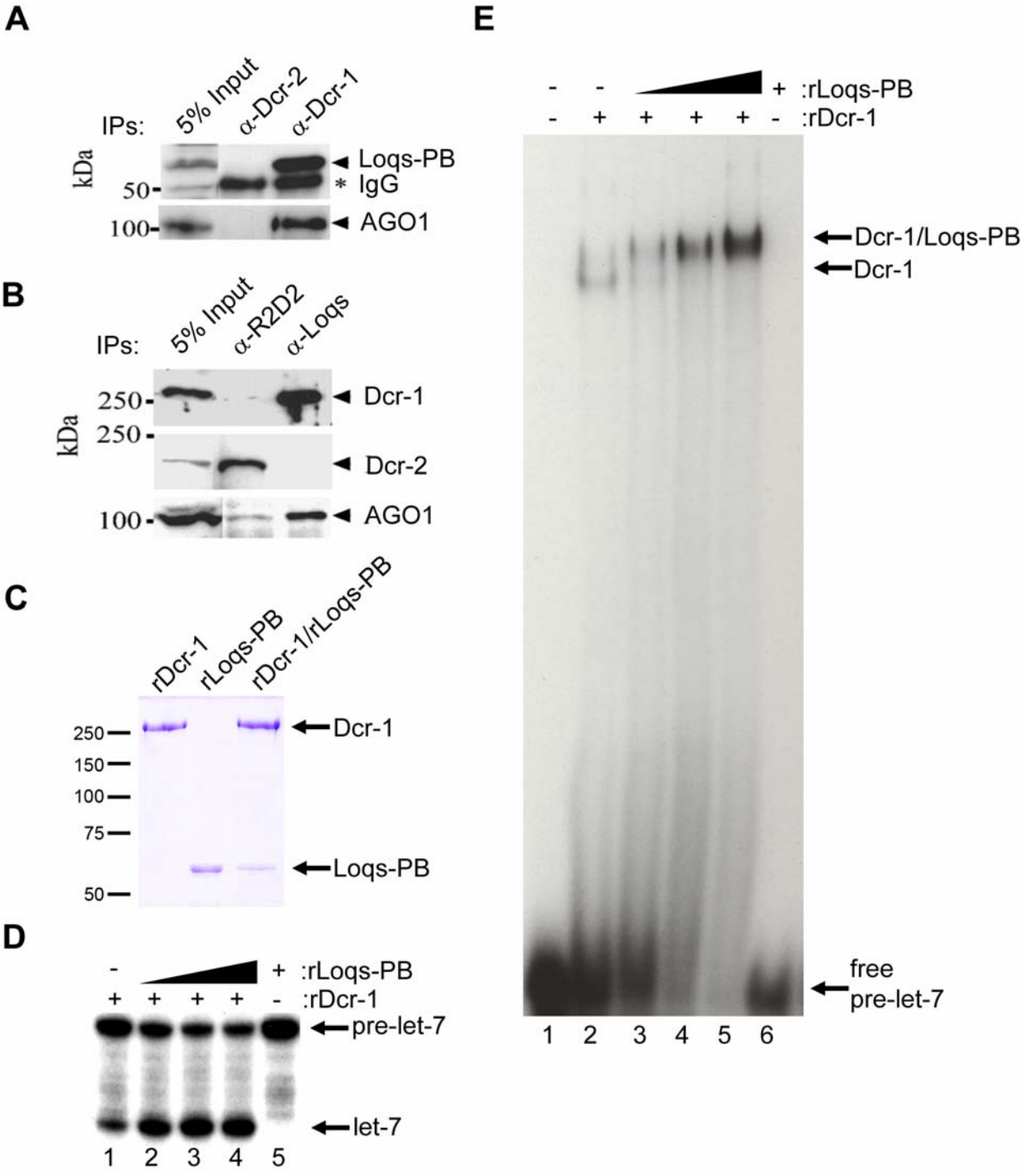
A
IPs:
5% Input
α-Dcr-2
α-Dcr-1
kDa
50
100
Loqs-PB
* IgG
AGO1
B
IPs:
5% Input
α-R2D2
α-Loqs
kDa
250
250
100
Dcr-1
Dcr-2
AGO1
C
rDcr-1
rLoqs-PB
rDcr-1/rLoqs-PB
250
150
100
75
50
Dcr-1
Loqs-PB
D
- + :rLoqs-PB
+ + + + - :rDcr-1
pre-let-7
let-7
1 2 3 4 5
E
- - + :rLoqs-PB
- + + + + - :rDcr-1
Dcr-1/Loqs-PB
Dcr-1
free
pre-let-7
1 2 3 4 5 6

Figure 4.3. Loqs-PB is a cofactor for Dcr-1. (A) Co-immunoprecipitations (coIPs) were performed in S100 of S2 cells with anti-Dcr-1 or anti-Dcr-2 antibodies followed by Western blot using anti-Loqs or anti-AGO1 antibodies. The asterisk refers to IgG heavy chain, which co-migrates with Loqs-PA. **(B)** coIPs were performed with anti-R2D2 or anti-Loqs antibodies followed by Western blots with corresponding antibodies to detect Dcr-1, Dcr-2, and AGO1. S100 lanes represent 5% input for IPs. **(C)** A Coomassie blue-stained SDS–polyacrylamide gel (PAGE) showing purified recombinant Dcr-1, Loqs-PB, and Dcr-1/Loqs-PB complex. Courtesy of Dr. Xuecheng Ye. **(D)** Loqs-PB enhances miRNA production by Dcr-1. The pre-miRNA-processing assays were performed with 25 pmol Dcr-1 alone (lane 1) or in combination with 30, 100, or 300 pmol Loqs-PB (lanes 2-4), or 300 pmol Loqs-PB (lane 5). Courtesy of Dr. Xuecheng Ye. **(E)** Loqs-PB increases Dcr-1's affinity for pre-miRNA. The gel-shift assays were performed without Mg^{2+}, in buffer alone (lane 1) or with 1 nmol Dcr-1 alone (lane 2) or in combination with 1, 3, or 10 nmol Loqs-PB (lanes 3–5), or 10 nmol Loqs-PB alone (lane 6).

recombinant Dcr-1, Loqs, and Dcr-1/Loqs complex (Fig. 4.3.C, data by Dr. Xuecheng Ye). Recombinant Dcr-1 and Loqs-PB, formed a stable complex and cofractionated on multiple columns (final fraction shown in Fig. 4.3.C, lane 3). Addition of purified Loqs-PB to Dcr-1 greatly enhanced its miRNA-generating activity in a dose-dependent manner (Fig. 4.3.D, data by Dr. Xuecheng Ye). Purified Loqs-PA has a similar role but to a lesser degree (data by Dr. Xuecheng Ye, not shown). To compare the substrate affinity of Dcr-1 and Dcr-1/Loqs-PB, I performed gel mobility shift experiments in the absence of Mg^{2+}, which blocked cleavage activity of pre-miRNA by Dcr-1 (Fig. 4.3.E). Addition of Loqs-PB to Dcr-1 greatly enhanced its affinity for pre-miRNA in a dose-dependent manner (Fig. 4.3.E). Taken together, these studies suggest that Loqs-PB can enhance miRNA-generating activity of Dcr-1 by increasing its substrate affinity.

Loqs-PB is required for miRNA biogenesis in S2 cells

To determine if Loqs is required for miRNA biogenesis *in vivo*, I knocked down Dcr-1, Loqs, or both in S2 cells by RNAi followed by Northern blotting to measure the levels of pre-bantam and bantam miRNA. Surprisingly, only Loqs-PB (~55 kDa), but not Loqs-PA (~50 kDa), protein level was efficiently knocked down by treatment of dsLoqs (Fig. 4.4.A, lanes 6 and 7). The Loqs (~1.1 kb) dsRNA should efficiently target both Loqs-PB and Loqs-PA mRNA, which differ by 138 nt. It was likely that Loqs-PA co-migrated with a cross-reacting protein on the Western blot. As shown previously (Okamura et al., 2004), depletion of AGO1, a key component of miRISC, resulted in a specific reduction of bantam miRNA in S2 cells (Fig. 4.4.B, cf. lanes 3 and 1,2). On the other hand, knocking down Dcr-1 caused accumulation of pre-bantam but no reduction in bantam (Fig. 4.4.B, cf. lanes 4 and 1, 2). Targeting Loqs produced a similar phenotype as Dcr-1 depletion (Fig. 4.4.B, cf. lanes 4 and 6). When Dcr-1 and Loqs were both targeted, there was a greater accumulation of pre-bantam and a modest reduction in bantam (Fig. 4.4.B, lane 7). Since RNAi is transient and rarely a complete knockout, the lack of significant bantam reduction is probably because the remaining Dcr-1 is sufficient to maintain the level of miRNA production. Consistent with these results, the pre-miRNA processing activity was significantly reduced S2 cell extract from Dcr-1, Loqs or both targeted cells (Fig. 4.4.C). By quantitation through Phosphor Imager, the activity in Dcr-1 or Loqs depleted cells was one half of dsGFP treated cells, and one third in cells of double RNAi treatment (Fig. 4.4.D). Thus, like Dcr-1, Loqs is required for miRNA generation in S2 cells.

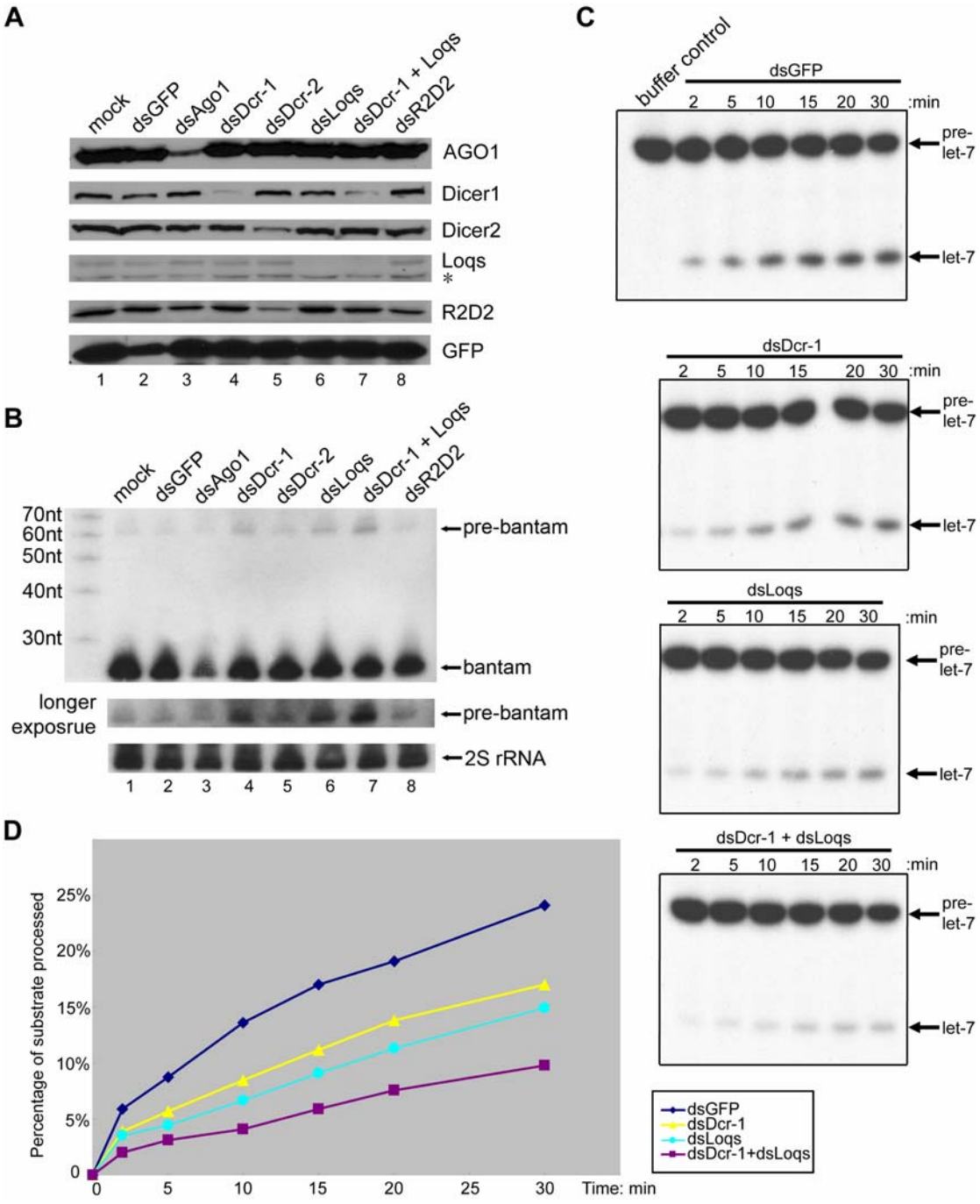
A
mock
dsGFP
dsAgo1
dsDcr-1
dsDcr-2
dsLoqs
dsDcr-1 + Loqs
dsR2D2
AGO1
Dicer1
Dicer2
Loqs
*
R2D2
GFP
1 2 3 4 5 6 7 8
B
mock
dsGFP
dsAgo1
dsDcr-1
dsDcr-2
dsLoqs
dsDcr-1 + Loqs
dsR2D2
70nt
60nt
50nt
40nt
30nt
pre-bantam
bantam
longer exposrue
pre-bantam
2S rRNA
1 2 3 4 5 6 7 8
C
buffer control
dsGFP
2 5 10 15 20 30 :min
pre-let-7
let-7
dsDcr-1
2 5 10 15 20 30 :min
pre-let-7
let-7
dsLoqs
2 5 10 15 20 30 :min
pre-let-7
let-7
dsDcr-1 + dsLoqs
2 5 10 15 20 30 :min
pre-let-7
let-7
D
Percentage of substrate processed
25%
20%
15%
10%
5%
0
0 5 10 15 20 25 30 Time: min
dsGFP
dsDcr-1
dsLoqs
dsDcr-1+dsLoqs

Figure 4.4. Loqs-PB is required for miRNA biogenesis in S2 cells. (A) Western blots were performed with corresponding antibodies to measure the protein levels in S2/GFP cells following various dsRNA treatments. The asterisk refers to Loqs-PA and a co-migrating cross-reacting protein. **(B)** Northern blots were performed to measure the levels of pre-bantam and bantam miRNA. In the middle panel, a longer exposure was used to obtain clear signals of pre-bantam. 2S rRNA was used as loading control. **(C)** The pre-miRNA processing assays were performed in a time-course experiment with 4 μg of extracts from S2/GFP cells treated with dsRNA of GFP (top), Dcr-1 (middle top), Loqs (middle bottom), or Dcr-1 + Loqs (bottom). **(D)** The results shown in panel C was quantified using Phosphor Imager and plotted against time. Blue line represents activity from dsGFP treated cells, yellow line represents activity from dsDcr-1 treated cells, green line represents activity from dsLoqs treated cells, and purple line represents activity from dsDcr-1 plus dsLoqs treated cells,

loqs mutant flies are defective for miRNA biogenesis

To study the physiological function of R3D1 in flies, we obtained a piggyBac (PB) fly strain in which the piggyBac transposon was inserted in the vicinity of the Loqs gene (Bloomington, #18371). By cloning and sequencing the flanking sequences, we found that the PB-element was inserted within the first exon and 221 nt upstream of the translational start codon of the loqs gene (Fig. 4.5.A, data by Dr. Xiang Liu). The levels of Loqs-PB and Loqs-PA mRNA were dramatically reduced in the homozygous flies when compared with wild type or heterozygotes by semiquantitative RT–PCR (Jiang et al., 2005). However, we could not verify corresponding reductions in Loqs protein levels by Western blots due to masking by cross-reacting proteins (data by Dr. Xiang Liu, not shown). Nevertheless, this suggests that the PB-insertion creates a hypomorphic mutant allele of the loqs gene by attenuating its transcription.

To examine if miRNA biogenesis was defective in the *loqs*^{PB} mutant flies, the levels of pre-miR277 and miR-277 in wild-type, heterozygous, and homozygous adult flies were compared. As shown by Northern blots, there was significant accumulation

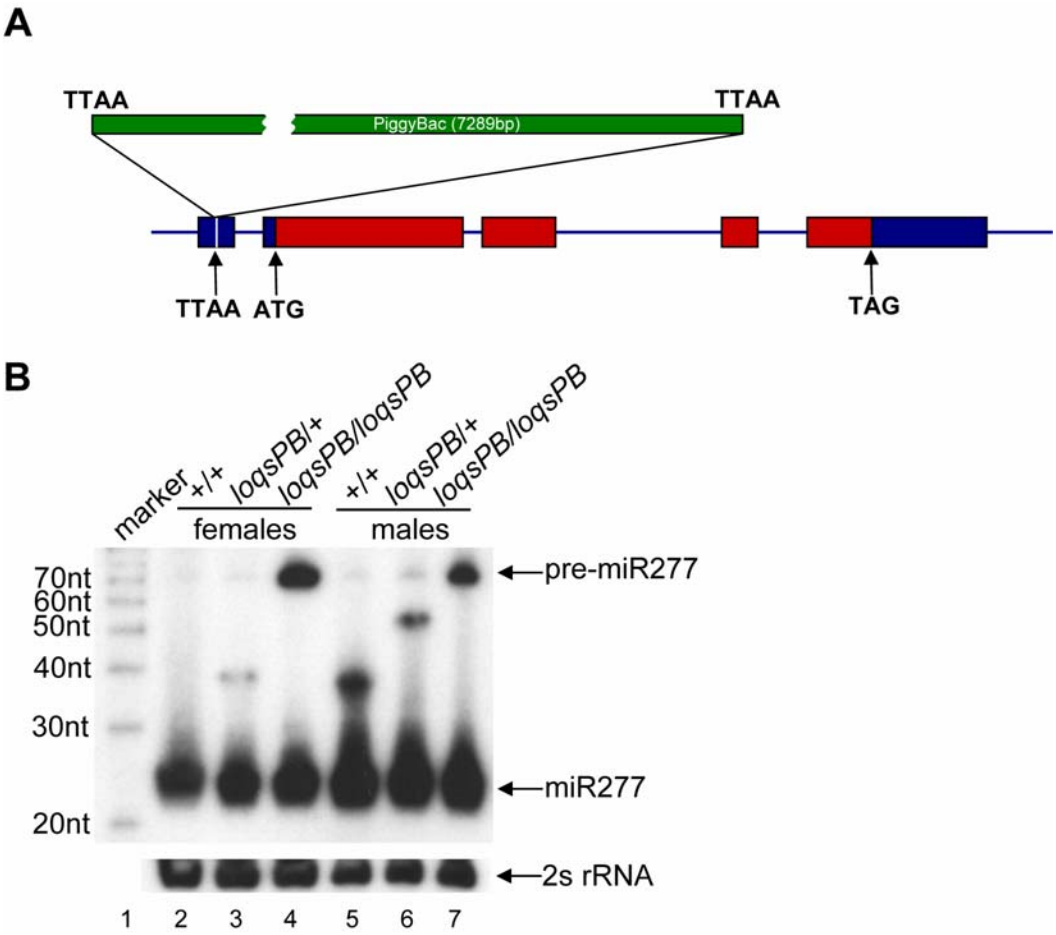

Figure 4.5. Loqs mutant flies are defective in miRNA biogenesis. (A) A schematic diagram of the insertion site of piggyBac. **(B)** The levels of pre-miR277 and miR277 were measured by Northern blots in wild-type, heterozygous, and homozygous *loqs*^{PB} female (lanes 2-4) and male (lanes 5-7) flies. Lane 1 are RNA markers.

of pre-miR277 in both male and female homozygotes (Fig. 4.5.B). The lack of reduction in mature miR277 may be explained by the fact that *loqs*^{PB} is a partial loss-of-function allele. These data may also suggest that miRNA production is not the rate-limiting step in the *Drosophila* miRNA pathway. Together, these results indicate that *loqs*^{PB} mutant flies are defective for miRNA biogenesis.

Dcr-1, but not loqs, is required for RISC activity

In the siRNA branch of RNAi pathway in *Drosophila*, both Dcr-2 and R2D2 are critical components of the RISC loading complex (RLC), the formation of which precedes and is required for RISC activation (Pham et al., 2004; Pham and Sontheimer, 2005; Tomari et al., 2004a). Dcr-2 and R2D2 coordinately bind siRNAs to promote efficient assembly of the siRISC complexes (Liu et al., 2003; Liu et al., 2006; Tomari et al., 2004b). It will be important to determine if Dcr-1 and Loqs play a similar role in loading miRNAs onto the miRISC complexes. To examine this possibility, I first performed native gel-shift assays to compare the binding of recombinant Dcr-1 proteins to a radiolabeled let-7/let-7* duplex in the absence or presence of Loqs-PA and Loqs-PB. Recombinant Dcr-1 alone efficiently interacted with miRNA duplex (Fig. 4.6.A, lane 3), while neither Loqs-PB or Loqs-PA interacted with miRNA duplex (Fig. 4.6.A, lanes 4-7). Loqs-PA reduced the binding of Dcr-1 to let-7/let-7* duplex (Fig. 4.6.A, lane 8), and Loqs-PB slightly enhanced it (Fig. 4.6.A, lane 9). Adding all three recombinant proteins together showed similar binding affinity as Dcr-1 alone (Figl 4.6.A, lane 10). By contrast, only Dcr-2/R2D2 complex,

but neither Dcr-2 nor R2D2 alone, efficiently interacts with duplex siRNA (Liu et al., 2006).

To determine if Dcr-1 and Loqs were required for Drosophila miRISC assembly, *dcr-1* or *loqs* null extract were generated by using the FLP/ovo^{D} system (Chou et al., 1993). This mosaic germline system allowed us to bypass the lethality of homozygous *dcr-1*^{Q1147X} or *loqs*^{KO} animals and to produce only mutant eggs that lack maternal and zygotic Dcr-1 or Loqs proteins (Fig. 4.2). The *dcr-1*^{Q1147X} was considered a null allele because of a nonsense mutation before the catalytic RIII domains (Lee et al., 2004b). The *loqs*^{KO} animals were generated by ends-out homologous recombination (Park et al., 2007), and it was also considered as a null allele.

In vitro assays were performed using wild-type (WT), *dcr-1* or *loqs* null extracts. While all extracts possessed similar dsRNA processing activity (Fig. 4.6.B), the duplex siRNA induced RISC activity was greatly diminished in *dcr-1* null extract (Fig. 4.6.C, lane 3). The role of Dcr-1 in siRISC assembly was consistent with previous analysis of the *dcr-1*^{Q1147X} mutant (Lee et al., 2004b). miRNA duplex initiated RISC activity was also significantly impaired in *dcr-1* null extract (Fig. 4.6.D, lane 3). The minimal RISC – single-stranded let-7 initiated RISC activity was modestly reduced in *dcr-1* null extract (Fig. 4.6.E, lane 3), suggesting the absence of Dcr-1 affects the catalytic activity of AGO1 or AGO2. In contrast, we observed equivalent siRNA and miRNA duplex, single-stranded RNA initiated RISC activities between wild-type and *loqs* null extracts (Fig. 4.6.C-E), suggesting that Dcr-1, but not Loqs, is critical for *Drosophila* RISC assembly.

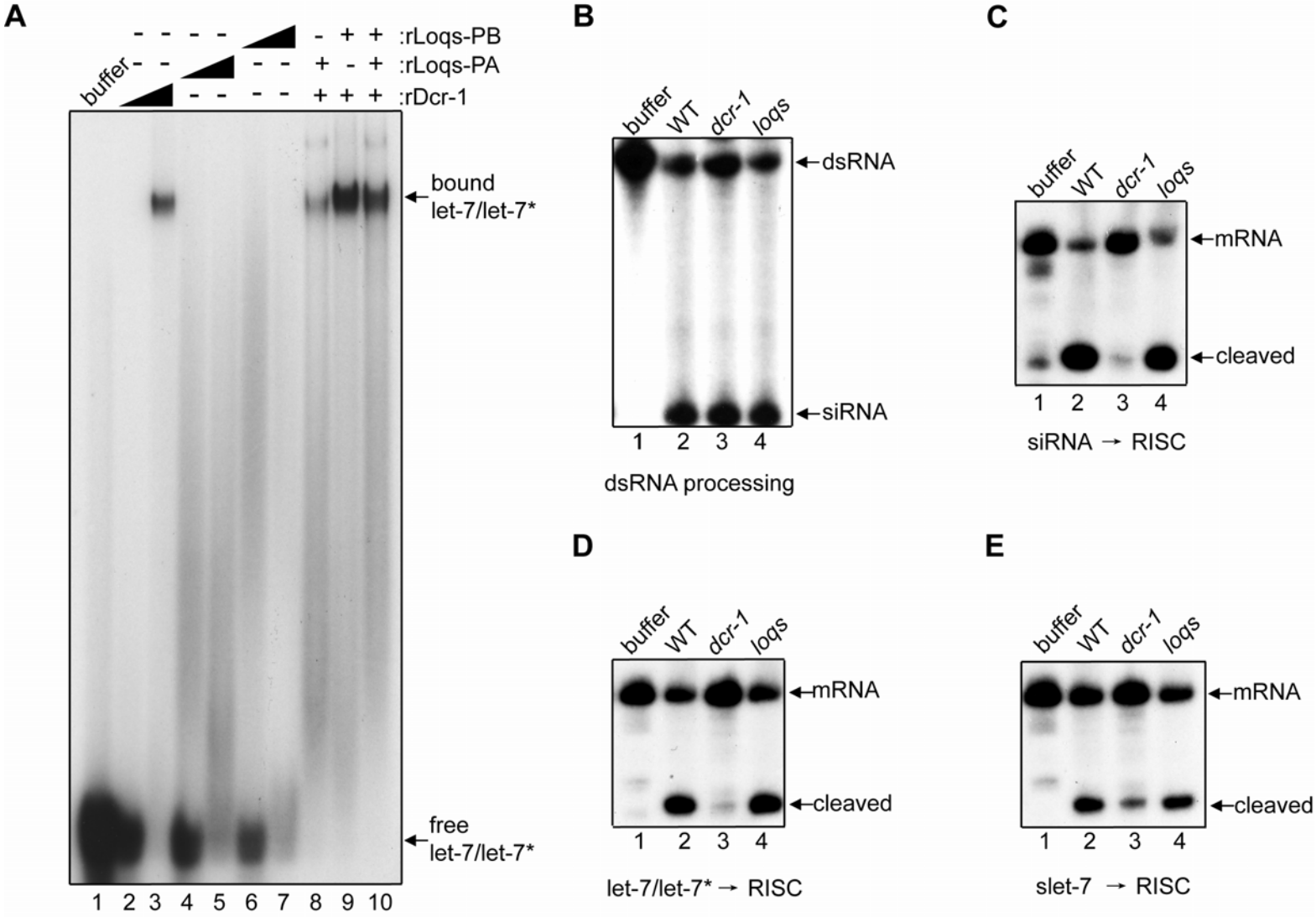
A
:rLoqs-PB
:rLoqs-PA
:rDcr-1
buffer
bound
let-7/let-7*
free
let-7/let-7*
1 2 3 4 5 6 7 8 9 10
B
buffer
WT
dcr-1
loqs
dsRNA
siRNA
1 2 3 4
dsRNA processing
C
buffer
WT
dcr-1
loqs
mRNA
cleaved
1 2 3 4
siRNA → RISC
D
buffer
WT
dcr-1
loqs
mRNA
cleaved
1 2 3 4
let-7/let-7* → RISC
E
buffer
WT
dcr-1
loqs
mRNA
cleaved
1 2 3 4
slet-7 → RISC

Figure 4.6. Dcr-1, but not Loqs, is essential for assembly of RISC complexes. (A) Native gel-shift assays were performed by incubating radiolabeled let-7/let-7* with 2 pmol or 8 pmol recombinant Dcr-1 alone (lanes 2,3), recombinant Loqs-PA alone (lanes 4,5), recombinant Loqs-PB alone (lanes 6,7), or recombinant Dcr-1 in combination with 8 pmol Loqs-PA (lane 8), or Loqs-PB (lanes 9), or Loqs-PA + Loqs-PB (lanes 10). **(B)** dsRNA processing assay was performed in buffer (lane 1) or 25 μg wild-type (WT) (lane 2), or *dcr-1* (lane 3), or *loqs* (lane 4) null egg extract. **(C)** Duplex siRNA initiated RISC assay was performed in buffer or 25 μg wild-type (WT) (lane 2), or *dcr-1* (lane 3), or *loqs* (lane 4) null egg extract. **(D)** Duplex miRNA initiated RISC assay was performed in buffer or 25 μg wild-type (WT) (lane 2), or *dcr-1* (lane 3), or *loqs* (lane 4) null egg extract. **(E)** Single-stranded let-7 initiated RISC assays was performed in buffer or 25 μg wild-type (WT) (lane 2), or *dcr-1* (lane 3), or *loqs* (lane 4) null egg extract.

Interestingly, the RISC assembly defect of dcr-1 null extract could not be rescued by recombinant Dcr-1 or Dcr-1/Loqs complex (data not shown). It is possible that the lack of Dcr-1 causes reduction in other critical RNAi components. Alternatively, the dcr-1 mutant may fail to produce a miRNA that normally represses an inhibitor of RNAi. *dcr-1* null extract produced an equal level of dsRNA processing activity as WT and *loqs* extracts (Fig. 4.6.B), indicating that it was not completely incapable to possess any *in vitro* RNAi activity. Thus, Dcr-1 is likely to be directly or indirectly involved in miRISC or siRISC assembly.

AGO1 is a slicer

It was previously shown that recombinant human Argonaute 2 could be programmed with a single-stranded siRNA to perform minimal RISC activity (Rivas et al., 2005). This minimal RISC assay is the most straightforward method to determine whether a protein possesses slicer activity. I expressed N-terminal His-tagged *Drosophila* AGO1 by using Bac-to-Bac expression system. Unlike human

Ago2, recombinant *Drosophila* AGO1 was salt-sensitive in that high salt (500 mM NaCl) wash significantly reduced the minimal RISC activity (data not shown). However, without high salt wash, the preparation was very dirty (Fig. 4.7.A, lane 1). To overcome this problem, I engineered another 3× Flag tag between the N-terminal 6× His tag and AGO1. By performing tandem steps of purification, the quality of preparation was significantly improved. There was only one major band visible by coomassie stain (Fig. 4.7.A, lane 2), and it migrated at the molecular weight of 100 kDa, which is the predicted size of *Drosophila* AGO1.

Recombinant fly AGO1 was capable of cleaving the mRNA substrate if programmed by single-stranded RNA (ssRNA) (Fig. 4.7.B). The activity was specific because when ssRNAs targeting different positions of substrate mRNA lead to different sized cleavage product (Fig. 4.7.B). Interestingly, the amount of ssRNA required for generating decent cleavage activity was 20 fold higher in S2 S100 extract than recombinant AGO1. The requirement of large amount of slet-7 in S100 extract can be explained by the abundance of nuclease existing in the extract while single-stranded RNA is extremely susceptible for nuclease degradation. In fact, if large amount of slet-7 was added to recombinant AGO1, the activity became inhibited (data not shown). It is possible that if the ratio of ssRNA versus mRNA substrate becomes too high, all the mRNA will anneal with ssRNA and make it inaccessible for AGO1.

To further demonstrate the slicer activity from recombinant AGO1 is specific, I generated three AGO1 mutants based on the conserved “DDH” catalytic domain

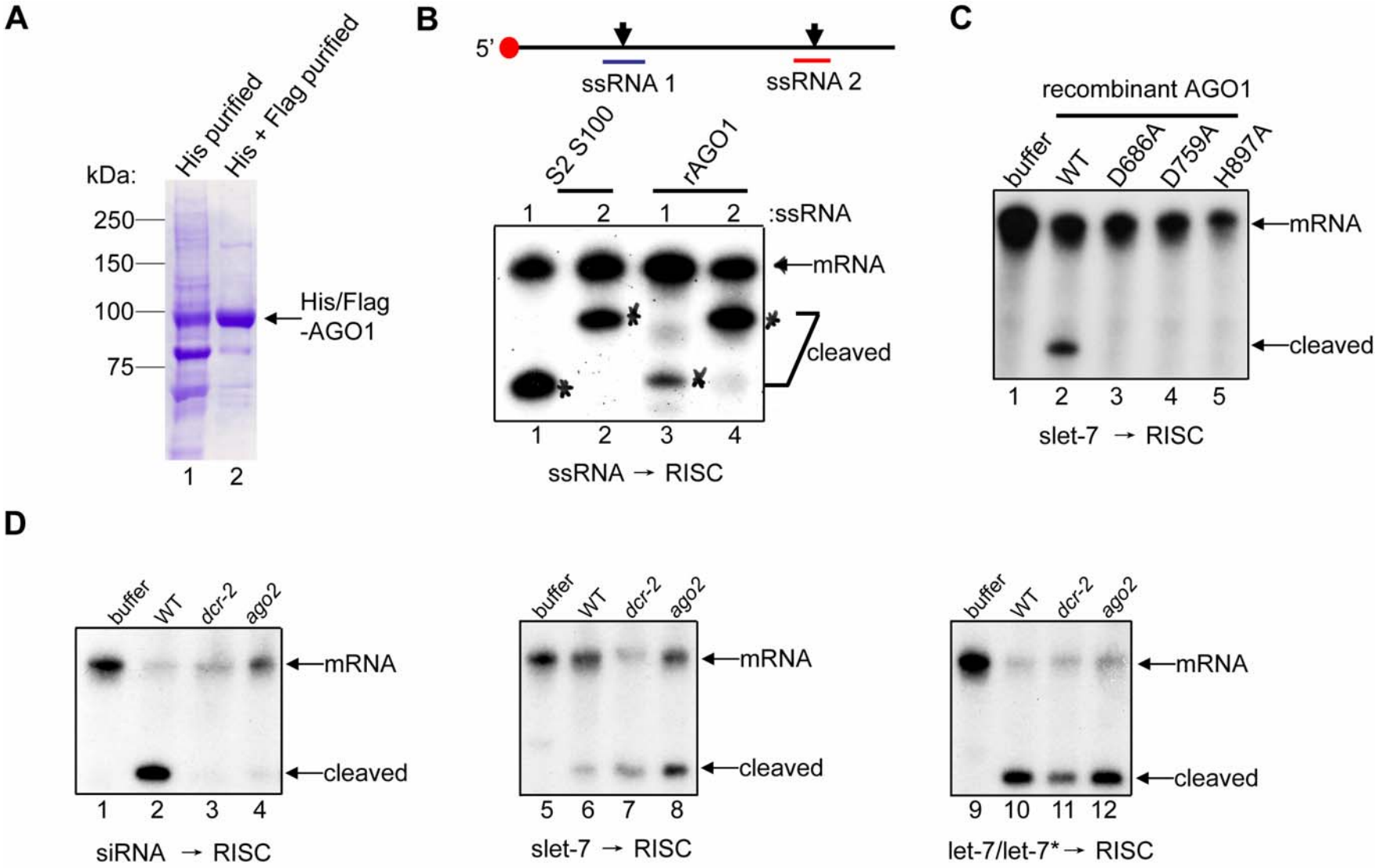
A
His purified
His + Flag purified
kDa:
250
150
100
75
His/Flag
-AGO1
1 2
B
5'
ssRNA 1
ssRNA 2
S2 S100
rAGO1
1 2 1 2 :ssRNA
mRNA
cleaved
1 2 3 4
ssRNA → RISC
C
recombinant AGO1
buffer
WT
D686A
D759A
H897A
mRNA
cleaved
1 2 3 4 5
slet-7 → RISC
D
buffer
WT
dcr-2
ago2
mRNA
cleaved
1 2 3 4
siRNA → RISC
buffer
WT
dcr-2
ago2
mRNA
cleaved
5 6 7 8
slet-7 → RISC
buffer
WT
dcr-2
ago2
mRNA
cleaved
9 10 11 12
let-7/let-7* → RISC

Figure 4.7. AGO1 is a slicer. (A) A Coomassie blue-stained SDS–polyacrylamide gel (PAGE) showing purified recombinant AGO1 after one-step affinity purification – Ni column (lane 1), or two-step affinity purification – Ni column followed by Flag beads (lane 2). (B) Single-stranded RNA (ssRNA) initiated RISC assay was performed with buffer, or 50 μg S2 S100 extract (lane 2), or 10 ng recombinant AGO1. Two ssRNAs containing complementary sequence to the same mRNA were used. The concentration of ssRNA used in S100 was 200 nM, while 10 nM was used for AGO1 catalyzed reaction. **(C)** Single-stranded let-7 initiated RISC assay was performed with buffer, or 10 ng recombinant AGO1 wildtype (WT) (lane 2), or "DDH" mutants (lane 3-6). **(D)** Duplex siRNA (lanes 1-4), sslet-7 (lanes 5-8) and miRNA duplex (lanes 9-12) initiated RISC assays were performed in buffer or 25 μg wild-type (WT), *dcr-2* or *ago2*^{414} ovary extract.

among Argonaute family of proteins. The corresponding "DDH" residues in AGO1 are: aspartate 686, aspartate 759, and histidine 897 (Fig. 4.9, red arrows) and I mutated each residue to alanine. While all three mutants had similar expression levels as the wildtype (WT) (data not shown), only WT AGO1 showed minimal RISC activity (Fig. 4.7.C). Taken together, these results indicate that like *Drosophila* AGO2 and human Ago2, Drosophila AGO1 also has slicer function.

The siRISC and miRISC activity can be distinguished by performing RISC assays in different mutant extracts. The *dcr-2*^{R416X} was considered a null allele because of a nonsense mutation before the catalytic RIII domains (Lee et al., 2004b). The *ago2*^{414} was generated by imprecise excision of EP element which resulted in deletion of exon 1 and 2 of the AGO2 gene and no detectable expression of AGO2 (Okamura et al., 2004). Both homozygous mutant flies are healthy and can be maintained indefinitely. Mutations in AGO1 resulted in lethality during development (Williams and Rubin, 2002), and we are in the process of obtaining *ago1* mutant extract through the FLP/ovo^{D} system. However, we were able to extract some information from *dcr-2* and

ago2 null extracts. Consistently, absence of the two core enzymatic components of the siRISC machinery – Dcr-2 and AGO2, resulted in no siRNA induced RISC activity (Fig. 4.7.D, lanes 1-4), while both minimal RISC and miRNA duplex induced RISC activity remained (Fig. 4.7.D, lanes 5-12). The minimal RISC and miRISC activity was likely contributed by AGO1 since I have previously shown that AGO1 is a slicer, and it is critical for miRNA mediated RNA cleavage *in vivo* (Okamura et al., 2004).

Reconstitution of the miRNA pathway

One of the critical issues for illuminating the molecular mechanisms of the RNAi pathways is to have reconstituted machineries. In the miRNA pathway, we obtained the initiation step enzymatic complex – Dcr-1/Loqs for miRNA biogenesis, and the effector step catalytic component – AGO1 as the slicer in RISC. Then we asked a simple question: if we put all three recombinant proteins together, will RISC cleavage be observed when pre-miRNA is added? At first, when I used pre-let-7 as trigger for RISC reaction, target mRNA was cleaved by recombinant AGO1 alone (data not shown). To dtermine whether AGO1 alone can reconstitute miRISC assembly, careful examination of the structure of pre-miRNA trigger is required. Pre-miRNAs possess a stem-loop structure, and the miRNA can be located on the upper arm (the 5' end, Fig. 4.8.A, structure 1) or the lower arm (the 3' end, Fig. 4.8.A, structure 2). Due to imperfect complementarity in the stem-loop structure, the pre-miRNA could denature at the assay temperature of 30°C and become a single-stranded RNA and be loaded onto AGO1 without being processed by Dcr-1/Loqs. In the case of pre-let-7, the 5'

end 21 nt is identical to mature let-7 sequence (Fig. 4.8.A, structure 1). Since catalytic Argonautes count from the anchored 5' end of the guiding strand and cleave the target RNA at the complementary position between the tenth and eleventh nucleotides of the guiding strand, single-stranded pre-let-7 and let-7 will induce the same cleavage pattern. In this case, recombinant AGO1 could not distinguish the difference between single-stranded pre-let-7 and let-7, and it cleaves the target mRNA guided by single-stranded pre-let -7 without it being processed by Dcr-1/Loqs first.

On the other hand, pre-miRNA possessing the second structure shown in Fig. 4.8.A can not initiate cleavage on an mRNA having only complementary sequence to the mature miRNA because the 5' end of mature miRNA is not exposed. Pre-bantam belongs to this class. When pre-bantam was used as a trigger, no cleavage product by AGO1 alone was detected (Fig. 4.8.B, lane 3). However, while there was RISC activity from S2 cell extract (Fig. 4.8.B, lane 2), miRISC could not be reconstituted by combining recombinant AGO1 with Dcr-1/Loqs complex (Fig. 4.8.B, lane 4). This result suggests that additional factor(s) may be required for the connection between Dicer processing and Ago2 slicing, which is the RISC assembly process.

Partial purification of miRISC

I have established an in vitro system to detect miRISC activity by using pre-bantam initiated RISC assay. Since recombinant Dicer-1, Loqs and AGO1 are not sufficient to reconstitute the miRNA pathway, I tested whether the additional factor(s) could be purified from S2 cell extract. The principle is simple. If the miRISC can be

broken apart and reconstituted by combining different fractions, we would be able to purify the factor(s) essential for miRISC activity. Fractions containing Dcr-1, Loqs, or AGO1 will be excluded through Western blotting. To determine the feasibility of this strategy, I fractionated S2 cell S100 by using Q-Sepharose and found that the activity resided in the Q bound pool (Fig. 4.8. C). This result was surprising because previous study on siRISC showed that siRISC was extremely salt sensitive unless it was pre-loaded with siRNA before high salt exposure (Rand et al., 2004). The salt sensitivity refers to irreversible damage upon salt addition. Thus, there is difference between the physical character of siRISC and miRISC. The salt tolerance of miRISC enables us to further purify the component(s) required for *de novo* RISC assembly.

Ammonium sulfate (AS) precipitation is another common fractionation method of protein purification. It separates proteins with different solubility according to the ionic strength of the solution. Different AS saturations, 10% through 40% with a 10% increment, were examined. miRISC resided in the supernatant of 10 and 20% AS saturation, while it was in the pellet of 30 and 40% (Fig. 4.8.D). A good purification step would be precipitation in 30% AS saturation and then to resuspend the pellet in 20% AS. Western blots showed that Dcr-1 and AGO1 correlated with miRISC activity, while the siRISC components Dcr-2 and AGO2 did not (Fig. 4.8.E). These preliminary experiments suggest miRISC can be purified through traditional biochemical fractionation. This provides a platform to identify unknown factors that are essential for miRISC activity, and much more future work is needed.

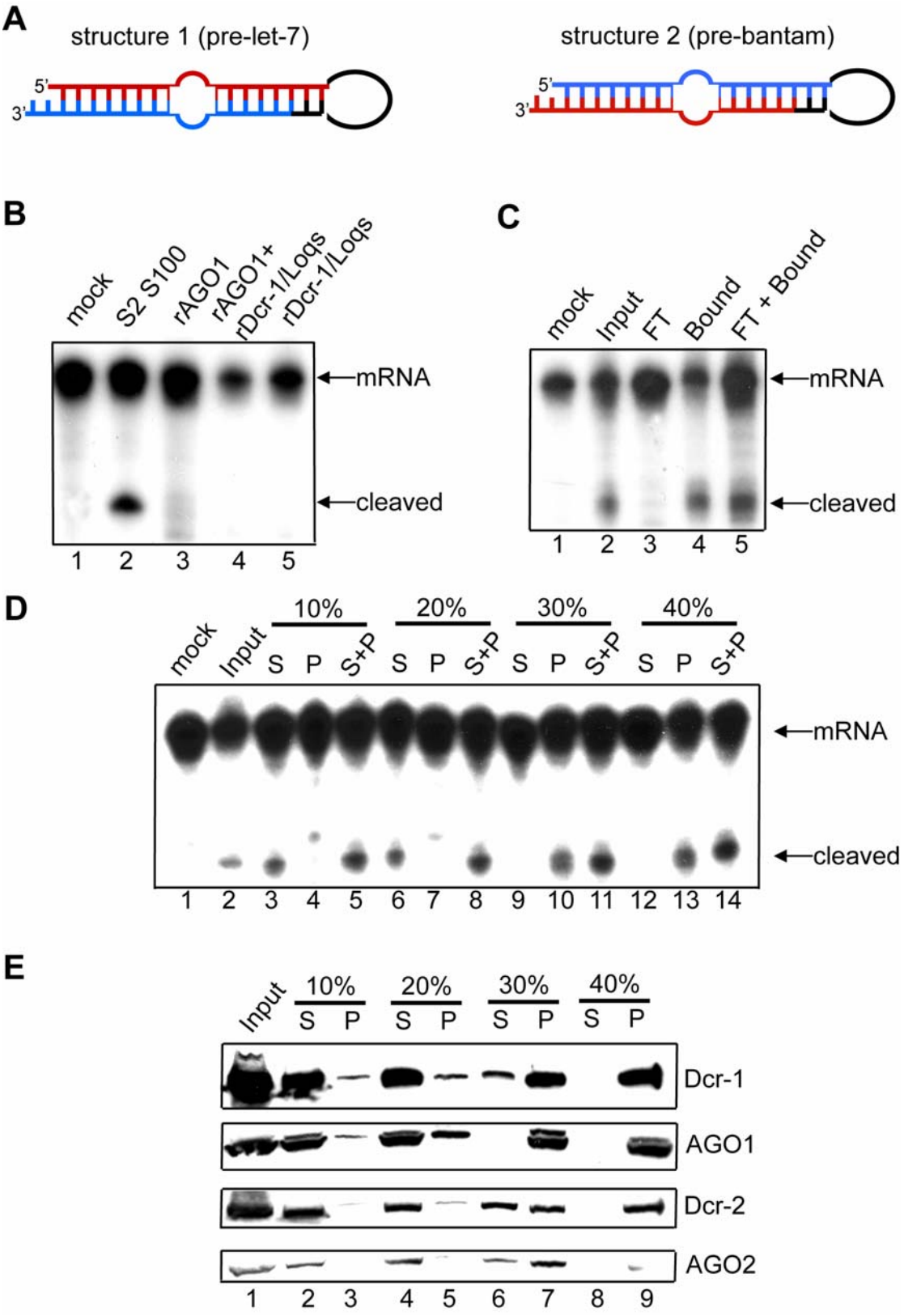
A
structure 1 (pre-let-7)
5'
3'
structure 2 (pre-bantam)
5'
3'
B
mock
S2 S100
rAGO1
rAGO1+ rDcr-1/Loqs
rDcr-1/Loqs
mRNA
cleaved
1 2 3 4 5
C
mock
Input
FT
Bound
FT + Bound
mRNA
cleaved
1 2 3 4 5
D
mock
Input
10%
20%
30%
40%
S P S+P S P S+P S P S+P S P S+P
mRNA
cleaved
1 2 3 4 5 6 7 8 9 10 11 12 13 14
E
Input
10%
20%
30%
40%
S P S P S P S P
Dcr-1
AGO1
Dcr-2
AGO2
1 2 3 4 5 6 7 8 9

Figure 4.8. Partial purification of endogenous miRISC complex. (A) A diagram showing two pre-miRNA structures. Red lines denotes mature miRNA, while blue lines denotes miRNA*. In structure 1, the mature miRNA resides in the 5' region of pre-miRNA, while in structure 2, the mature miRNA resides in the 3' end. **(B)** pre-bantam initiated RISC assay was performed with buffer, or 25 μg S2 S100 extract (lane 2), or 10 ng recombinant AGO1 alone (lane 3), or 10 ng recombinant Dcr-1/Loqs-PB complex (lane 5), or 10ng recombinant AGO1 plus 10 ng recombinant Dcr-1/Loqs-PB complex (lane 4). **(C)** Q-Sepharose purification of miRISC. Pre-bantam initiated RISC assay was performed in S100 input (lane 2), or Q flow-through (FT), or Q bound (lane 4), or Q flow-through plus Q bound (lane 5). **(D)** Ammonium sulfate (AS) precipitation of S2 S100. Four AS saturations were tested: 10%, 20%, 30% and 40%. In each AS saturation, pre-bantam initiated RISC activity was tested in supernatant (S) (lanes 3, 6, 9, 12),or pellet (P) (lanes 4, 7, 10, 13), or supernatant plus pellet (S+P) (lanes 5, 8, 11, 14). **(E)** Western blots were performed with corresponding antibodies to detect Dcr-1, AGO1, Dcr-2, and AGO2 following different saturation AS precipitation.

Discussion

Dicers in flies, worms, and humans

miRNA and siRNA can be viewed as two parallel branches of the RNAi pathway. Our biochemical studies demonstrate that Dcr-1/Loqs-PB and Dcr-2/R2D2 are used as distinct initiation complexes for the miRNA and siRNA pathways, respectively, in *Drosophila* cells. The same concept can also be applied to species containing a single Dicer, such as *C. elegans* and human. In *C. elegans*, DCR-1/RDE-4 functions as the initiation complex for the siRNA pathway. However, RDE-4 is not required for miRNA-mediated silencing as supported by the lack of developmental defects in *rde-4* mutant worms (Tabara et al., 1999). It is likely that DCR-1 functions in concert with another dsRNA-binding protein in the worm miRNA pathway.

By reconstitution, we establish that Drosophila Dcr-1 and Dcr-2 enzymes are functional distinct enzymes with distinct substrate specificities. While Dcr-1 is more

suited for processing pre-miRNA, Dcr-2 favors long dsRNA as its ideal substrate (Liu et al., 2003). Thus, it will be important to identify the protein sequence and structural features that determine the evolutionary and functional differences between Dcr-1 and Dcr-2.

Partnerships of RNase III enzymes and dsRNA-binding proteins

In *Drosophila*, while Dcr-2/R2D2 cleaves long dsRNA into siRNA, Drosha/Pasha (DGCR8 in human) and Dcr-1/Loqs-PB catalyze sequential steps of miRNA biogenesis, processing of pri-miRNA into pre-miRNA and of pre-miRNA into miRNA, respectively (Denli et al., 2004; Forstemann et al., 2005; Gregory et al., 2004; Han et al., 2004; Jiang et al., 2005; Landthaler et al., 2004; Liu et al., 2003; Saito et al., 2005). Although R2D2 does not regulate siRNA production, it remains in a tight complex with Dcr-2 and facilitates the role of Dcr-2 in loading siRNA onto siRISC (Liu et al., 2003; Liu et al., 2006). Similar to $Pasha^{fly}$ ($DGCR8^{human}$), which is essential for Drosha to process pri-miRNA (Gregory et al., 2004; Han et al., 2004), Loqs-PB greatly enhances miRNA generation by Dcr-1. Taken together, these studies indicate that all known RNase III enzymes in *Drosophila* (Drosha, Dicer-1, and Dicer-2) are paired with specific dsRNA-binding proteins (Pasha, Loqs-PB, and R2D2) in catalyzing small RNA biogenesis and/or function. It remains to be tested if the same scheme will repeat in other species.

Two modes of function for dsRBPs

The Dcr-2/R2D2 complex not only generates siRNA, but also coordinately binds siRNA and decides which siRNA strand get loaded onto the siRISC complex (Liu et al., 2003; Liu et al., 2006; Tomari et al., 2004b). It is different for Loqs. *In vitro* experiments demonstrate that neither does Loqs interact with miRNA duplex nor does it enhance the interaction between Dcr-1 and miRNA duplex. Consistent with that, Loqs is also dispensible for miRISC assembly *in vivo*. Therefore, my studies identify two different modes of functions for dsRBPs: (1) R2D2 does not regulate siRNA production, but is required for loading siRNA onto the siRISC complexes (Liu et al., 2006). (2) Loqs plays a prominent role in miRNA biogenesis, but is largely dispensable for assembly of the miRISC complexes (Jiang et al., 2005; Liu et al., 2007). These studies will have important implications for understanding the functions of dsRBPs in other RNAi model systems.

The slicer function of AGO1

Structural and biochemical studies on Argonaute proteins demonstrate that Ago is an RNase H –like enzyme, and the "DDH" motif forms the catalytic center of the enzyme (Liu et al., 2004; Rivas et al., 2005; Song et al., 2004). Based on primary sequence alignment, the "DDH" motif is conserved in AGO1 and AGO2 in *Drosophila* (data not shown). Mutation in any one of the DDH residues resulted in obliteration of the slicer activity, supporting the "DDH" model. Siomi group also discovered that *Drosophila* AGO1 can slice (Miyoshi et al., 2005). Sequence

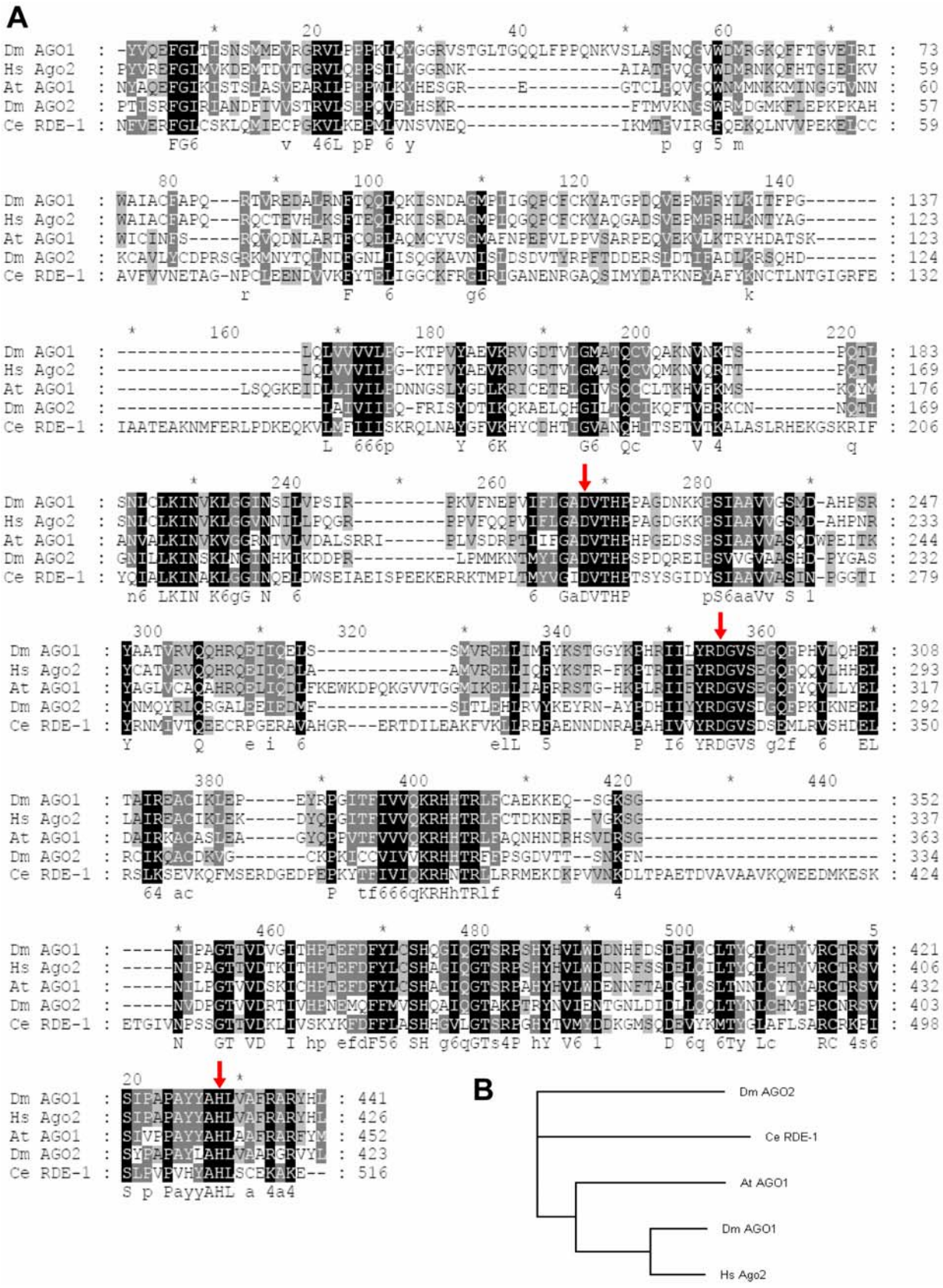
A
Dm AGO1
Hs Ago2
At AGO1
Dm AGO2
Ce RDE-1
B
Dm AGO2
Ce RDE-1
At AGO1
Dm AGO1
Hs Ago2

Figure 4.9. Sequence alignment of PIWI domains among several members of Argonaute family of proteins. (A) The protein sequences of PIWI domains of *Drosophila* AGO1 and AGO2, human Ago2, *Arabidopsis* AGO1, and *C. elegans* RDE-1 were aligned by using Clustal X. The most conserved two sequences were shown on the top: *Drosophila* AGO1 and human Ago2. Red arrows point to the conserved DDH catalytic residues. **(B)** A phylogenic tree of the PIWI domains of the five Ago2s was generated by TreeView.

alignment of the PIWI domains among human Ago2, *Drosophila* AGO1 and AGO2, *C. elegans* RDE-1 and *Arabidopsis* AGO1 reveals that the highest similarity exists between two PIWI domains are human Ago2 and *Drosophila* AGO1 (76% identity and 85% homology) (Fig. 4.9), while *Drosophila* AGO2 is distinct from other four Agos (Fig. 4.9, right bottom panel) . Therefore, from the sequence and structure point of view, it is reasonable that AGO1 possesses slicer function.

However, it brings a question what is the purpose for *Drosophila* AGO1 to have slicer activity? AGO1 functions in the miRNA pathway, and it is widely accepted that miRNA-mediated gene regulation in animals usually does not involve sequence-specific cleavage of the target. Even if AGO1 is the slicing-competent, most animal miRNAs do not share sufficient sequence complementarity to trigger sequence-specific cleavage. Instead, most miRNA-mediated gene regulation in animals is carried out through translational repression (Bartel, 2004). There is as yet no definitive explanation to the slicer function of AGO1, but it provides a tempting hypothesis that animal miRNAs can also mediate mRNA degradation. In fact, the dogma that animal miRNAs do not influence the stability of target RNA has been challenged. It was discovered that regulation by let-7 or lin-4 miRNA in *C. elegans* resulted in degradation of their target mRNAs, though the 3'UTR regulatory

sequences of lin-41 has imperfect base-pairing interaction with let-7 (Bagga et al., 2005). Thus, it raises the possibility that regulation at the level of mRNA stability may be more common than previously perceived for the miRNA pathway in animals. It remains to be tested whether mRNAs containing partial miRNA complementary sites or endogenous target sites can be targeted for degradation by recombinant Drosophila AGO1.

On the other hand, most plant miRNA share near perfect sequence complementarity to their target mRNAs and have been shown to guide sequence-specific cleavage (Bartel, 2004). This notion has also been challenged by the discovery that miR172 regulated the expression of a floral homeotic gene APETALA2 through translational inhibition in *Arabidopsis*, despite the near-perfect complementarity between miR172 and the sequences in APETALA2 ORF (Aukerman and Sakai, 2003; Chen, 2004). A recent unbiased genetic study in *Arabidopsis* showed widespread plant miRNA-mediated translational repression and this regulation required AGO1, AGO10, and the decapping component VARICOSE (VCS) (Brodersen et al., 2008). Thus, like Drosophila AGO1, *Arabidopsis* AGO1 can either slice its target or inhibit mRNA translation depending on the context.

Taken together, these studies illustrate that there is no exclusive mode of miRNA action in animals or plants, and the degree of complementarity can no longer be the decisive criterion for execution through slicing or translational inhibition (Mallory et al., 2008). Yet it raises another question of how slicing is avoided during translational repression. It also remains unclear whether the two mechanisms coexist within the

same cells, or whether they can be spatially and/or temporally separated. Different cofactors involved, tissue specificity of miRNA and its target expression could be the differential factors that influence the prevalence of one process over the other.

More factor(s) remain to be identified in the miRNA pathway

While the minimal siRISC machinery in *Drosophila* can be reconstituted by recombinant Dcr-2/R2D2 and AGO2, the miRISC cannot be reconstituted by the parallel proteins, Dcr-1/Loqs and AGO1. In addition, while the siRISC is irreversibly damaged by exposure to high salt, the miRISC can sustain activity after high salt treatment. By comparison, these two parallel pathways are not exact mirror images of each other, and there may be mechanistic differences between them. Resistance of miRISC to salt enables us to identify novel factor(s) through protein purification procedures in the future.

To date, one of the most important problems in understanding the mechanism of RNAi lies in how siRNA and miRNA duplexes unwind and get loaded onto RISC. Though it has been shown that the passenger strand was cleaved in a Ago-dependent manner (Leuschner et al., 2006; Matranga et al., 2005; Miyoshi et al., 2005; Rand et al., 2005), it may not be the only mechanism for conversion of siRNA or miRNA duplex into single-stranded state because siRNAs bearing uncleavable anti-guide strand were still able to induce RISC cleavage. The inability of Dcr-1/Loqs and AGO1 to reconstitute miRISC may be due to the absence of the unwinding factor. Another distinguishable feature of the miRNA pathway is that only mature miRNA strand

exists in vivo while the processing by Dcr-1/Loqs generates a duplex. The factor that senses the asymmetry of miRNA duplex may determine the selectivity of RISC toward one strand versus another. I hope that our continued effort to discover novel component(s) would contribute to solve the above mysteries.

Chapter V

Perspective and Future Directions

***Drosophila* AGO2**

In other proteins, polyQ regions are associated with protein aggregation (Ross and Poirier, 2004). Thus, we hypothesize that the extensive polyQ regions at the N terminus of AGO2 may be problematic for expression. Truncation of part of the polyQ region leads to higher expression level than wildtype protein, while truncation of the whole polyQ region results in loss of the slicer activity, indicating that the polyQ region is necessary for the RISC activity. Furthermore, the recombinant AGO2 is extremely labile in that the pellet of insect cells expressing AGO2 can not be stored at -80ºC for over two weeks and purified recombinant AGO2 can not be stored at -80ºC for over one month. Otherwise, the activity will be lost. At the same time, most other recombinant enzymes that we have purified retain activity for at least one year, and the S2 cell extract sustains RISC activity after more than two-year storage. There is no clear mechanism discovered either, though we can speculate that it may contribute to the aggregative nature of the polyQ region of AGO2. The truncated AGO2 with 4 long polyQ repeat has the molecular weight of 100 kDa, and it runs between the molecular weight markers 158 kDa and 44 kDa on the gel filtration column, indicating that active AGO2 possibly exists in a monomeric form. These data suggest that aggregation possibly through polyQ region leads to inactivation of AGO2, while AGO2 requires the polyQ region to function.

The biggest breakthrough in expressing AGO2 comes from the significant increase in AGO2 expression when co-expressed with AGO1. However, the mechanism of enhancement remains largely unknown except the observation that

AGO1 interacts with AGO2. The interaction between endogenous AGO1 and AGO2 remains to be examined by co-immunoprecipitation experiments. If endogenous AGO1 and AGO2 interact with each other, the interaction domain(s) will be identified through truncation analysis and the mechanism of enhancement can be examined by making truncated recombinant proteins.

There are other unsolved mysteries about AGO2. Where does the salt sensitivity come from? In the process of spliceosome assembly, some complexes such as U1 snRNP have been discovered to contain salt-sensitive subunits (Gottschalk et al., 1998). The exact nature of the salt-sensitive association as yet remains to be determined. We can speculate that there may be small molecule or RNA component which forms labile interaction with AGO2

How is siRNA loaded onto AGO2?

1) Helicase model.

While newly synthesized siRNA is double-stranded, siRNA exists as a single-stranded form in an active siRISC complex (Martinez et al., 2002). Thus, the nascent siRNA duplex must be unwound during siRISC assembly. It is reasonable to speculate that the Dcr-2/R2D2 complex facilitates unwinding of the siRNA duplex, thereby promoting incorporation of single-stranded siRNA into the siRISC complex. Dcr-2 is a candidate for the siRNA-unwinding helicase because it carries putative DExDc and HELICc helicase domains and physically contacts the siRNA end that is easier to unwind (Tomari et al., 2004b).

However, two mutations in the dcr-2 helicase domain were able to reconstitute the double-stranded siRNA-initiated RISC activity with AGO2, while they lost dsRNA processing activity. This result suggests that a DExDc and HELICc helicase domains are possibly involved in ATP hydrolysis and unwinding long dsRNA or product release, but not required for Dcr-2 to promote siRISC assembly. In addition, recombinant Dcr-2 or Dcr-2/R2D2 complex cannot unwind the siRNA duplex in vitro (Tomari et al., 2004b). An explanation can be offered that Dcr-2/R2D2 may not possess helicase activity in the absence of AGO2. Or the helicase domain that is responsible for unwinding siRNA may reside in other regions of the 190 kDa Dcr-2 protein.

2) Passenger strand cleavage by Ago2 model.

Recent studies suggest an alternative model for separation of siRNA strands and activation of the siRISC complex (Matranga et al., 2005; Rand et al., 2005). Both studies above used tissue extract or cell extract instead of purified protein, therefore, it remains unclear whether AGO2 directly mediates cleavage-assisted dissociation of siRNA. My observation that AGO2 alone is unable to perform double-stranded siRNA initiated RISC cleavage indicates that the recruitment of duplex siRNA to AGO2 by Dcr-2/R2D2 complex is essential, or the cleaved passenger strand can not be released without the help of Drc-2/R2D2 complex. Only after siRNA loading will the PIWI domain of AGO2 cleave the passenger strand and facilitate the formation of an active siRISC complex containing only the guide strand. It is likely that the

orientation of siRNA binding by the Dcr-2/R2D2 complex allows AGO2 to access and cleave only one of the two siRNA strands. Therefore, the Dcr-2/R2D2 complex determines which strand of siRNA duplex becomes the guide strand and AGO2 slices the opposite strand.

The two mechanistic models of siRISC assembly are not mutually exclusive. Since siRNAs bearing uncleavable passenger strand was still able to induce RISC cleavage (Matranga et al., 2005; Rand et al., 2005) , it indicates the possible existence of unwinding mechanism for conversion of siRNA duplex into single-stranded state. In either model, the Dcr-2/R2D2 complex plays a critical role in facilitating the strand separation of the duplex siRNA. Future studies are needed to identify the helicase that unwinds siRNA and to assess the passenger cleavage mechanism in the reconstitution system.

Reconstituted system as a tool

The minimal reconstituted system will enable us to identify positive or negative regulators of the RNAi pathway by "biochemical supplementation". Since the *Drosophila* siRISC is salt-sensitive, we can use salt to inactivate the siRISC in the S2 cell extract, fractionate the S2 cell extract, and identify the fraction(s) that will enhance or inhibit the siRISC activity of the reconstituted system. After purifying the fraction(s) to homogeneity, we will be able to discover the novel factor(s) involved in the RNAi pathway.

Slicer function of *Drosophila* AGO1

I have discovered that like human AGO2, *Drosophila* AGO1 also possesses minimal RISC activity. AGO1 functions in the miRNA pathway, and it is widely accepted that miRNA-mediated gene regulation in animals usually does not involve sequence-specific cleavage of the target. Even if AGO1 is slicing-competent, most animal miRNAs do not share sufficient sequence complementarity to trigger sequence-specific cleavage. Instead, most miRNA-mediated gene regulation in animals is carried out through translational repression (Bartel, 2004). There is as yet no definitive explanation to the slicer function of AGO1, but it provides a tempting hypothesis that animal miRNAs can also mediate mRNA degradation. In fact, the dogma that animal miRNAs do not influence the stability of target RNA has been challenged. It was discovered that regulation by let-7 or lin-4 miRNA in *C. elegans* resulted in degradation of their target mRNAs, though the 3'UTR regulatory sequences of lin-41 has imperfect base-pairing interaction with let-7 (Bagga et al., 2005). Thus, it raised the possibility that regulation at the level of mRNA stability may be more common than previously perceived for the miRNA pathway in animals. It remains to be tested whether mRNAs containing partial miRNA complementary sites or endogenous target sites can be targeted for degradation by recombinant *Drosophila* AGO1.

On the other hand, most plant miRNA share near perfect sequence complementarity to their target mRNAs and have been shown to guide sequence-specific cleavage (Bartel, 2004). This notion has also been challenged by

the discovery that miR172 regulated the expression of a floral homeotic gene APETALA2 through translational inhibition in *Arabidopsis*, despite the near-perfect complementarity between miR172 and the sequences in APETALA2 ORF (Aukerman and Sakai, 2003; Chen, 2004). A recent unbiased genetic study in *Arabidopsis* showed widespread plant miRNA-mediated translational repression and this regulation required AGO1, AGO10, and the decapping component VARICOSE (VCS) (Brodersen et al., 2008). Thus, like Drosophila AGO1, *Arabidopsis* AGO1 can either slice its target or inhibit mRNA translation depending on the context.

Taken together, these studies illustrate that there is no exclusive mode of miRNA action in animals or plants, and the degree of complementarity can no longer be the decisive criterion for execution through slicing or translational inhibition (Mallory et al., 2008). Yet it raises another question of how slicing is avoided during translational repression. It also remains unclear whether the two mechanisms coexist within the same cells, or whether they can be spatially and/or temporally separated. Different cofactors involved, tissue specificity of miRNA and its target expression could be the differential factors that influence the prevalence of one process over the other.

More factor(s) remain to be identified in the miRNA pathway

While the minimal siRISC machinery in *Drosophila* can be reconstituted by recombinant Dcr-2, R2D2, and AGO2, the miRISC can not be reconstituted by the parallel proteins, Dcr-1, Loqs, and AGO1. In addition, while the siRISC is irreversibly damaged by exposure to high salt, the miRISC can sustain activity after high salt

treatment. By comparison, these two parallel pathways are not exact mirror images of each other, and there may be mechanistic differences between them. Resistance of miRISC to salt enables us to identify novel factor(s) through protein purification procedure in the future.

Again, one of the most important problems in understanding the mechanism of RNAi lies in how siRNA and miRNA duplexes unwind and get loaded onto RISC. The inability of Dcr-1/Loqs and AGO1 to reconstitute miRISC may be due to the absence of the unwinding factor. Another distinguishable feature of the miRNA pathway is that only mature miRNA strand exists in vivo while the processing by Dcr-1/Loqs generates a duplex. The factor that senses the asymmetry of miRNA duplex may determine the selectivity of RISC toward one strand versus another. I hope that our continued effort through fractionation to discover novel component(s) would contribute to solve the above mysteries.

Bibliography

Aravin, A. A., Lagos-Quintana, M., Yalcin, A., Zavolan, M., Marks, D., Snyder, B., Gaasterland, T., Meyer, J., and Tuschl, T. (2003). The small RNA profile during Drosophila melanogaster development. Dev Cell 5, 337-350.

Aukerman, M. J., and Sakai, H. (2003). Regulation of flowering time and floral organ identity by a MicroRNA and its APETALA2-like target genes. Plant Cell 15, 2730-2741.

Aukerman, M.J., and Sakai, H. (2003). Regulation of flowering time and floral organ identity by a MicroRNA and its APETALA2-like target genes. Plant Cell 15, 2730-2741.

Bagga, S., Bracht, J., Hunter, S., Massirer, K., Holtz, J., Eachus, R., and Pasquinelli, A.E. (2005). Regulation by let-7 and lin-4 miRNAs results in target mRNA degradation. Cell 122, 553-563.

Bartel, D.P. (2004). MicroRNAs: genomics, biogenesis, mechanism, and function. Cell 116, 281-297.

Baulcombe, D. (2004). RNA silencing in plants. Nature 431, 356-363.

Bentwich, I., Avniel, A., Karov, Y., Aharonov, R., Gilad, S., Barad, O., Barzilai, A., Einat, P., Einav, U., Meiri, E., et al. (2005). Identification of hundreds of conserved and nonconserved human microRNAs. Nat Genet 37, 766-770.

Bernstein, E., Caudy, A. A., Hammond, S. M., and Hannon, G. J. (2001). Role for a bidentate ribonuclease in the initiation step of RNA interference. Nature 409, 363-366.

Bitko, V., and Barik, S. (2001). Phenotypic silencing of cytoplasmic genes using sequence-specific double-stranded short interfering RNA and its application in the reverse genetics of wild type negative-strand RNA viruses. BMC Microbiol 1, 34.

Blaszczyk, J., Tropea, J.E., Bubunenko, M., Routzahn, K.M., Waugh, D.S., Court, D.L., and Ji, X. (2001). Crystallographic and modeling studies of RNase III suggest a mechanism for double-stranded RNA cleavage. Structure 9, 1225-1236.

Bohmert, K., Camus, I., Bellini, C., Bouchez, D., Caboche, M., and Benning, C.

(1998). AGO1 defines a novel locus of Arabidopsis controlling leaf development. Embo J 17, 170-180.

Bohnsack, M. T., Czaplinski, K., and Gorlich, D. (2004). Exportin 5 is a RanGTP-dependent dsRNA-binding protein that mediates nuclear export of pre-miRNAs. Rna 10, 185-191.

Bohnsack, M.T., Czaplinski, K., and Gorlich, D. (2004). Exportin 5 is a RanGTP-dependent dsRNA-binding protein that mediates nuclear export of pre-miRNAs. Rna 10, 185-191.

Brennecke, J., Hipfner, D. R., Stark, A., Russell, R. B., and Cohen, S. M. (2003). bantam encodes a developmentally regulated microRNA that controls cell proliferation and regulates the proapoptotic gene hid in Drosophila. Cell 113, 25-36.

Brodersen, P., Sakvarelidze-Achard, L., Bruun-Rasmussen, M., Dunoyer, P., Yamamoto, Y. Y., Sieburth, L., and Voinnet, O. (2008). Widespread translational inhibition by plant miRNAs and siRNAs. Science 320, 1185-1190.

Burgyan, J. (2008). Role of silencing suppressor proteins. Methods Mol Biol 451, 69-79.

Cerutti, L., Mian, N., and Bateman, A. (2000). Domains in gene silencing and cell differentiation proteins: the novel PAZ domain and redefinition of the Piwi domain. Trends Biochem Sci 25, 481-482.

Chapman, E.J., Prokhnevsky, A.I., Gopinath, K., Dolja, V.V., and Carrington, J.C. (2004). Viral RNA silencing suppressors inhibit the microRNA pathway at an intermediate step. Genes Dev 18, 1179-1186.

Chen, P.Y., Manninga, H., Slanchev, K., Chien, M., Russo, J.J., Ju, J., Sheridan, R., John, B., Marks, D.S., Gaidatzis, D., et al. (2005). The developmental miRNA profiles of zebrafish as determined by small RNA cloning. Genes Dev 19, 1288-1293.

Chen, X. (2004). A microRNA as a translational repressor of APETALA2 in Arabidopsis flower development. Science 303, 2022-2025.

Chou, T.B., Noll, E., and Perrimon, N. (1993). Autosomal P[ovoD1] dominant female-sterile insertions in Drosophila and their use in generating germ-line chimeras. Development 119, 1359-1369.

Cullen, B.R. (2004). Transcription and processing of human microRNA precursors. Mol Cell 16, 861-865.

Denli, A.M., Tops, B.B., Plasterk, R.H., Ketting, R.F., and Hannon, G.J. (2004). Processing of primary microRNAs by the Microprocessor complex. Nature 432, 231-235.

Eamens, A., Wang, M. B., Smith, N. A., and Waterhouse, P. M. (2008). RNA silencing in plants: yesterday, today, and tomorrow. Plant Physiol 147, 456-468.

Elbashir, S. M., Harborth, J., Lendeckel, W., Yalcin, A., Weber, K., and Tuschl, T. (2001a). Duplexes of 21-nucleotide RNAs mediate RNA interference in cultured mammalian cells. Nature 411, 494-498.

Elbashir, S. M., Lendeckel, W., and Tuschl, T. (2001b). RNA interference is mediated by 21- and 22-nucleotide RNAs. Genes Dev 15, 188-200.

Elbashir, S. M., Martinez, J., Patkaniowska, A., Lendeckel, W., and Tuschl, T. (2001c). Functional anatomy of siRNAs for mediating efficient RNAi in Drosophila melanogaster embryo lysate. Embo J 20, 6877-6888.

Filippov, V., Solovyev, V., Filippova, M., and Gill, S. S. (2000). A novel type of RNase III family proteins in eukaryotes. Gene 245, 213-221.

Fire, A., Xu, S., Montgomery, M.K., Kostas, S.A., Driver, S.E., and Mello, C.C. (1998). Potent and specific genetic interference by double-stranded RNA in Caenorhabditis elegans. Nature 391, 806-811.

Forstemann, K., Tomari, Y., Du, T., Vagin, V. V., Denli, A. M., Bratu, D. P., Klattenhoff, C., Theurkauf, W. E., and Zamore, P. D. (2005). Normal microRNA maturation and germ-line stem cell maintenance requires Loquacious, a double-stranded RNA-binding domain protein. PLoS Biol 3, e236.

Gottschalk, A., Tang, J., Puig, O., Salgado, J., Neubauer, G., Colot, H.V., Mann, M., Seraphin, B., Rosbash, M., Luhrmann, R., et al. (1998). A comprehensive biochemical and genetic analysis of the yeast U1 snRNP reveals five novel proteins. Rna 4, 374-393.

Gregory, R. I., Yan, K. P., Amuthan, G., Chendrimada, T., Doratotaj, B., Cooch, N., and Shiekhattar, R. (2004). The Microprocessor complex mediates the genesis of microRNAs. Nature 432, 235-240.

Gregory, R.I., Yan, K.P., Amuthan, G., Chendrimada, T., Doratotaj, B., Cooch, N., and

Shiekhattar, R. (2004). The Microprocessor complex mediates the genesis of microRNAs. Nature 432, 235-240.

Hamilton, A. J., and Baulcombe, D. C. (1999). A species of small antisense RNA in posttranscriptional gene silencing in plants. Science 286, 950-952.

Hammond, S. M., Bernstein, E., Beach, D., and Hannon, G. J. (2000). An RNA-directed nuclease mediates post-transcriptional gene silencing in Drosophila cells. Nature 404, 293-296.

Hammond, S. M., Boettcher, S., Caudy, A. A., Kobayashi, R., and Hannon, G. J. (2001). Argonaute2, a link between genetic and biochemical analyses of RNAi. Science 293, 1146-1150.

Hammond, S.M., Boettcher, S., Caudy, A.A., Kobayashi, R., and Hannon, G.J. (2001). Argonaute2, a link between genetic and biochemical analyses of RNAi. Science 293, 1146-1150.

Han, J., Lee, Y., Yeom, K.H., Kim, Y.K., Jin, H., and Kim, V.N. (2004). The Drosha-DGCR8 complex in primary microRNA processing. Genes Dev 18, 3016-3027.

Hartig, J.V., Tomari, Y., and Forstemann, K. (2007). piRNAs--the ancient hunters of genome invaders. Genes Dev 21, 1707-1713.

Hutvagner, G., and Simard, M.J. (2008). Argonaute proteins: key players in RNA silencing. Nat Rev Mol Cell Biol 9, 22-32.

Hutvagner, G., McLachlan, J., Pasquinelli, A. E., Balint, E., Tuschl, T., and Zamore, P. D. (2001). A cellular function for the RNA-interference enzyme Dicer in the maturation of the let-7 small temporal RNA. Science 293, 834-838.

Ishizuka, A., Siomi, M. C., and Siomi, H. (2002). A Drosophila fragile X protein interacts with components of RNAi and ribosomal proteins. Genes Dev 16, 2497-2508.

Ishizuka, A., Siomi, M.C., and Siomi, H. (2002). A Drosophila fragile X protein interacts with components of RNAi and ribosomal proteins. Genes Dev 16, 2497-2508.

Jiang, F., Ye, X., Liu, X., Fincher, L., McKearin, D., and Liu, Q. (2005). Dicer-1 and R3D1-L catalyze microRNA maturation in Drosophila. Genes Dev 19, 1674-1679.

Jin, Z., and Xie, T. (2007). Dcr-1 maintains Drosophila ovarian stem cells. Curr Biol 17, 539-544.

Kataoka, Y., Takeichi, M., and Uemura, T. (2001). Developmental roles and molecular characterization of a Drosophila homologue of Arabidopsis Argonaute1, the founder of a novel gene superfamily. Genes Cells 6, 313-325.

Kennerdell, J. R., Yamaguchi, S., and Carthew, R. W. (2002). RNAi is activated during Drosophila oocyte maturation in a manner dependent on aubergine and spindle-E. Genes Dev 16, 1884-1889.

Ketting, R. F., Fischer, S. E., Bernstein, E., Sijen, T., Hannon, G. J., and Plasterk, R. H. (2001). Dicer functions in RNA interference and in synthesis of small RNA involved in developmental timing in C. elegans. Genes Dev 15, 2654-2659.

Klattenhoff, C., and Theurkauf, W. (2008). Biogenesis and germline functions of piRNAs. Development 135, 3-9.

Lagos-Quintana, M., Rauhut, R., Lendeckel, W., and Tuschl, T. (2001). Identification of novel genes coding for small expressed RNAs. Science 294, 853-858.

Lagos-Quintana, M., Rauhut, R., Meyer, J., Borkhardt, A., and Tuschl, T. (2003). New microRNAs from mouse and human. Rna 9, 175-179.

Lagos-Quintana, M., Rauhut, R., Yalcin, A., Meyer, J., Lendeckel, W., and Tuschl, T. (2002). Identification of tissue-specific microRNAs from mouse. Curr Biol 12, 735-739.

Lai, E. C., Tomancak, P., Williams, R. W., and Rubin, G. M. (2003). Computational identification of Drosophila microRNA genes. Genome Biol 4, R42.

Lakatos, L., Szittya, G., Silhavy, D., and Burgyan, J. (2004). Molecular mechanism of RNA silencing suppression mediated by p19 protein of tombusviruses. Embo J 23, 876-884.

Lamontagne, B., Larose, S., Boulanger, J., and Elela, S. A. (2001). The RNase III family: a conserved structure and expanding functions in eukaryotic dsRNA metabolism. Curr Issues Mol Biol 3, 71-78.

Landthaler, M., Yalcin, A., and Tuschl, T. (2004). The human DiGeorge syndrome critical region gene 8 and Its D. melanogaster homolog are required for miRNA biogenesis. Curr Biol 14, 2162-2167.

Lau, N.C., Lim, L.P., Weinstein, E.G., and Bartel, D.P. (2001). An abundant class of

tiny RNAs with probable regulatory roles in Caenorhabditis elegans. Science 294, 858-862.

Lee, R. C., and Ambros, V. (2001). An extensive class of small RNAs in Caenorhabditis elegans. Science 294, 862-864.

Lee, R. C., Feinbaum, R. L., and Ambros, V. (1993). The C. elegans heterochronic gene lin-4 encodes small RNAs with antisense complementarity to lin-14. Cell 75, 843-854.

Lee, Y. S., Nakahara, K., Pham, J. W., Kim, K., He, Z., Sontheimer, E. J., and Carthew, R. W. (2004b). Distinct roles for Drosophila Dicer-1 and Dicer-2 in the siRNA/miRNA silencing pathways. Cell 117, 69-81.

Lee, Y., Ahn, C., Han, J., Choi, H., Kim, J., Yim, J., Lee, J., Provost, P., Radmark, O., Kim, S., and Kim, V. N. (2003). The nuclear RNase III Drosha initiates microRNA processing. Nature 425, 415-419.

Lee, Y., Kim, M., Han, J., Yeom, K.H., Lee, S., Baek, S.H., and Kim, V.N. (2004a). MicroRNA genes are transcribed by RNA polymerase II. Embo J 23, 4051-4060.

Lee, Y.S., Nakahara, K., Pham, J.W., Kim, K., He, Z., Sontheimer, E.J., and Carthew, R.W. (2004b). Distinct roles for Drosophila Dicer-1 and Dicer-2 in the siRNA/miRNA silencing pathways. Cell 117, 69-81.

Leuschner, P.J., Ameres, S.L., Kueng, S., and Martinez, J. (2006). Cleavage of the siRNA passenger strand during RISC assembly in human cells. EMBO Rep 7, 314-320.

Lim, L. P., Glasner, M. E., Yekta, S., Burge, C. B., and Bartel, D. P. (2003a). Vertebrate microRNA genes. Science 299, 1540.

Lim, L. P., Lau, N. C., Weinstein, E. G., Abdelhakim, A., Yekta, S., Rhoades, M. W., Burge, C. B., and Bartel, D. P. (2003b). The microRNAs of Caenorhabditis elegans. Genes Dev 17, 991-1008.

Lin, H., and Spradling, A.C. (1997). A novel group of pumilio mutations affects the asymmetric division of germline stem cells in the Drosophila ovary. Development 124, 2463-2476.

Lingel, A., Simon, B., Izaurralde, E., and Sattler, M. (2003). Structure and nucleic-acid binding of the Drosophila Argonaute 2 PAZ domain. Nature 426, 465-469.

Liu, J., Carmell, M.A., Rivas, F.V., Marsden, C.G., Thomson, J.M., Song, J.J., Hammond, S.M., Joshua-Tor, L., and Hannon, G.J. (2004). Argonaute2 is the catalytic engine of mammalian RNAi. Science 305, 1437-1441.

Liu, Q., Rand, T.A., Kalidas, S., Du, F., Kim, H.E., Smith, D.P., and Wang, X. (2003). R2D2, a bridge between the initiation and effector steps of the Drosophila RNAi pathway. Science 301, 1921-1925.

Liu, X., Jiang, F., Kalidas, S., Smith, D., and Liu, Q. (2006). Dicer-2 and R2D2 coordinately bind siRNA to promote assembly of the siRISC complexes. Rna 12, 1514-1520.

Liu, X., Park, J. K., Jiang, F., Liu, Y., McKearin, D., and Liu, Q. (2007). Dicer-1, but not Loquacious, is critical for assembly of miRNA-induced silencing complexes. Rna 13, 2324-2329.

Liu, X., Park, J.K., Jiang, F., Liu, Y., McKearin, D., and Liu, Q. (2007). Dicer-1, but not Loquacious, is critical for assembly of miRNA-induced silencing complexes. Rna 13, 2324-2329.

Llave, C., Xie, Z., Kasschau, K.D., and Carrington, J.C. (2002). Cleavage of Scarecrow-like mRNA targets directed by a class of Arabidopsis miRNA. Science 297, 2053-2056.

Lund, E., Guttinger, S., Calado, A., Dahlberg, J.E., and Kutay, U. (2004). Nuclear export of microRNA precursors. Science 303, 95-98.

Ma, J. B., Ye, K., and Patel, D. J. (2004). Structural basis for overhang-specific small interfering RNA recognition by the PAZ domain. Nature 429, 318-322.

Ma, J. B., Yuan, Y. R., Meister, G., Pei, Y., Tuschl, T., and Patel, D. J. (2005). Structural basis for 5'-end-specific recognition of guide RNA by the A. fulgidus Piwi protein. Nature 434, 666-670.

Macrae, I.J., Zhou, K., Li, F., Repic, A., Brooks, A.N., Cande, W.Z., Adams, P.D., and Doudna, J.A. (2006). Structural basis for double-stranded RNA processing by Dicer. Science 311, 195-198.

Mallory, A.C., Elmayan, T., and Vaucheret, H. (2008). MicroRNA maturation and action-the expanding roles of ARGONAUTEs. Curr Opin Plant Biol.

Martinez, J., and Tuschl, T. (2004). RISC is a 5' phosphomonoester-producing RNA endonuclease. Genes Dev 18, 975-980.

Martinez, J., Patkaniowska, A., Urlaub, H., Luhrmann, R., and Tuschl, T. (2002). Single-stranded antisense siRNAs guide target RNA cleavage in RNAi. Cell 110, 563-574.

Matranga, C., Tomari, Y., Shin, C., Bartel, D.P., and Zamore, P.D. (2005). Passenger-strand cleavage facilitates assembly of siRNA into Ago2-containing RNAi enzyme complexes. Cell 123, 607-620.

Meister, G., Landthaler, M., Dorsett, Y., and Tuschl, T. (2004a). Sequence-specific inhibition of microRNA- and siRNA-induced RNA silencing. Rna 10, 544-550.

Meister, G., Landthaler, M., Patkaniowska, A., Dorsett, Y., Teng, G., and Tuschl, T. (2004). Human Argonaute2 mediates RNA cleavage targeted by miRNAs and siRNAs. Mol Cell 15, 185-197.

Meyer, W. J., Schreiber, S., Guo, Y., Volkmann, T., Welte, M. A., and Muller, H. A. (2006). Overlapping functions of argonaute proteins in patterning and morphogenesis of Drosophila embryos. PLoS Genet 2, e134.

Miyoshi, K., Tsukumo, H., Nagami, T., Siomi, H., and Siomi, M. C. (2005). Slicer function of Drosophila Argonautes and its involvement in RISC formation. Genes Dev 19, 2837-2848.

Napoli, C., Lemieux, C., and Jorgensen, R. (1990). Introduction of a Chimeric Chalcone Synthase Gene into Petunia Results in Reversible Co-Suppression of Homologous Genes in trans. Plant Cell 2, 279-289.

Nykanen, A., Haley, B., and Zamore, P.D. (2001). ATP requirements and small interfering RNA structure in the RNA interference pathway. Cell 107, 309-321.

Okamura, K., and Lai, E. C. (2008). Endogenous small interfering RNAs in animals. Nat Rev Mol Cell Biol 9, 673-678.

Okamura, K., Ishizuka, A., Siomi, H., and Siomi, M.C. (2004). Distinct roles for Argonaute proteins in small RNA-directed RNA cleavage pathways. Genes Dev 18, 1655-1666.

Park, J. K., Liu, X., Strauss, T. J., McKearin, D. M., and Liu, Q. (2007). The miRNA pathway intrinsically controls self-renewal of Drosophila germline stem cells. Curr Biol 17, 533-538.

Parker, J.S., Roe, S.M., and Barford, D. (2005). Structural insights into mRNA

recognition from a PIWI domain-siRNA guide complex. Nature 434, 663-666.

Pasquinelli, A. E., Reinhart, B. J., Slack, F., Martindale, M. Q., Kuroda, M. I., Maller, B., Hayward, D. C., Ball, E. E., Degnan, B., Muller, P., et al. (2000). Conservation of the sequence and temporal expression of let-7 heterochronic regulatory RNA. Nature 408, 86-89.

Pham, J. W., and Sontheimer, E. J. (2005). Molecular requirements for RNA-induced silencing complex assembly in the Drosophila RNA interference pathway. J Biol Chem 280, 39278-39283.

Pham, J. W., Pellino, J. L., Lee, Y. S., Carthew, R. W., and Sontheimer, E. J. (2004). A Dicer-2-dependent 80s complex cleaves targeted mRNAs during RNAi in Drosophila. Cell 117, 83-94.

Poy, M.N., Eliasson, L., Krutzfeldt, J., Kuwajima, S., Ma, X., Macdonald, P.E., Pfeffer, S., Tuschl, T., Rajewsky, N., Rorsman, P., et al. (2004). A pancreatic islet-specific microRNA regulates insulin secretion. Nature 432, 226-230.

Rand, T. A., Ginalski, K., Grishin, N. V., and Wang, X. (2004). Biochemical identification of Argonaute 2 as the sole protein required for RNA-induced silencing complex activity. Proc Natl Acad Sci U S A 101, 14385-14389.

Rand, T. A., Petersen, S., Du, F., and Wang, X. (2005). Argonaute2 cleaves the anti-guide strand of siRNA during RISC activation. Cell 123, 621-629.

Reed, J.C., Kasschau, K.D., Prokhnevsky, A.I., Gopinath, K., Pogue, G.P., Carrington, J.C., and Dolja, V.V. (2003). Suppressor of RNA silencing encoded by Beet yellows virus. Virology 306, 203-209.

Reinhart, B.J., Slack, F.J., Basson, M., Pasquinelli, A.E., Bettinger, J.C., Rougvie, A.E., Horvitz, H.R., and Ruvkun, G. (2000). The 21-nucleotide let-7 RNA regulates developmental timing in Caenorhabditis elegans. Nature 403, 901-906.

Rhoades, M.W., Reinhart, B.J., Lim, L.P., Burge, C.B., Bartel, B., and Bartel, D.P. (2002). Prediction of plant microRNA targets. Cell 110, 513-520.

Rivas, F.V., Tolia, N.H., Song, J.J., Aragon, J.P., Liu, J., Hannon, G.J., and Joshua-Tor, L. (2005). Purified Argonaute2 and an siRNA form recombinant human RISC. Nat Struct Mol Biol 12, 340-349.

Robertson, H. D., Webster, R. E., and Zinder, N. D. (1968). Purification and properties

of ribonuclease III from Escherichia coli. J Biol Chem 243, 82-91.

Rodriguez, A., Griffiths-Jones, S., Ashurst, J.L., and Bradley, A. (2004). Identification of mammalian microRNA host genes and transcription units. Genome Res 14, 1902-1910.

Ross, C.A., and Poirier, M.A. (2004). Protein aggregation and neurodegenerative disease. Nat Med 10 Suppl, S10-17.

Rudenko, G., Henry, L., Henderson, K., Ichtchenko, K., Brown, M.S., Goldstein, J.L., and Deisenhofer, J. (2002). Structure of the LDL receptor extracellular domain at endosomal pH. Science 298, 2353-2358.

Saito, K., Ishizuka, A., Siomi, H., and Siomi, M.C. (2005). Processing of pre-microRNAs by the Dicer-1-Loquacious complex in Drosophila cells. PLoS Biol 3, e235.

Sasaki, T., Shiohama, A., Minoshima, S., and Shimizu, N. (2003). Identification of eight members of the Argonaute family in the human genome small star, filled. Genomics 82, 323-330.

Scholthof, H.B. (2007). Heterologous expression of viral RNA interference suppressors: RISC management. Plant Physiol 145, 1110-1117.

Silhavy, D., and Burgyan, J. (2004). Effects and side-effects of viral RNA silencing suppressors on short RNAs. Trends Plant Sci 9, 76-83.

Silhavy, D., Molnar, A., Lucioli, A., Szittya, G., Hornyik, C., Tavazza, M., and Burgyan, J. (2002). A viral protein suppresses RNA silencing and binds silencing-generated, 21- to 25-nucleotide double-stranded RNAs. Embo J 21, 3070-3080.

Siomi, M.C., Tsukumo, H., Ishizuka, A., Nagami, T., and Siomi, H. (2005). A potential link between transgene silencing and poly(A) tails. Rna 11, 1004-1011.

Song, J. J., Liu, J., Tolia, N. H., Schneiderman, J., Smith, S. K., Martienssen, R. A., Hannon, G. J., and Joshua-Tor, L. (2003). The crystal structure of the Argonaute2 PAZ domain reveals an RNA binding motif in RNAi effector complexes. Nat Struct Biol 10, 1026-1032.

Song, J. J., Smith, S. K., Hannon, G. J., and Joshua-Tor, L. (2004). Crystal structure of Argonaute and its implications for RISC slicer activity. Science 305, 1434-1437.

Tabara, H., Sarkissian, M., Kelly, W.G., Fleenor, J., Grishok, A., Timmons, L., Fire, A., and Mello, C.C. (1999). The rde-1 gene, RNA interference, and transposon silencing in C. elegans. Cell 99, 123-132.

Tabara, H., Yigit, E., Siomi, H., and Mello, C. C. (2002). The dsRNA binding protein RDE-4 interacts with RDE-1, DCR-1, and a DExH-box helicase to direct RNAi in C. elegans. Cell 109, 861-871.

Tang, G., Reinhart, B. J., Bartel, D. P., and Zamore, P. D. (2003). A biochemical framework for RNA silencing in plants. Genes Dev 17, 49-63.

Tomari, Y., and Zamore, P. D. (2005). Perspective: machines for RNAi. Genes Dev 19, 517-529.

Tomari, Y., Du, T., Haley, B., Schwarz, D. S., Bennett, R., Cook, H. A., Koppetsch, B. S., Theurkauf, W. E., and Zamore, P. D. (2004a). RISC assembly defects in the Drosophila RNAi mutant armitage. Cell 116, 831-841.

Tomari, Y., Matranga, C., Haley, B., Martinez, N., and Zamore, P.D. (2004b). A protein sensor for siRNA asymmetry. Science 306, 1377-1380.

Tuschl, T., Zamore, P.D., Lehmann, R., Bartel, D.P., and Sharp, P.A. (1999). Targeted mRNA degradation by double-stranded RNA in vitro. Genes Dev 13, 3191-3197.

Vargason, J.M., Szittya, G., Burgyan, J., and Hall, T.M. (2003). Size selective recognition of siRNA by an RNA silencing suppressor. Cell 115, 799-811.

Vaucheret, H. (2005). MicroRNA-dependent trans-acting siRNA production. Sci STKE 2005, pe43.

Weber, M. J. (2005). New human and mouse microRNA genes found by homology search. Febs J 272, 59-73.

Wightman, B., Ha, I., and Ruvkun, G. (1993). Posttranscriptional regulation of the heterochronic gene lin-14 by lin-4 mediates temporal pattern formation in C. elegans. Cell 75, 855-862.

Williams, R.W., and Rubin, G.M. (2002). ARGONAUTE1 is required for efficient RNA interference in Drosophila embryos. Proc Natl Acad Sci U S A 99, 6889-6894.

Wu, H., Xu, H., Miraglia, L. J., and Crooke, S. T. (2000). Human RNase III is a 160-kDa protein involved in preribosomal RNA processing. J Biol Chem 275,

36957-36965.

Xie, Z., Kasschau, K. D., and Carrington, J. C. (2003). Negative feedback regulation of Dicer-Like1 in Arabidopsis by microRNA-guided mRNA degradation. Curr Biol 13, 784-789.

Yan, K.S., Yan, S., Farooq, A., Han, A., Zeng, L., and Zhou, M.M. (2003). Structure and conserved RNA binding of the PAZ domain. Nature 426, 468-474.

Ye, K., Malinina, L., and Patel, D. J. (2003). Recognition of small interfering RNA by a viral suppressor of RNA silencing. Nature 426, 874-878.

Yekta, S., Shih, I.H., and Bartel, D.P. (2004). MicroRNA-directed cleavage of HOXB8 mRNA. Science 304, 594-596.

Yi, R., Qin, Y., Macara, I. G., and Cullen, B. R. (2003). Exportin-5 mediates the nuclear export of pre-microRNAs and short hairpin RNAs. Genes Dev 17, 3011-3016.

Yuan, Y. R., Pei, Y., Ma, J. B., Kuryavyi, V., Zhadina, M., Meister, G., Chen, H. Y., Dauter, Z., Tuschl, T., and Patel, D. J. (2005). Crystal structure of A. aeolicus argonaute, a site-specific DNA-guided endoribonuclease, provides insights into RISC-mediated mRNA cleavage. Mol Cell 19, 405-419.

Zamore, P.D., Tuschl, T., Sharp, P.A., and Bartel, D.P. (2000). RNAi: double-stranded RNA directs the ATP-dependent cleavage of mRNA at 21 to 23 nucleotide intervals. Cell 101, 25-33.

Zhang, H., Kolb, F. A., Jaskiewicz, L., Westhof, E., and Filipowicz, W. (2004). Single processing center models for human Dicer and bacterial RNase III. Cell 118, 57-68.